

3rd Mid-European Clay Conference – MECC 06
Field Trip Guidebook

edited by Igor VLAHOVIĆ, Darko TIBLJAŠ & Goran DURN

CONTENTS

FIELD TRIP 1

Clay mineralogy of bauxites and palaeosols in Istria formed during regional subaerial exposures of the Adriatic Carbonate Platform

DURN, G., OTTNER, F., MINDSZENTY, A., TIŠLJAR, J. & MILEUSNIĆ, M.: Clay mineralogy of bauxites and palaeosols in Istria formed during regional subaerial exposures of the Adriatic Carbonate Platform.....	3
--	---

FIELD TRIP 2

Ceramic and brick clays deposits and excessive flysch erosion

KRUK, B., BROZOVIĆ, I., KASTMÜLLER, Ž., ZAJC, J., TIBLJAŠ, D. & KRUK, Lj.: Stop 1 – Deposit of brick clays Rečica.....	33
AVANIĆ, R., BAKRAČ, K., GRIZELJ, A., WACHA, L., ŠIMIĆ-STANKOVIĆ, M., HEĆIMOVIĆ, Lj., TIBLJAŠ, D. & KRUK, B.: Stop 2 – Ivošević Gaj ceramic clay deposit in the vicinity of Vojnić.....	39
JURAK, V., SLOVENEČ, D. & MILEUSNIĆ, M.: Stop 3 – Excessive flysch erosion – Slani Potok.....	48

FIELD TRIP 3

Clay minerals and selected ecological aspects of soils on Veli Brijun Island, Croatia

OTTNER, F., SIEGHARDT, M., ERSTIĆ, T. & MILEUSNIĆ, M.: Clay minerals and selected ecological aspects of soils on Veli Brijun Island, Croatia.....	55
---	----

Field Trip 1

Clay mineralogy of bauxites and palaeosols in Istria formed during regional subaerial exposures of the Adriatic Carbonate Platform

Clay mineralogy of bauxites and palaeosols in Istria formed during regional subaerial exposures of the Adriatic Carbonate Platform

Goran DURN¹, Franz OTTNER², Andrea MINDSZENTY³, Josip TIŠLJAR¹ and Marta MILEUSNIĆ¹

This excursion is largely based upon the Field Trip P8 (Regional Subaerial Unconformities in Shallow-Marine Carbonate Sequences of Istria: Sedimentology, Mineralogy, Geochemistry and Micromorphology of Associated Bauxites, Palaeosols and Pedo-Sedimentary Complexes) of the 22nd IAS Regional Meeting held in Opatija, Croatia (DURN et al., 2003). Unlike the aforementioned field trip, this excursion comprises 3 stops instead of 8, but data on clays are presented in more detail.

1. INTRODUCTION AND GEOLOGICAL SETTING

The Istrian peninsula represents the NW part of the spacious Adriatic Carbonate Platform (for more details see VLAHOVIĆ et al., 2005). This part of the platform is composed of a succession of carbonate deposits more than 2000 m thick, of Middle Jurassic (Bathonian) to Eocene age, and is overlain by Palaeogene (Eocene) *Foraminiferal limestones*, *Transitional beds (Globigerina marls)* and flysch deposits (Fig. 1).

The most important geological structure of the Istrian peninsula is the Western Istrian Anticline (POLŠAK & ŠIKIĆ, 1973; MARINČIĆ & MATIČEC, 1991), as shown on Fig. 1.

According to VELIĆ et al. (1995a) carbonate and flysch deposits of Istria can be divided into four large-scale sequences. The 1st, 2nd and 3rd large-scale sequences are composed of carbonates, each terminated by important, long-lasting emersions, i.e. type 1 sequence boundaries (TIŠLJAR et al., 1998). They are divided into several laterally continuous units exhibiting gradual changes, typical of the facies diversity on carbonate platforms (Fig. 2).

The Jurassic and Lower Cretaceous deposits of Istria, ranging from the Bathonian to the Upper Albian (1st and 2nd large-scale sequences – Fig. 2), are characterized predominantly by shallow-marine deposition, only sporadically interrupted by periods of emersion (TIŠLJAR, 1978; TIŠLJAR et al., 1995; VELIĆ & TIŠLJAR, 1988; TIŠLJAR & VELIĆ, 1991; VELIĆ et al., 1995a, b). Limestones deposited in peritidal, tidal flat, tidal bar, and lagoonal to low-energy shallow marine environments predominate. Late-diagenetic dolomites only occur in the Upper Tithonian, Berriasian and Albian strata, whereas supratidal early-diagenetic dolomites are abundant in the Berriasian deposits.

During the emersion phases breccia, clay and bauxite deposits were formed.

Recent investigations in Istria (VLAHOVIĆ et al., 1994; MATIČEC et al., 1996; TIŠLJAR et al., 1998), especially in its southern and northern parts, indicate the important role of synsedimentary tectonics which significantly modified the effects of eustatic sea-level fluctuations on this part of the Adriatic Carbonate Platform. In the Istrian part, these include the diachronism of the beginning of the regional Aptian–Early Albian emersion in Istria (Fig. 2): starting from the Late Barremian, Early or Late Aptian, distinct facies differentiation around the emerged parts, and contemporaneous transgression of deposits of different ages during the Middle Albian indicates the important influence of synsedimentary tectonics (VELIĆ et al., 1989), most probably expressed as low-amplitude folding (TIŠLJAR et al., 1995).

MATIČEC et al. (1996) presented new data on the age of the footwall of transgressive Palaeogene deposits in Istria (from Valanginian to Coniacian–Santonian). They reviewed the influence of Cretaceous synsedimentary tectonics, and also the palaeogeographic implications for the Istrian part of the Adriatic Carbonate Platform. For example, they pointed out that Late Cenomanian beds are the youngest Cretaceous deposits in northern Istria, which are karstified and covered by Eocene Foraminiferal limestones (column B on Fig. 2, after VLAHOVIĆ et al., 1994). In contrast, in southern Istria, sedimentation continued until the Upper Santonian (column A on Fig. 2, after TIŠLJAR et al., 1998), including the Late Cenomanian/Early Turonian eustatic sea-level rise which caused temporary drowning over a large part of the Adriatic Carbonate Platform (JENKYNS, 1991; GUŠIĆ & JELASKA, 1993; VLAHOVIĆ et al., 1994, 2002a), while in Central Istria there are localities where transgressive Palaeogene deposits overlie Lower Cretaceous limestones (MATIČEC et al., 1996).

Carbonate deposits of the Istrian Peninsula exhibit numerous exposure surfaces reflecting emergence. On this field trip, subaerial exposure surfaces associated with bauxites and palaeosols will be presented. Special attention will be given to clay mineralogy, sedimentology, geochemistry and the micromorphology of these materials. The following will be presented: (1) clayey bauxites associated with Kimmeridgian to Early Tithonian emergence, and

¹ University of Zagreb, Faculty of Mining, Geology and Petroleum Engineering, Pierottijeva 6, HR-10000 Zagreb, Croatia (gdurn@rgn.hr)

² University of Natural Resources and Applied Life Sciences, Department of Applied Geology, Peter Jordan Strasse 70, A-1190 Vienna, Austria

³ Eötvös Loránd University, Dept. of Applied & Environmental Geology, Pázmány Péter sétány 1/c, 1117 Budapest XI, Hungary

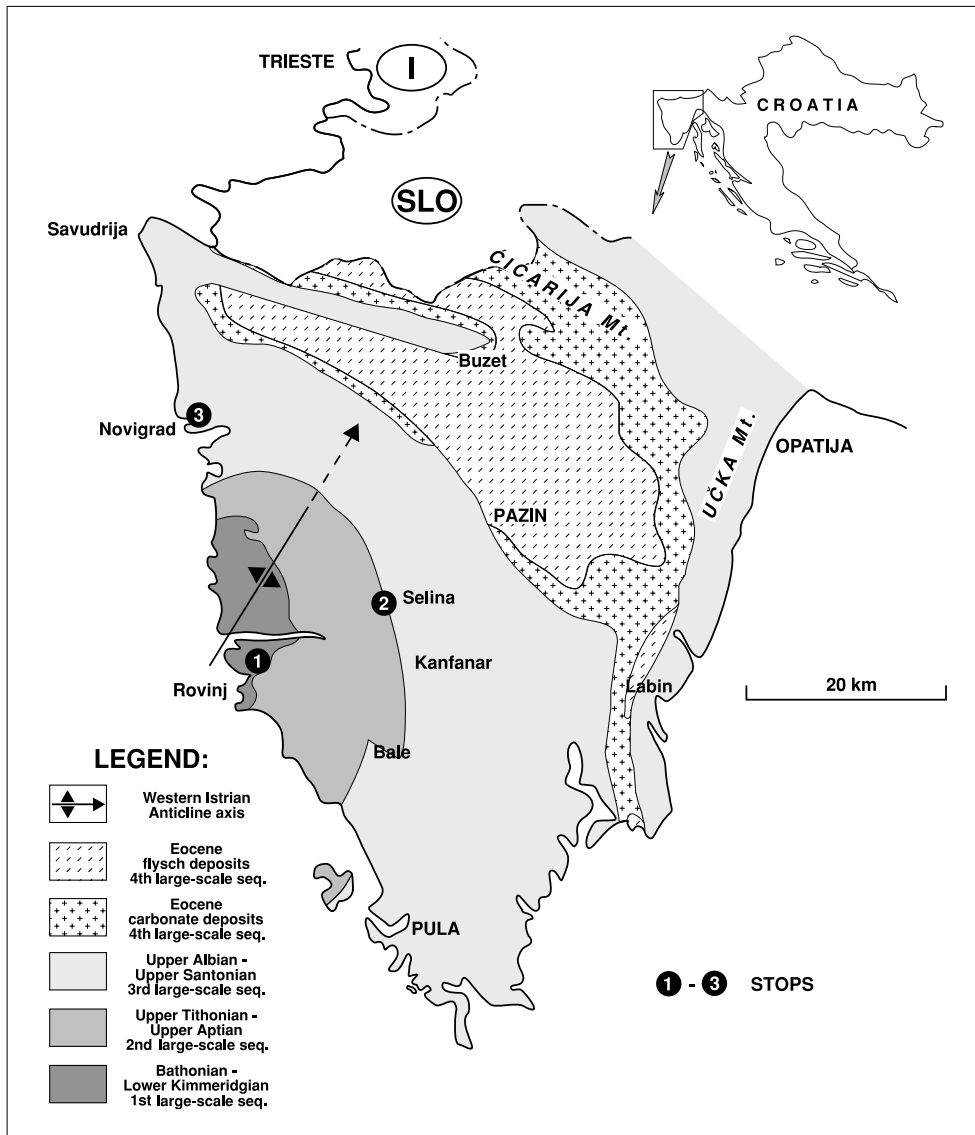


Fig. 1 Map showing the schematic distribution of large-scale sequences in Istria and location of the Western Istrian anticline (partly modified after VELIĆ et al., 1995a), with locations of the field trip stops.

(2) greenish–gray clays associated with Late Aptian–Late Albian regional emergence and relict polygenetic *terra rossa* soil.

2. JURASSIC BAUXITES

2.1. Introduction

Bauxites are humid tropical weathering products, similar to ferrallitic soils, the formation of which requires lengthy (>1 MY) subaerial exposure. The occurrence of bauxites is therefore generally considered as an indication of great periods of exposure and a hot humid climate. According to BÁRDOSSY & DERCOURT (1990), D'ARGENIO & MINDSZENTY (1991, 1992, 1995), MINDSZENTY & D'ARGENIO (1994) and COMBES & BÁRDOSSY (1994), subaerial exposure conducive to bauxitization is almost always the result of tectonically controlled uplift and the associated relative sea-level fall (which may or may not be coincident with a lower order eustatic event). As to the possible tectonic settings, three major cases are considered (D'ARGENIO & MINDSZENTY, 1995): (1) collisional settings, on the exposed/eroded tops of nappe-stacks or on

flexural fore-bulges, (2) in passive plate interior settings affected by the change of intraplate stress, and (3) in strike-slip affected sectors at places of transpression-related uplift or on the tip of fault-bounded blocks (Fig. 3). In this excursion, one of three major settings will be presented: the Rovinj–1 bauxite deposit of Jurassic age is considered that of a passive plate interior under interplate stress (Type 2 sensu D'ARGENIO & MINDSZENTY, 1995).

2.2. Stop 1: Late Kimmeridgian–Early Tithonian emersion with bauxite deposit (Bauxite Pit near Rovinj, western Istria)

2.2.1. General framework

Although the likely palaeogeographic position of Istria in the Late Jurassic period was well within the inter-tropical belt (according to CHANNELL, 1996; STAMPFLI & MOSAR, 1999), the mechanism which resulted in the sufficiently lengthy exposure deserves attention, since it apparently counteracted the uniform thermal subsidence considered to be characteristic of most Jurassic Periadriatic carbonate platforms (e.g. BERNOULLI, 2001). The bauxitiferous unconformity of Rovinj, indicates that in the Kim-

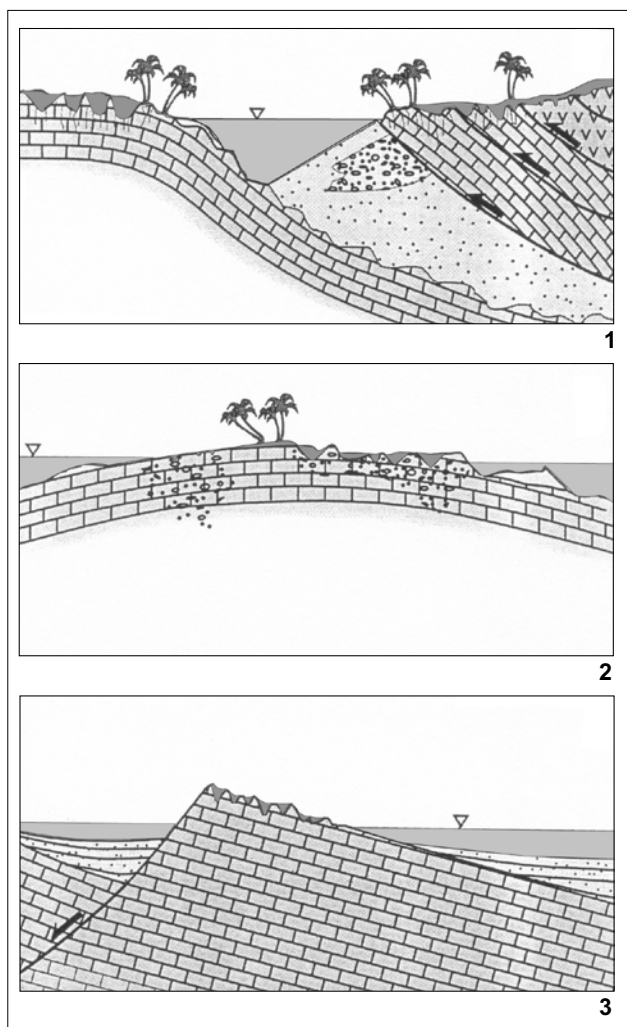


Fig. 3 Diagram showing three principal types of bauxites (after MINDSZENTY & D'ARGENIO, 1994). For explanation see text.

meridgian to the Tithonian, the subsidence of the Istrian part of the Adriatic Carbonate Platform domain was interrupted for some reason. Considering the Jurassic palaeo-position of Istria (e.g. on the palaeogeographic maps of DERCOURT et al. 1986; MANATSCHAL & BERNOULLI, 1998 or STAMPFLI & MOSAR, 1999), it is very likely that the tectonic setting of the Rovinj bauxite is that of a passive plate interior under intraplate stress (Type 2): on all three maps the Istrian peninsula plots close to the northern tip of, but still clearly within the Apulian Promontory (or Adria Microplate) (Fig. 4). Ongoing closure of the Vardar ocean along the distant eastern margins of the Apulian Promontory may have been responsible for intraplate stress generating gentle deformation in the Adriatic sector, resulting in exposure and bauxite formation. The associated relatively short stratigraphic gap (about 6 MY), lack of an appreciable angular unconformity between the bauxite, its bedrock and cover, and the fact that there is no abrupt facies change across the unconformity, (platform-type sedimentation continues apparently unchanged after the subaerial event) all reinforce the idea that the bauxite of Rovinj belongs to the aforementioned Type 2.

It should be noted that the Rovinj-1 deposit is not an isolated bauxite occurrence. According to BÁRDOSSY (1982), ŠINKOVEC & SAKAČ (1991), and others, in late Jurassic times, roughly contemporaneous bauxites, fossilized by Kimmeridgian to Tithonian shallow water carbonate sediments, occur at several localities within Greater Apulia (Fig. 5). From Greece through Montenegro to Slovenia (Amorgos, Parnass, Euboea, Viduša, Prokletije, Hrušica etc.), smaller or larger occurrences testify that this event of gentle deformation, though probably not strictly contemporaneous and of varying intensity, was of regional significance. Instead of having been restricted to the Adriatic sector, it also affected the Adriatic Carbonate Platform and seems to correlate very well with karst bauxite deposits as far south as the Hellenides or the attached shelf of the African craton (the bauxite of Mte Gallo/Sicily – Di STEFANO et al., 2002).

2.2.2. Geological setting and sedimentological characteristics below and above the Late Kimmeridgian–Early Tithonian emersion surface in the Rovinj-1 bauxite deposit

At Stop 1 within the Rovinj-1 bauxite deposit we will see the end of the Late Kimmeridgian–Early Tithonian emersion bauxite deposit and the beginning of the Late Tithonian–Late Aptian large-scale sequence (2nd large-scale sequence on Figs. 2 and 6). The Bathonian–Early Kimmeridgian sequence is approximately 200 m thick, and is characterized by shallowing- and coarsening-upward trends. It is terminated either by the Kimmeridgian–Early Tithonian emersion with bauxite deposits, or with erosion and emersion breccia. Carbonate deposits of this lengthy sequence are divided into three units (TIŠLJAR & VELIĆ, 1987; VELIĆ & TIŠLJAR, 1988): (1) “*Monsena unit*”; (2) “*Lim unit*” and (3) “*Muča unit*” (Fig. 6).

Monsena unit (“*Monsena micrites*”) contains well-bedded foraminiferal wackestones to mudstones and fossiliferous wackestones, and rarely oncolite floatstones, deposited in the shallow subtidal lagoon and/or in restricted shallows. Debris of molluscs, hydrozoans and echinoderms drifted sporadically into environments where mud deposition predominated. The biofacies is characterized by benthic foraminiferal assemblages, which indicate a Bathonian age and, from the sequence of superposition, a Callovian age.

Lim unit (Oxfordian “*Lim pelletal limestones*”) is composed of thick-bedded and massive fine-grained pelletal packstone/wackestones deposited in low-energy subtidal environments. On the basis of the fossil association these deposits are attributed to the lower parts of the Upper Jurassic, i.e. to the Oxfordian and Lower Kimmeridgian (*Salpingoporella sellii* zone).

Muča unit (Oxfordian “*Ooid and bioclastic limestones*”) is the lateral counterpart of the *Lim unit*. The main lithofacies characteristic of the *Muča unit* is rhythmical alternation, i.e. cyclic deposition of three limestone types:

(a) *Peloidal and skeletal wackestones* deposited in a shallow subtidal environment under low energy conditions;

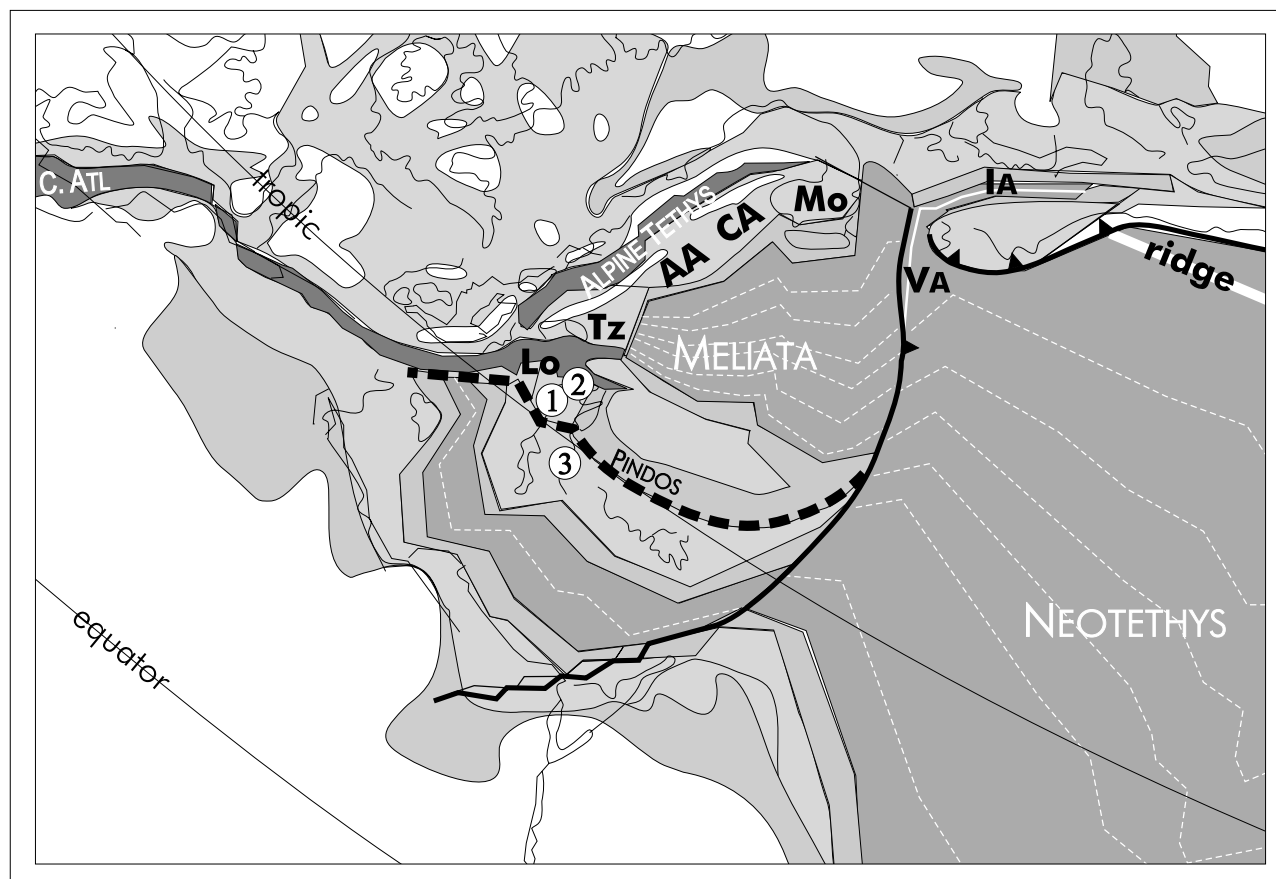


Fig. 4 The palaeographic map of the Sinemurian (after STAMPFLI & MOSAR, 1999), with the position of Jurassic bauxites in Istria (1), Slovenia (2) and Herzegovina and Montenegro (3). Locations of the bauxites after BARDOSSY & DERCOURT (1990), slightly modified.

- (b) *Oolitic grainstones with cross-bedding* deposited on a tidal bar under a predominantly tidal influence, and
- (c) *Thick-bedded oolitic grainstones and bioclastic rudstones* composed of coarse hydrozoans, corals, and mollusc bioclasts (cortoids), foraminiferal tests and *Cladocoropsis* and other stromatoporoid debris.

The biofacies of the *Muča unit* is characterized by different groups of organisms, especially in the *b* and *c* members. The most frequent components of the *c* member are reef-builders (corals, hydrozoans and other stromatoporoids), echinoderms, molluscs and foraminifera. Thickening-upward and coarsening-upward cycles were produced by migration of coarse-grained biodetritus. These deposits were produced by the disintegration of reefs during storm events and deposited in high-energy conditions in the form of prograding tidal-bar facies (TIŠLJAR & VELIĆ, 1987). On the basis of the fossil association these deposits are, like their lateral counterpart – *Lim unit* – attributed to the lower parts of the Upper Jurassic – to the Oxfordian and Lower Kimmeridgian.

Lowermost part of the *Kirmenjak unit* above the underlying bauxite is characterized by an oscillating transgression (Figs. 6 and 7). It represents the first part of the second transgressive–regressive large-scale sequence of Jurassic–Cretaceous shallow-water carbonates of western and southern Istria (Figs. 2 and 6). The lower part of the *Kirmenjak unit* represents (after TIŠLJAR, 1986, and

TIŠLJAR et al., 1995) shallowing-upward cycles composed of three members (Fig. 6):

- (a) a thin, laterally variable bed of black-pebble breccia with carbonate, clayey or marly matrix. This member was formed by the redeposition of material originating from marsh deposits, enriched in organic matter, which was eroded and transported by storm activity over the black, supratidal and upper intertidal, oxygen-deficient, brackish and/or partly freshwater deposits, during a relative sea-level rise. They occur as fragments of intertidal or subtidal black-pebbles (breccia and conglomerates), partly in the form of tidal channel fills (TIŠLJAR, 1986);
- (b) a thick-bedded (100 to 200 cm) stylolitized mudstone with rare bioclasts of *Clypeina jurassica* FAVRE, *Salpingoporella annulata* CAROZZI, and *Campbelliella striata* (CAROZZI). In some of the cycles the upper part is characterized by vertical bioturbation, fenestral fabric, desiccation cracks and erosion surfaces. This member was deposited in a low-energy subtidal to low intertidal environment;
- (c) in this part of the *Kirmenjak unit* the third member is not always present (it is typical of the middle and upper parts of the unit); it is characterized by variable lithology and textures including vadose fabrics, intraclasts with pisoid coatings, and in places by brackish to freshwater(?) stromatolites. The upper bedding surfaces are sharp, irregular with desiccation cracks and/or erosion

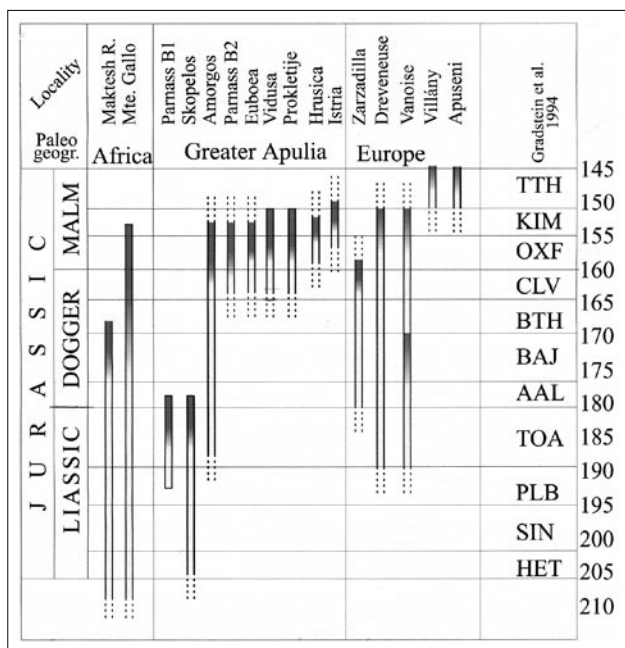


Fig. 5 Stratigraphic position of Jurassic bauxites. Data from BARDOSSY (1982), BARDOSSY & DER COURT (1990), BORDEA & MANTEA (1991), COMBES (1990), DI STEFANO et al. (2002), DUDICH & MINDSZENTY (1984), ELLENBERGER (1955), FERLA & BOMMARITO (1988), MOLINA et al. (1991), NICHITTA (1988), ŠINKOVEC & SAKAČ (1991), SIMMONE et al. (1991), RADOJČIĆ (1982), TIŠLJAR et al. (1995), VERA et al. (1988).

features. This member was formed in an intertidal and/or vadose zone.

For more information on the palaeogeographical and sedimentological characteristics below and above the Kimmeridgian–Early Tithonian emersion surface in the western Istria see VLAHOVIĆ et al. (2003).

2.2.3. Bauxite and immediate cover

The Rovinj bauxite occurs at the contact of Upper Oxfordian–Lower Kimmeridgian and Upper Tithonian strata in an apparent stratigraphic gap of relatively short duration (about 6 MY) (Fig. 6). There is no noticeable angular unconformity associated with the erosion surface. According to TIŠLJAR et al. (1995, see Fig. 6), the subaerial phase is supposed to have lasted from the latest Oxfordian/earliest Kimmeridgian to the Middle Tithonian. Palaeokarstified thick-bedded ooid grainstones and bioclastic rudstones (*Muča unit*) are exposed in the bauxite pit, interrupted by the subaerial unconformity associated with bauxites. They are overlain by the *Kirmenjak unit* consisting of clay, breccia and mudstone followed by black-pebble breccia, stylolitized mudstone and fenestral mudstone. The uneven karstic surface of the bedrock contains medium-size (2.0 to 2.5 m high) sub-soil pinnacles exposed by mining activity. Closer examination of the bedrock reveals evidence of several superimposed phases of dissolution, brecciation and cementation.

The bauxite deposit is about 400 m long and 300 m wide and its thickness decreases gradually from 20 m to 0 m towards the margin of the deposit (ŠINKOVEC, 1974). The bauxite is red in colour, muddy (pelitomorphic) with

occasional round grains, and small ooliths. On the outcrop scale it is massive and shows a characteristic nodular to spheroidal parting. Joint surfaces are coated by Mn-oxide and/or kaolinite. The quality of the ore is medium to poor. It is highly argillaceous; the alumina to silica ratio is just above 2.6, with alumina around 46% and silica above 15% (ŠINKOVEC, 1974). Major minerals are boehmite, kaolinite, haematite, anatase and minor chlorite. Extraclasts identified by ŠINKOVEC (1974) include rare zircon, tourmaline and apatite grains, which testify to the relative isolation of the depositional environment from the non-carbonatic surroundings. As a possible source material, the dissolution residue of the host carbonates, plus windblown dust is proposed by ŠINKOVEC & SAKAČ (1991), whereas VLAHOVIĆ et al. (2000) put forward the idea of an additional fine-grained volcanoclastic contribution.

The uppermost 20–30 cm of the bauxite is heavily altered: its colour is greenish–grey to yellowish–white with vertical to subvertical extensions penetrating the underlying deep red bauxite (Fig. 7). The alteration having affected the iron-minerals is clearly of a redox nature and is closely related to the environmental change associated with the deposition of the cover-beds. After the long subaerial period, when bauxite has accumulated and partly even passed the early stages of diagenesis under vadose meteoric conditions, relative sea-level rise induced an obvious hydrological change. Leaching throughflow must have effectively ceased, pores became saturated first by freshwater then by seawater, and, as a result of microbial destruction of organic matter, (living plants or plant-litter), all free oxygen was extracted from the pores. Ongoing plant destruction under stagnant, oxygen-poor conditions resulted in what soil scientists call “gleying” – the characteristic patchy iron-removal around roots and other plant residue. Later on, interaction with saline pore-waters may have resulted in the formation of fine-grained pyrite. Deferrified veins with traces of organic matter, observed at the top of the bauxite, are interpreted as an effect of root activity. Namely, they probably represent the remains of roots from the soil which may have developed on the top of bauxite in an already marshy/brackish environment.

2.2.3.1. The “blue hole” sequence

Above the altered bauxite the lowermost part of the cover records the establishment of a palustrine–lacustrine environment with greyish, organic-rich marl and brecciated limestone, characterized by a very restricted fauna, (mainly ostracods according to VLAHOVIĆ et al., 2000), and probably representing a freshwater pond, formed as the groundwater table was pushed upwards by seawater rising through karstic channels from below. According to VLAHOVIĆ (1999) in the wider surroundings of the quarry, this basal layer shows considerable facies diversity reflecting the dissected karst topography resulting from the preceding lengthy subaerial episode. An analogous situation was described in detail by CARANNANTE et al. (1994) from above Cretaceous bauxites of Southern Italy, where the change from freshwater to the eventual fully marine environment, with intervening schizohaline episodes was documented by faunal changes, sedimentary struc-

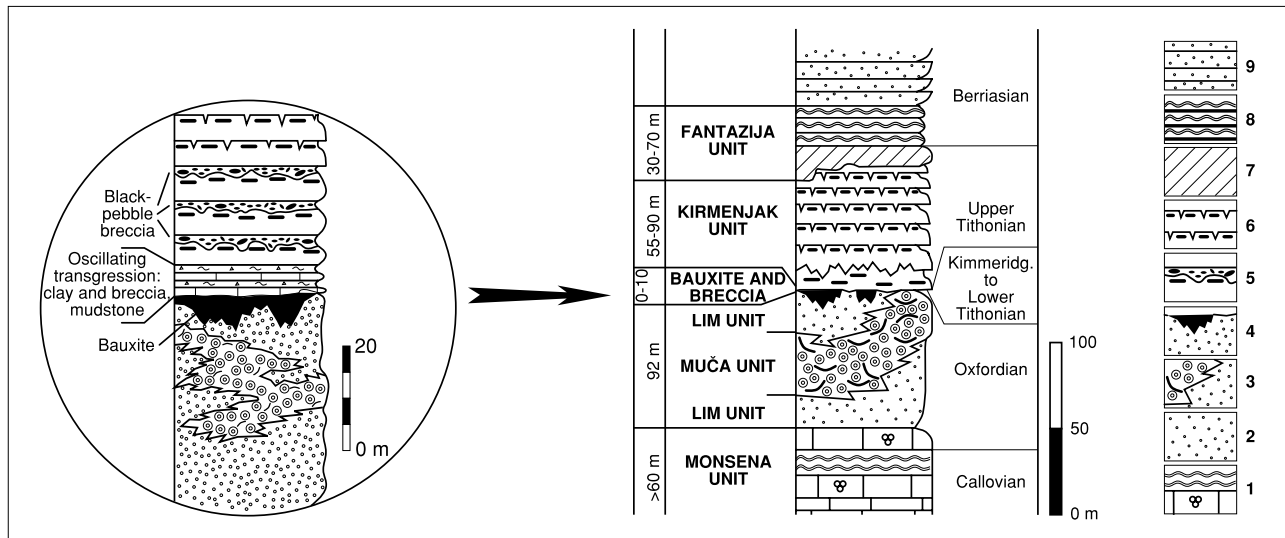


Fig. 6 Schematic geological column of Jurassic and older Lower Cretaceous deposits of western Istria with the location of stop 1 and details of emersions with bauxite deposits (after TIŠLJAR et al., 1994, partly modified according to lithostratigraphic units from VELIĆ & TIŠLJAR, 1988). Legend: 1) *Monsena unit*: well-bedded foraminiferal wackestone/mudstones (low-energy subtidal or lagoon); 2) *Lim unit*: thick-bedded and massive fine-grained pelletal packstone/wackestones (low-energy subtidal), with its lateral counterpart *Muča unit*; 3) *Muča unit*: thick-bedded ooid grainstones and bioclastic rudstones composed of ooids and bioclasts of bryozoans, corals, stromatoporoids and foraminifera (high-energy tidal-bar facies); 4) *Rovinj unit*: regressive breccia and bauxite (formed during a long-lasting emersion phase); 5) Lowermost part of the *Kirmenjak unit*: alternation of clay, breccia and mudstone (deposits of an oscillating transgression); 6) Lower part of the *Kirmenjak unit*: peritidal shallowing-upward cycles consisting mostly of black-pebble breccia, stylolitic mudstone and fenestral mudstone with erosion surfaces or desiccation cracks, frequently capped by storm-tide deposits with vadose diagenesis; 7) Late-diagenetic dolomites (= dolomitised limestones of the *Kirmenjak unit*); 8) *Fantazija dolomites*: shallowing-upward cycles consisting mostly of late-diagenetically dolomitised subtidal-intertidal deposits and supratidal early-diagenetic dolomites capped by fenestral stromatolites, desiccation cracks and erosion surfaces; 9) Berriasian shallowing-upward cycles consisting mostly of pelletal wackestones and *Favreina* packstone/grainstones and/or LLH stromatolites.

tures and diagenetic features. Based on the striking similarity with a Pleistocene/Holocene scenario described by RASMUSSEN & NEUMANN (1988) from the Bahamas, they compared the establishment of freshwater ponds on top of the bauxite-filled karst terrain to the establishment of the “blue holes” of the Bahamas and introduced the term “internal transgression” as opposed to “overland transgression”. We have good reason to think that the lowermost part of the cover sequence of the Rovinj bauxite is another

example of the filling of a karst relief from below, while higher up, shallowing-upward peritidal sequences and associated palaeosols show that after the initial “blue hole” stage, the sea encroached the whole platform, and normal marine conditions were again established.

2.2.3.2. Intercalations of green clay

Greenish–grey to yellow clay intercalations in the coverbeds may be signs of ephemeral exposure or, alternatively



Fig. 7 Bauxite deposit Rovinj–1. Contact of bauxite and first part of the second transgressive–regressive large-scale sequence of Jurassic–Cretaceous shallow-water carbonates.

represent clay influx from adjoining, slightly more highly elevated areas (still exposed when the depositional environment was already inundated).

When occurring at the top of shallowing-upward cycles and displaying associated dissolution phenomena, they are claimed to be signs of ephemeral exposure. It is worth noticing that the distribution of cm-sized palaeokarstic cavities seems to have been controlled by the pre-existing burrows of benthic organisms (or alternatively by roots of aquatic plants) having affected the muddy sediment while it was still soft. Differential hardening on exposure has fossilized these structures, which later became filled by clay washed in from the thin argillaceous soil blanket above, and cemented by calcite during the later stages of burial. Embedded in the green clay, corroded limestone fragments (occasionally also black pebbles) are interpreted as a dissolution breccia accumulated on the exposed surface.

When clay intercalations occur without accompanying palaeokarst features, they were possibly introduced to the depositional environment from external sources. The most plausible source would be the redeposited material of the bauxitic blanket covering adjoining slightly more highly elevated (and therefore not yet inundated) areas. Though no detailed mineralogical data on this material are available as yet, it is highly possible that early diagenesis in the lagoonal submarine environment would have substantially altered the bauxitic clay.

2.2.3.3. Chemical and mineralogical composition of bauxite and the lowermost part of the immediate cover

For the purpose of this fieldtrip, seven samples for chemical and mineralogical analyses were taken along a profile situated in the uppermost part of the bauxite and the lowermost part of the immediate cover (Fig. 8, Table 1). The uppermost sample analysed is situated 90 cm above the grey bauxite and represents a greenish-grey clay. Immediately above this sample there is a coarse brecciated zone, infilled with greenish-grey clay which probably represents a dissolution breccia accumulated on the exposed surface.

The chemical analyses were performed after LiBO₂ fusion with ICP-ES (major elements) and ICP-MS (trace elements). REE were analysed with ICP-MS. A semi-quantitative mineral composition was calculated from XRD, TG, FTIR and ICP-ES data.

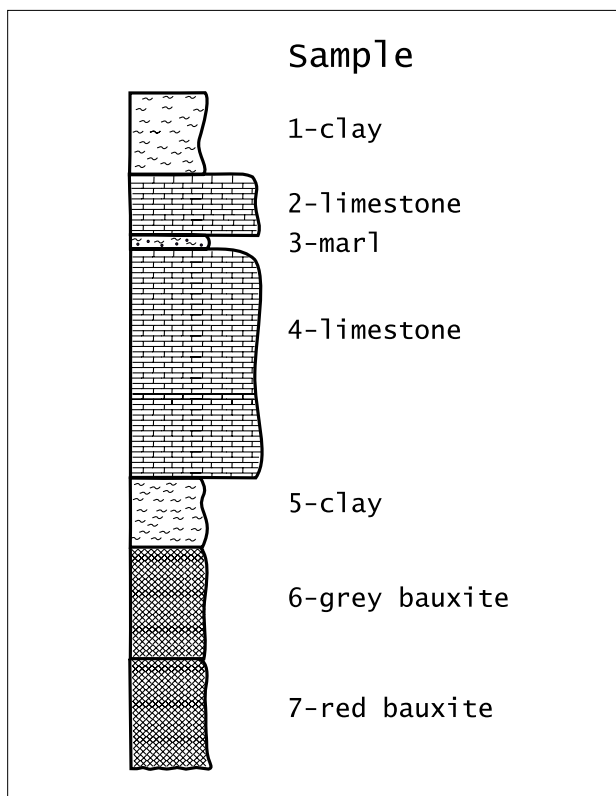


Fig. 8 Bauxite deposit Rovinj-1. Profile situated in the uppermost part of the bauxite and the lowermost part of the immediate cover.

2.2.3.3.1. Bauxite

The dominant mineral phases in both red and grey bauxite are kaolinite and boehmite (Table 2). The main iron-bearing phase in red bauxite is haematite and in grey bauxite pyrite. Both bauxites also contain chlorite and mixed-layer chlorite/vermiculite/illite (Tables 2 and 3). Compared to the red bauxite, grey bauxite is depleted in iron and arsenic, and, at the same time, enriched in sulphur (Table 4), and slightly enriched in cobalt, copper, zinc and lead (Table 5), i.e. in elements which have a general tendency to accumulate under reducing conditions. The mineralogy of the iron-bearing phases and the chemical composition, clearly indicates that red bauxites were deposited under oxidizing conditions (*vadose bauxites*), while grey bauxite (at the top of red bauxite), formed in a reducing environment as a result of hydrological change due to deposition of the coverbeds. Consequently, grey bauxite at the top of a

Sample	Description	Thickness	Munsell colour
1	clay	20 cm	greenish grey (6/1 for clay 1)
2	limestone (ostracod wackestone)	15 cm	-
3	marl	3 cm	yellow (2.5Y 7/6)
4	limestone (pyritized peloid-ostracod packstone)	55 cm	-
5	clay	17 cm	yellow (10YR 7/8)
6	grey bauxite	28 cm	greenish grey (6/1 for clay 1)
7	red bauxite	>800 cm	weak red red (10R 4/4)

Table 1 Bauxite deposit Rovinj-1. Description of profile situated in the uppermost part of the bauxite and lowermost part of the immediate cover.

	Kaolinite	Boehmite	Goethite	Haematite	Pyrite	Calcite	Other clay minerals
1	50	–	–	–	7	–	43
2	n.a.	n.a.	n.a.	n.a.	n.a.	n.a.	n.a.
3	20	–	4	–	–	40	36
4	n.a.	n.a.	n.a.	n.a.	n.a.	n.a.	n.a.
5	46	5	8	–	–	–	41
6	40	38	–	–	6	–	16
7	34	37	–	18	–	–	11

Table 2 Semiquantitative mineral composition of bauxites, clays and marl. Legend: n.a.) not analysed. For sample description see Table 1.

	Kaolinite	Illitic material	Mixed layer chlorite/ vermiculite/illite	Chlorite
1	+++	traces	++	++
2	n.a.	n.a.	n.a.	n.a.
3	++	++	+	+
4	n.a.	n.a.	n.a.	n.a.
5	+++	traces	++	++
6	++	–	+	+
7	++	–	+	+

Table 3 Clay mineral composition of the <2 µm fraction of bauxites, clays and marl. Legend: +++ dominant; ++ abundant; + minor; n.a.) not analysed. For sample description see Table 1.

red one can be considered *phreatic bauxite*. This is also supported by the distribution of REE (Figs. 9 and 10). The total REE content is 376.35 ppm in red and 261.76 ppm in grey bauxite. The $(La/Yb)_{CH}$ ratio in grey bauxite (6.36) is lower than that in red bauxite (8.50), and significantly lower than that of ES indicating HREE enrichment relative to LREE. Enrichment of HREE in grey bauxite is the result of the higher mobility of LREE in acidic reducing conditions.

Since chlorite is present in similar amounts in red and grey bauxite, its origin cannot be related solely to the reducing processes which affected the top of the red bauxite

and converted it to grey bauxite, but also to burial diagenesis. It is interesting to note that ŠINKOVEC (1974) observed that the appearance of chlorite in both red and grey bauxite is similar. For more about chlorite and mixed-layer chlorite/vermiculite/illite, which was also detected in both bauxites, see the next section.

2.2.3.3.2. Lowermost part of the immediate cover

The immediate cover of grey bauxite is yellow clay (Fig. 8 and Table 1) which can be traced as a layer of variable thickness (up to 30 cm) within the area of the whole de-

	SiO ₂ %	Al ₂ O ₃ %	Fe ₂ O ₃ %	MgO %	CaO %	Na ₂ O %	K ₂ O %	TiO ₂ %	P ₂ O ₅ %	MnO %	LOI %	TOTS %
1	40.15	29.89	6.08	1.89	1.09	0.09	2.43	1.54	0.02	0.02	16.6	3.70
2	n.a.	n.a.	n.a.	n.a.	n.a.	n.a.	n.a.	n.a.	n.a.	n.a.	n.a.	n.a.
3	26.24	15.99	4.98	1.97	21.76	0.04	2.66	0.79	0.02	0.07	25.2	0.06
4	n.a.	n.a.	n.a.	n.a.	n.a.	n.a.	n.a.	n.a.	n.a.	n.a.	n.a.	n.a.
5	37.20	32.18	8.04	2.08	0.62	0.09	1.81	1.50	0.04	0.02	15.9	0.09
6	22.58	50.15	5.55	0.66	0.12	0.06	0.30	2.42	0.03	0.06	17.9	3.38
7	18.87	46.89	18.22	0.60	0.16	0.05	0.25	2.20	0.04	0.14	12.3	0.07

Table 4 Chemical composition (major elements) of bauxites, clays and marl (in wt.%). Legend: n.a.) not analysed; TOTS) total sulphur. For sample description see Table 1.

	Co ppm	U ppm	Ba ppm	Ni ppm	Cu ppm	Pb ppm	Zn ppm	As ppm
1	36.4	27.0	169	146	24.8	23.3	145	14.5
2	n.a.	n.a.	n.a.	n.a.	n.a.	n.a.	n.a.	n.a.
3	78.8	9.1	108	99	18.4	21.7	153	41.0
4	n.a.	n.a.	n.a.	n.a.	n.a.	n.a.	n.a.	n.a.
5	283.0	4.9	129	315	222.9	223.3	714	34.7
6	136.5	6.9	46	244	15.3	124.3	107	1.2
7	27.6	5.3	47	205	6.2	72.5	96	5.6

Table 5 Chemical composition (trace elements) of bauxites, clays and marl (in ppm). Legend: n.a.) not analysed. For sample description see Table 1.

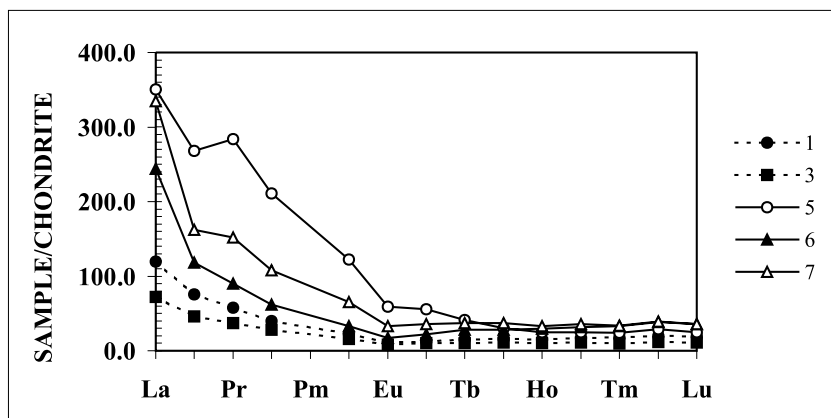


Fig. 9 Chondrite-normalized REE patterns of bauxites, clays and marl.

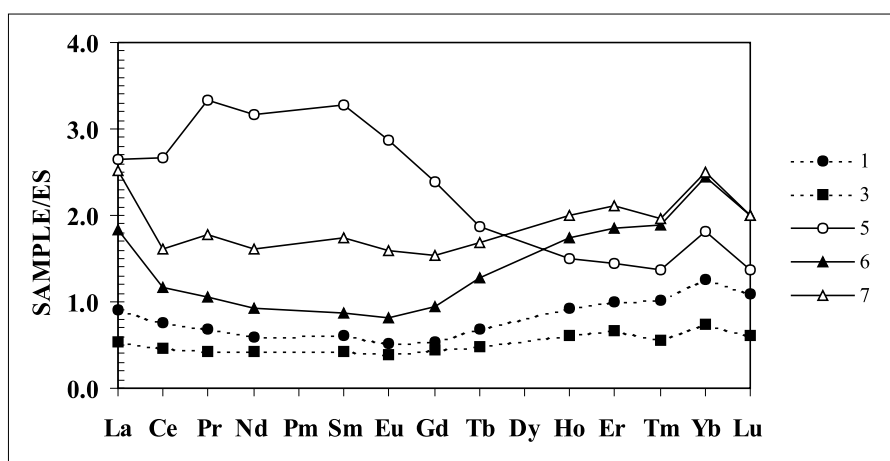


Fig. 10 European shale-normalized REE patterns of bauxites, clays and marl.

posit. The interesting point is its predominantly kaolinitic composition with boehmite as a minor phase (Table 2). The clay fraction is dominated by kaolinite, while chlorite and mixed-layer chlorite/vermiculite/illite are present in similar amounts as subordinate phases, and illitic material as traces (Table 3). This clay is especially enriched in Co, Ba, Ni, Cu, Pb, Zn, As (Table 5) and REE (the total REE content is 555.48 ppm). The chondrite normalized patterns and especially ES normalized patterns show that this clay is enriched in LREE and MREE, which can be an indication of repeated cycles of oxidation and reduction (Figs. 9 and 10). We tentatively propose that this clay represents redeposited material introduced to the depositional environment from the kaolinitic and bauxitic blanket covering adjoining slightly higher elevated areas. This clay is overlain by pyritized peloid/ostracod packstone and marl (Fig. 8, Table 1), which probably formed in a freshwater pond. The main mineral phase in marl is calcite (Table 2), while the clay fraction is dominated by illitic material and kaolinite, but chlorite and mixed-layer chlorite/vermiculite/illite are present in similar amounts as minor phases (Table 3). A high potassium content (Table 4), and, consequently, a high content of illitic material in this marl may be interpreted in two ways: either the external source of material supply altered (higher potassium input; e.g. K-feldspar, mica, illite), or weathering trends on land changed from *sialitization* (formation of kaolinite) and *allitization* (formation of Al-hydroxides) to *bisialitization* (formation of 2:1 clay minerals), as a consequence of climate change. A

low value for the $(La/Yb)_{ch}$ ratio in the marl (6.16) indicates HREE enrichment relative to LREE (Fig. 10) and may suggest formation under acidic and reducing conditions. The marl is overlain by an ostracod-bearing wackestone, which, in turn, is covered with greenish-grey kaolinitic clay containing pyrite (Fig. 8, Tables 1 and 2). Immediately above this clay there follows a coarse brecciated zone infilled with greenish-grey clay, which probably represents a dissolution breccia accumulated on the exposed surface.

The clay fraction is dominated by kaolinite, while chlorite and mixed-layer chlorite/vermiculite/illite are present in similar amounts as subordinate phases and illitic material as traces, i.e. the clay mineral composition is very similar to that of the clay overlying the grey bauxite (Table 3). The colour of the clay and the presence of pyrite framboids may imply that this clay was affected by hydromorphic pedogenic processes related to ephemeral exposure and represents a kind of a marshy soil. This is supported by its high U content (Table 5) and low $(La/Yb)_{ch}$ ratio (6.07). The mineralogical and chemical data support the “blue-hole” sequence story.

A few more words concerning the mineralogy of the clay fraction of the analysed samples.

Kaolinite

According to FTIR measurements it shows most properties of a poorly crystallized kaolinite (almost no absorption around 3670 nm). This is consistent with very low dehydroxylation temperatures ($\sim 550^\circ\text{C}$) and a low exothermal

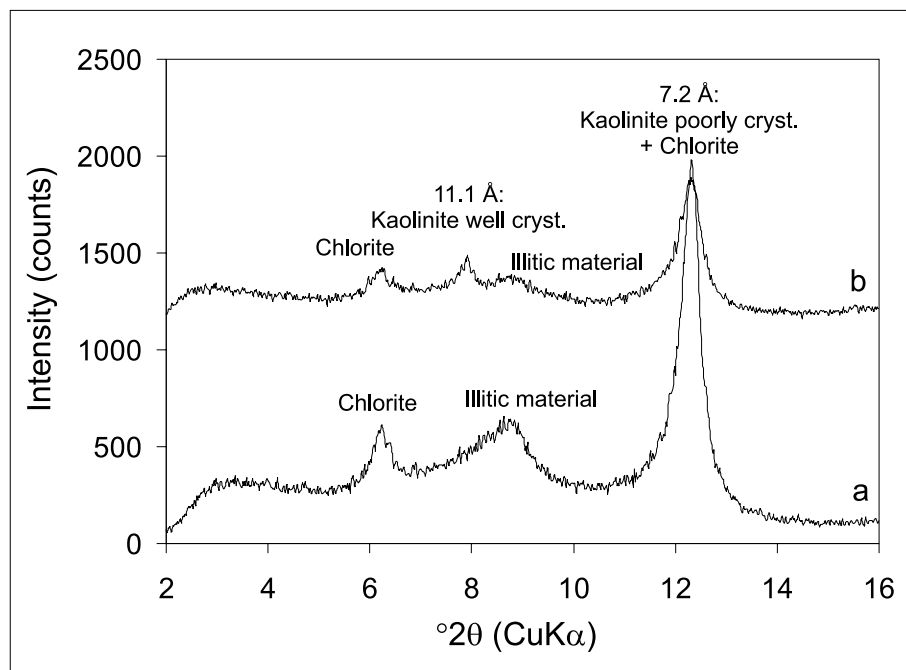


Fig. 11 Characteristic parts of XRD patterns of clay sample 1 (<2 μm fraction): (a) air dried; (b) K-saturated and DMSO-solvated.

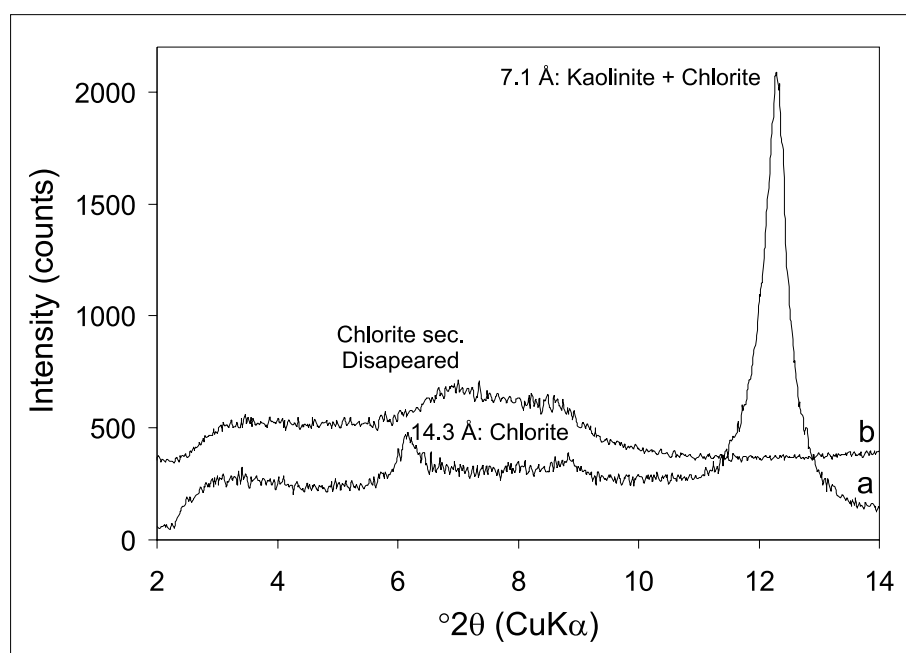


Fig. 12 Characteristic parts of XRD patterns of clay sample 5 (<2 μm fraction): (a) air dried; (b) Heated for one hour at 550°C.

reaction (950°C) in thermoanalysis. After treatment with DMSO and measurement by XRD, different amounts of well-crystallized kaolinite react by swelling (10 to 50%), but the rest of the kaolinite does not react, which means that it is poorly crystallized (Fig. 11).

Chlorite

All samples contain various amounts of chlorite, the highest content being observed in clays (samples 1 and 5). The very strong 003 reflexion (~4.77 Å) is noticeable which is typical for Al-rich chlorites, e.g. *sudowite*. The second important fact is that chlorite is not stable against heating to 550°C (Fig. 12), which is typical for secondary chlorites (formed in moderately acidic environment).

Mixed-layer mineral

This is more or less present in all samples, particularly in clays (samples 1 and 5). However, our investigations of this mixed-layer mineral are far from being complete. Namely, we tentatively interpret this mineral as mixed-layer chlorite/vermiculite/illite because it must consist of at least 3 components:

1) *Vermiculite*: because it contracts after treatment with K to 10 Å, and we know from the thermoanalysis that high amounts of interlayer water are present in the range between 100 and 200°C, which is typical for smectites and vermiculites. The presence of vermiculite in the mixed-layer mineral is also obvious from comparison of K and Mg treated samples (Fig. 13). After treatment with K the

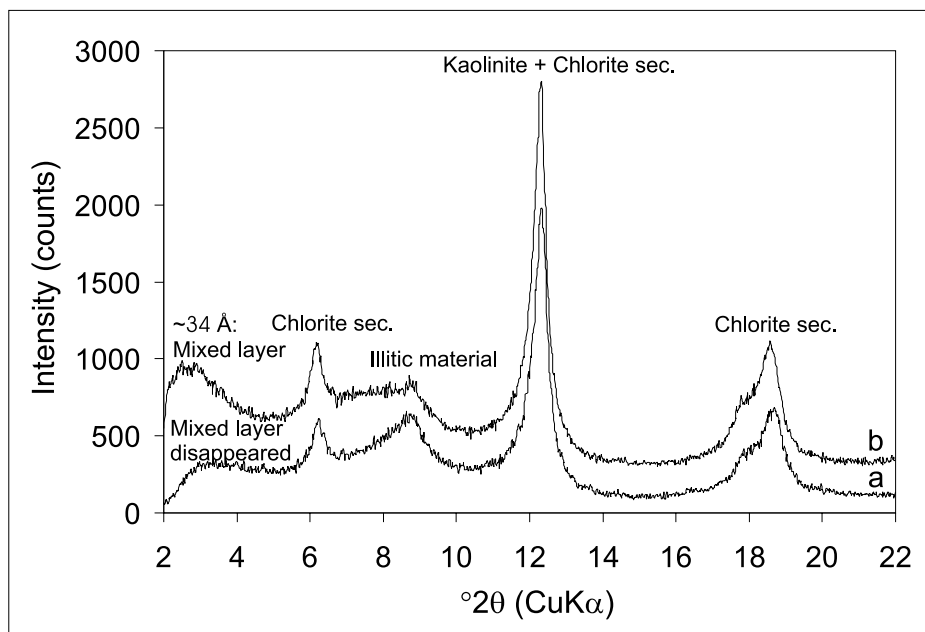


Fig. 13 Characteristic parts of XRD patterns of clay sample 1 (<2 μm fraction): (a) K-saturated; (b) Mg-saturated.

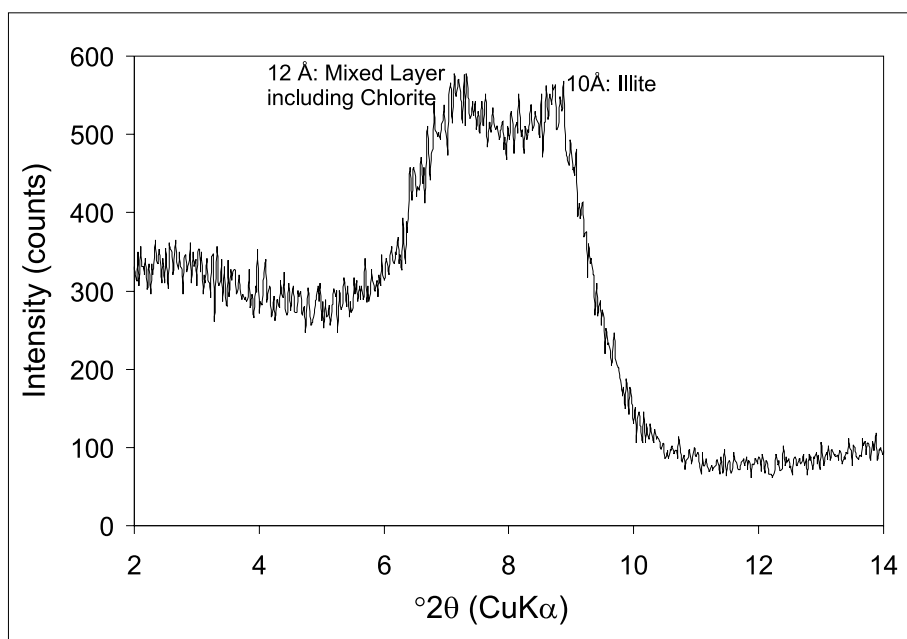


Fig. 14 Characteristic parts of XRD pattern of clay sample 1 (<2 μm fraction) heated for one hour at 550°C.

10 Å peak is much sharper (contraction of vermiculite in the mixed-layer mineral). Also, the change in the 34 Å area is caused by the vermiculite component in the mixed-layer mineral.

2) *Chlorite*: after heating to 550°C a very strong reflection appears around 12 Å, which is very typical of the 002 reflection of mixed-layer minerals containing chlorite (Fig. 14).

3) *Illitic material*: we know that K is present in relatively high amounts, no K bearing mineral other than illitic material is detected, and therefore it must occur in this mixed-layer mineral.

3. REGIONAL MIDDLE/LATE APTIAN–LATE ALBIAN EMERSION IN CENTRAL ISTRIA

3.1. General geological setting and sedimentological characteristics of the central Istrian area

At the beginning of the Aptian in the Istrian part of the Adriatic Carbonate Platform, spacious low-energy shallows and large lagoons were formed, where extensive amounts of fine carbonate detritus were deposited. The first 2–5 metres of the succession are commonly characterized by variable amounts of requieniid shells, mostly of *Toucasia* sp., and different benthic foraminifera, as well as numerous relatively large (1–8 cm) oncoids, with *Bacinella irregularis* RADOIČIĆ or gastropod shells as nuclei (=lower part of *Istarski žuti* zone).

The *Istarski žuti* zone of Lower Aptian age is characterized by rhythmic alternations of mudstone and *Bacinella*-

oncolites (i.e. oncolid floatstones), and it is yellow in colour (*Istarski žuti* = Istrian Yellow). It is subdivided into short and long rhythms (TIŠLJAR, 1978). *Short rhythms* are 25–50 cm thick, composed of layers of mudstone with rare oncolids and layers of oncolites. *Long rhythms* are 150–280 cm thick, composed of thick micrite beds (higher sedimentation rate) and a few short rhythms (lower sedimentation rate).

Bacinella-oncolids, which are typical components of the Lower Aptian limestones throughout the Dinarides, are always irregular in shape, and relatively large (mostly 5–80 mm), and are therefore sometimes referred to as “macroids”. They have encrusted *Bacinella* skeletons in the central part, surrounded by a thinner or thicker oncolid envelope. Oncolids usually comprise 40–80 vol.% of the rocks, and in some parts, where they form oncolid crusts like hardgrounds, they are practically the only rock constituents (TIŠLJAR, 1983).

Mudstones were deposited during periods of higher accumulation rates, while in periods of low accumulation rates oncolids were formed, and deposits were intensely bioturbated. The entire unit was characterized by deposition in relatively deeper environments, resulting in relative accumulation rates approximately three times lower than the average for Lower Cretaceous deposits in Istria (VLAHOVIĆ, 1999). Those deeper environments were sporadically connected with the open sea.

The thickness of the Lower Aptian oncolitic limestones is very variable, as a consequence of differences in the beginning and duration of the regional Middle/Late Aptian–Late Albian emersion on the Istrian part of the Adriatic Carbonate Platform (VELIĆ et al., 1989). Namely, the duration of the emersion phase was variable, from 11–19 MY, depending upon the palaeogeographical position of the different localities. This was caused by differential amounts of synsedimentary tectonics modifying the eustatic signal, resulting in variable levels of relative sea-level fall, erosion and karstification during the Late Aptian and Early Albian (VELIĆ et al., 1989; TIŠLJAR et al., 1995; MATIČEC et al., 1996). For example, in the area of Seline (Stop 2) and Bale, emersion started during the Middle Aptian, while in the area of Kanfanar, emersion began during the Late Aptian. Exposure-related features are represented by greenish–grey clays, mainly in palaeokarst pits and coarse brecciated regolith. Clays associated with this emersion range in thickness from several centimetres up to 1 metre. Transitional zones between the shallow-water carbonates and emergent parts of the platform were characterized by either clay and marl deposition, or extensive coastal marshes with reducing conditions and deposition of black sediments (black-pebbles) enriched in plant remains and pyrite formed by sulphate-reducing bacteria (TIŠLJAR et al., 1995). A specific characteristic of the succession in the Tri jezerca (Stop 2), Kanfanar and Bale quarries is the abundant occurrence of blackened peritidal deposits as a consequence of reducing swamp conditions.

The beginning of Late Albian deposition is characterized by an oscillating transgression, and deposition of peritidal limestones and high-energy conglomerates (TIŠLJAR et al., 1995). Within these sediments, features indicating 3

to 6 short emersions, represented mainly by coarse brecciated zones, infilled with greenish–grey and greenish–yellow clays can be observed. This oscillatory transgression gradually covered the entire Istrian area at the beginning of the Late Albian, marking the beginning of deposition of a new large-scale sequence (Fig. 2), which lasted in southern Istria until the Late Santonian (column A on Fig. 2), and in northern Istria (column B on Fig. 2) until the Late Cenomanian (VELIĆ et al., 1995a; TIŠLJAR et al., 1995).

3.2. Stop 2: Middle Aptian–Late Albian emersion phase in the Tri jezerca quarry (near Selina village, central Istria)

In the Tri jezerca quarry, near Selina village (Figs. 4 and 15), building-stone known under the name of *Istarski žuti* (Istrian Yellow) was exploited. This stone is presently exploited in a few quarries in central Istria by the “Kamen Pazin” company. It is part of the Lower Aptian massive limestones, forming the uppermost part of the second large-scale sequence over a predominant area of Istria (Fig. 2).

In the Tri jezerca quarry only the upper part, about 10 m thick, of these limestones crops out (Fig. 15). In the uppermost part there are indications of a relative sea-level fall, and the beginning of a regression phase culminating in the regional Late Aptian emersion. Besides intense vertical bioturbation, indicating lowered sedimentation rates, weakly expressed palaeokarstification effects occur. A further relative sea-level fall resulted in a clearly visible emersion with palaeokarstified relics of *Istarski žuti*, greenish–grey clays in palaeokarst pits and/or coarse brecciated regolith. This unit represents a stratigraphic gap, which started during the Middle Aptian and lasted until the beginning of the Late Albian (VELIĆ & TIŠLJAR, 1987; VELIĆ et al., 1989).

Greenish–grey clays in the Tri jezerca quarry are up to 93 cm thick, and are situated in palaeokarst pits. Morphologically, pits are conical and compound, and resemble those recognized in the Late Dinantian palaeokarst of England and Wales, where VANSTONE (1988) recognized four types of palaeokarst depression morphology. We can tentatively conclude that the morphology of palaeokarst in the Tri jezerca quarry resembles that of hummocky palaeokarstic depressions. We consider that the clays are the erosional remains of surficial soils and sediments, which were accumulated in palaeokarst pits following an oscillating marine transgression that terminated emergence. Samples of greenish–grey clay (5BG 4/1 to 10BG 6/1 – MUNSELL COLOUR CHARTS, 1994) were taken along one profile for detailed analyses (Fig. 16). A sample of limestone (*Istarski žuti*) situated immediately below the clay was also collected.

Clays are composed of phyllosilicates and pyrite (Table 6). Gypsum was detected only in the uppermost sample. The clay mineral distribution along the profile shows a clear trend (Fig. 17). The main clay mineral in the upper part is illitic material (Fig. 18). In the lower part of the profile illite values are below 50 wt.%. The second main clay mineral group are regularly ordered and randomly ordered illite/smectite mixed-layer minerals. Chlorite is sub-

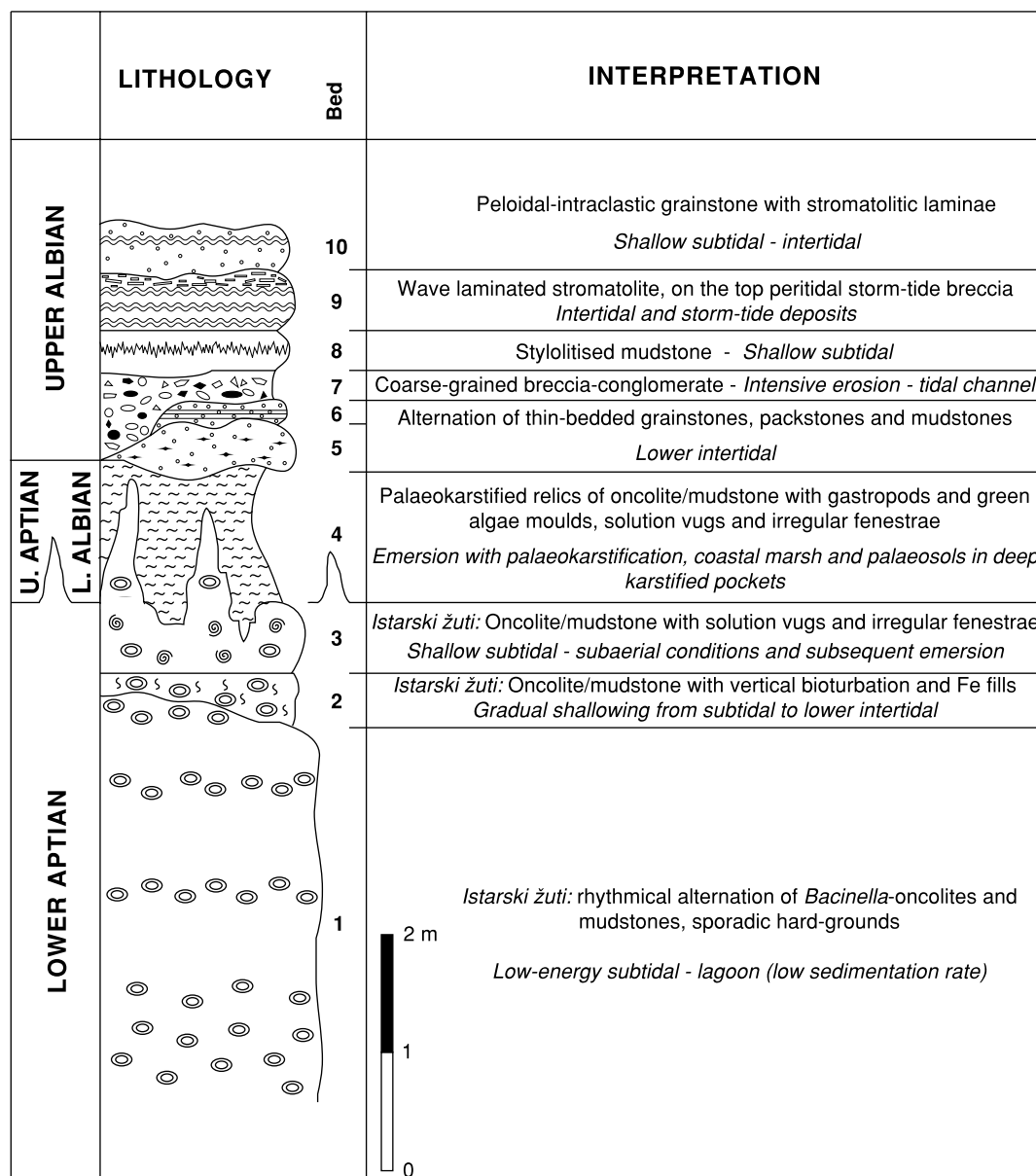


Fig. 15 Detailed geological column of the Lower Aptian *Istarski žuti* limestones, Late Aptian–Early Albian emersion with palaeokarstification and palaeosoil, and Upper Albian deposits in the Tri jezerca quarry (partly modified after TIŠLJAR et al., 1995).

		Phyllosilicates	Pyrite	Gypsum
1	0–8 cm	97	1	2
2	8–16 cm	97	3	
3	16–20 cm	98	2	
4	20–30 cm	99	1	
5	30–40 cm	99	1	
6	40–50 cm	99	1	
7	50–60 cm	99	1	
8	60–70 cm	99	1	
9	70–80 cm	99	1	
10	80–90 cm	99	1	
11	90–93 cm	99	1	
IRL		100		

Table 6 Semiquantitative mineral composition of greenish–grey clays from Tri jezerca quarry taken along a 93 cm thick profile. Sample 1 is uppermost and 11 is the lowermost sample. Legend: IRL insoluble residue of limestone (*Istarski žuti*) situated immediately bellow clay.

ordinate and present only in the lower part of the profile. The insoluble limestone residue is dominated by smectite and illitic material (Table 6 and Fig. 17). In contrast to the clays, mixed-layer minerals were not detected in the insoluble limestone residue. The higher content of illitic material in the upper part of the profile corresponds well with chemical data. Namely, the K₂O-content in the upper part is around 5 wt.% and decreases to 4 wt.% in the lower part of the profile (Fig. 19).

Lower Cretaceous deposits of Istria, characterized by shallow-marine deposition, sporadically interrupted by periods of emersion, are sedimentologically and palaeogeographically very similar to some Jurassic–Cretaceous marine carbonate sequences of NW Europe, called Purbeckian sediments. Important members of these sediments are greenish–grey marls, which form thin films between limestone beds (DECONINCK et al., 1988). According to DECONINCK & STRASSER (1987) they are characterized by a mineralogical composition of smectite–illite–kaolinite, and usually occur at the top of small



Fig. 16 Greenish-grey clays in the Trijezerca quarry. Cleaned profile prepared for detailed sampling.

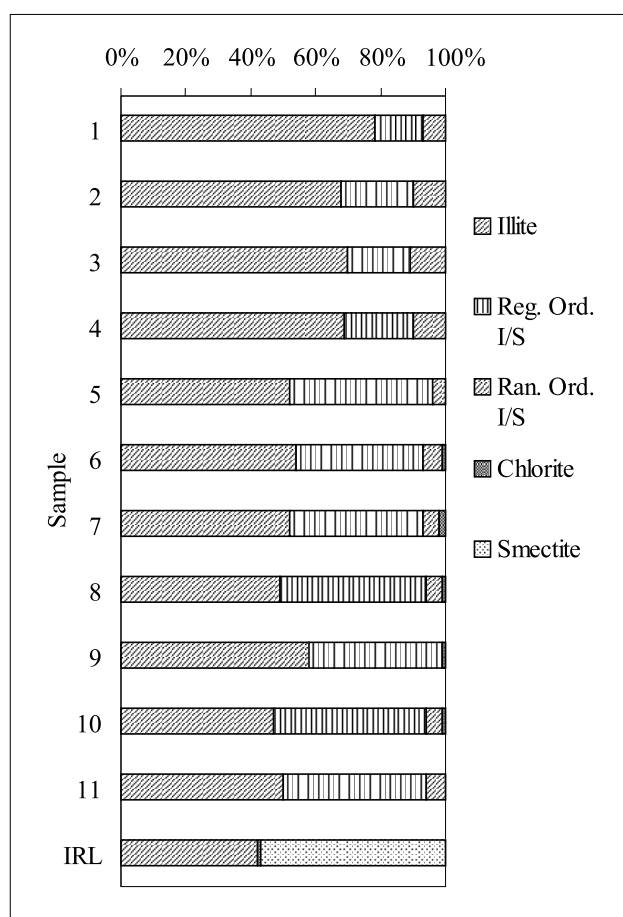


Fig. 17 Clay mineral composition of the <math><2\ \mu\text{m}</math> fraction along the profile in the Trijezerca quarry.

shallowing-upward sequences. They may also have been subaerially exposed for a long period. DECONINCK et al. (1988) noted that even in sections showing illite-rich clay-assemblages underlying formations contain smectite and kaolinite. This led them to the conclusion that the influence of burial diagenesis on the illitization of smectite seems to be negligible in the Jura Mountains. Namely, although il-

littization of smectites is commonly attributed to increasing temperature as burial diagenesis proceeds (HOWER et al., 1976), EBERL et al. (1986) suggested that K-fixation necessary for illitization of smectites could be achieved at surface temperatures by repeated wetting and drying. This led ROBINSON & WRIGHT (1987) to suggest that some mixed-layer illite/smectite could be produced from smectite during pedogenesis. DECONINCK et al. (1988) noted that illite occurred in areas closer to marine influences, and suggested that illite was formed by conversion from detrital smectite, as a result of repeated wetting by K-rich marine waters and subsequent drying in a hypersaline environment. The K^+ necessary for illitization of smectite was probably provided by marine waters, plant debris washed into ponds, leaching of volcanic rocks and from various other sources (DECONINCK et al., 1988).

The clay mineral composition of clays in the Trijezerca quarry clearly indicates the influence of both pedogenic and diagenetic processes. Mineralogical as well as chemical data indicate that transformation of smectite (from the mixed-layer minerals) to illite must have occurred. Wetting and drying experiments and layer charge measurements support this theory (Figs. 20 and 21). K-fixation necessary for illitization of smectites could have been achieved on the palaeolandscape by repeated wetting and drying. Potassium may have been provided by plants, marine waters, volcanic dust and other sources.

Based on micromorphological research, it can also be concluded that greenish-grey clays from the Trijezerca quarry were pedogenetically altered, i.e. they are palaeosols. The following facts favour this statement: (i) weakly developed soil structure (Fig. 22), (ii) presence of root remains, burrows and channels, now mainly filled with pyrite framboids (Fig. 23), (iii) nests of the faecal products of soil dwelling fauna, (iv) nodular pedofeatures (Fig. 24), and (v) microfabric (Figs. 25 and 26). The colour of palaeosols, the presence of root remains only in the upper part of the profile and high abundance of pyrite framboids may imply that they were probably seasonally marshy soils (partly or

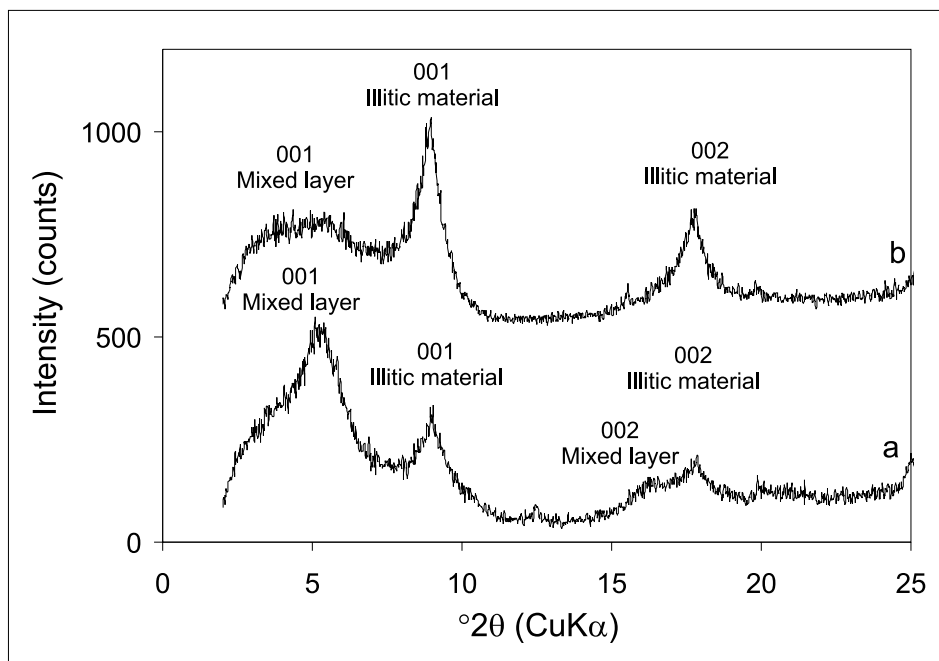


Fig. 18 Characteristic parts of XRD patterns of selected clay samples (<2 μm fraction) from Tri jezerca quarry: (a) upper part of profile, sample 1, glycol solvated; (b) lower part of the profile, sample 10, glycol solvated.

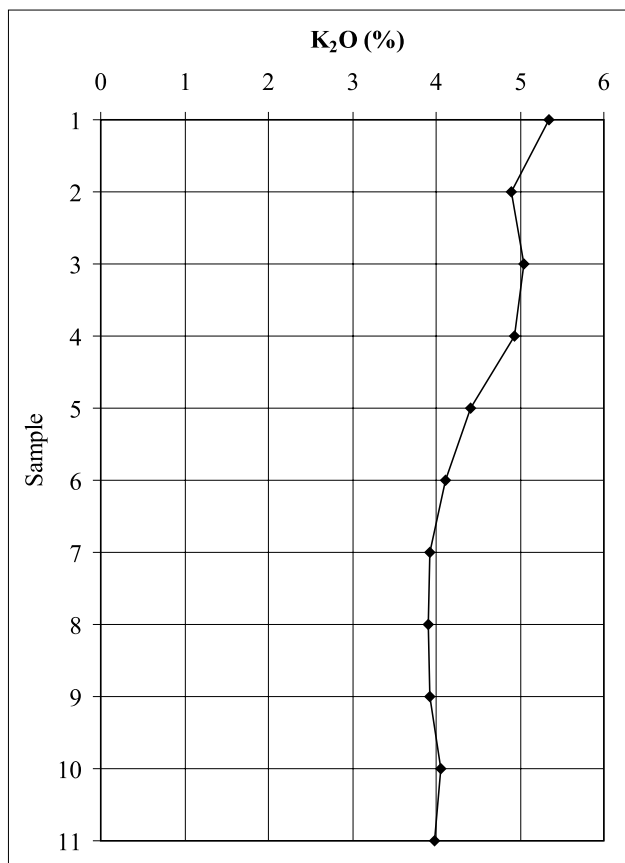


Fig. 19 Distribution of K₂O (in wt.%) along the profile in the Tri jezerca quarry.

wholly within the zone of water-table fluctuation), to permanently waterlogged soil (entirely below the water-table). This is also supported by the distribution of U, V and Mo along the profile (Fig. 27) and REE distribution. The total REE content of the clay profile ranges from 87.80–123.56 ppm. (La/Yb)_{ch} ratios in grey waterlogged palaeosols vary from 4.51–6.82 and are significantly lower than that of ES indicating HREE enrichment relative to LREE

(Fig. 28). The total REE content in the insoluble residue of limestone is 148.04 ppm and the (La/Yb)_{ch} ratio is 15.67. Enrichment of HREE in clays from the Tri jezerca quarry is probably the result of the higher mobility of LREE in an acidic pedogenic environment. Very low values of δ³⁴S in pyrites (δ³⁴S is -36‰) from the Tri jezerca quarry (sample SB2; 8–16 cm, Fig. 23) may also result from repeated cycles of oxidation and reduction, i.e. fluctuation of the water-table in wetland marshy soils.

The parentage of the material from which this soil was formed is still uncertain, but there are clear indications that materials other than the insoluble residue of limestones (e.g. volcanic dust, Fig. 29) may have contributed to the genesis of these clays. For example the Zr/Nb ratios in the insoluble limestone residue are much lower than these ratios in clays from the Tri jezerca quarry (Fig. 30). Namely, if we consider Zr and Nb as relatively immobile in soil (MUHS et al., 1987, 1990), then parent materials other than the insoluble residue of limestones may have influenced clay composition. This is also supported by the clay mineralogy results (Fig. 17).

The beginning of Upper Albian deposition (Fig. 15) is characterized by an oscillating transgression, and alternations of peritidal fenestral mudstones, fossiliferous wackestones and packstones, and high-energy shoreline and tidal-channel fill conglomerates and black-pebble breccias (TIŠLJAR et al., 1995). Within these sediments, features indicating 2 short emersions, represented mainly by coarse brecciated zones infilled with greenish–grey and greenish–yellow clays can be observed. The clay mineralogy of these clay infillings is similar to that of the lowest part of the greenish–grey clay situated in a palaeokarst pit (Fig. 17). E.g., the main clay minerals in clay infillings from the first brecciated zone are regularly ordered and randomly ordered illite/smectite mixed-layer minerals (52 wt.%). They are followed by illitic material (48 wt.%). These clays do not contain pyrite and chlorite.

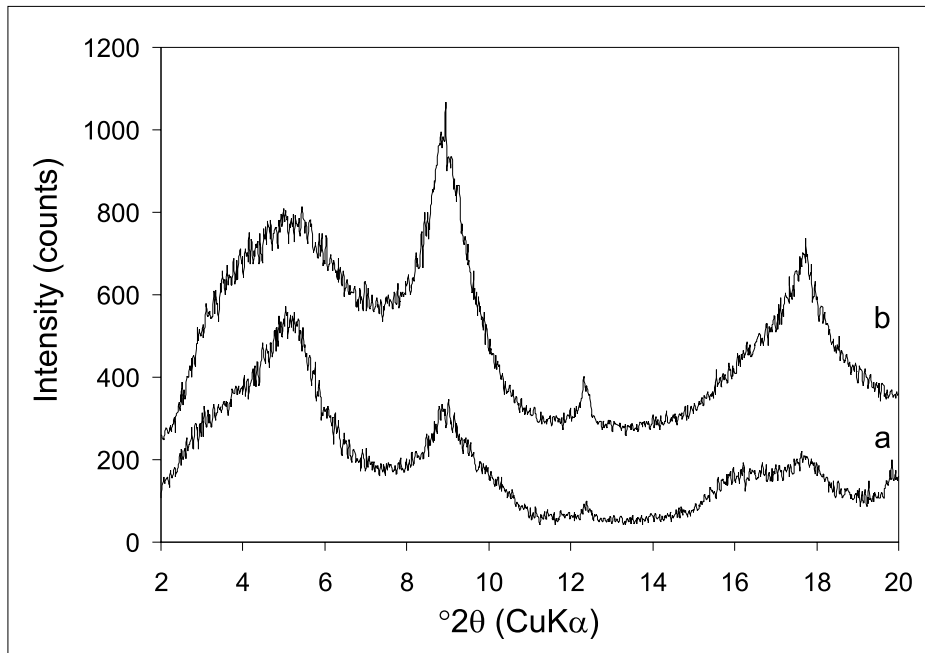


Fig. 20 Characteristic parts of XRD patterns of clay sample 10 (<2 μm fraction) from Tri jezerca quarry: (a) Sr treated, glycol solvated, after 0 wetting/drying cycles; (b) Sr treated, glycol solvated, after 100 wetting/drying cycles.

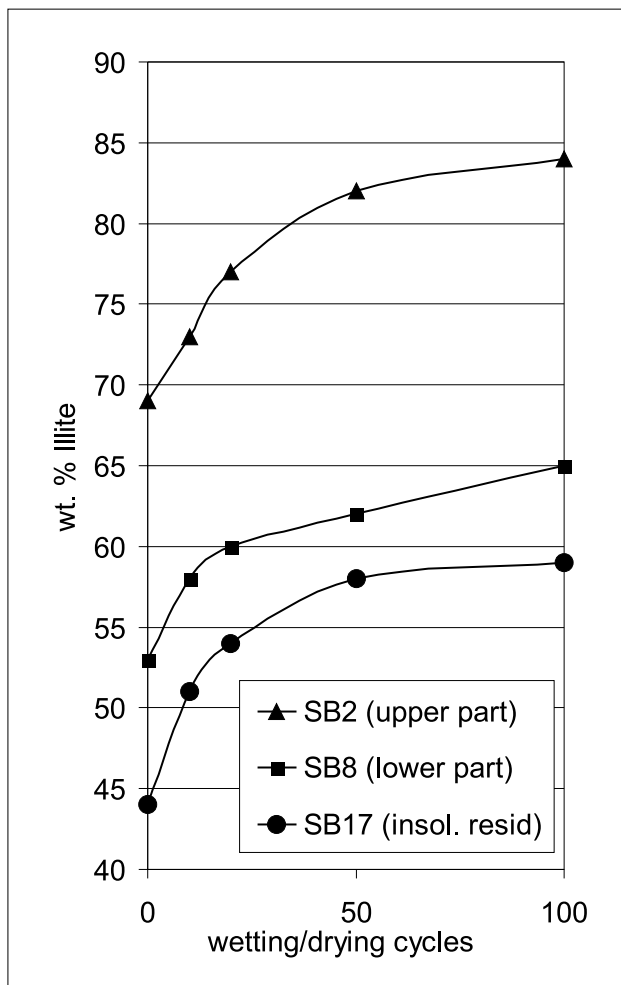


Fig. 21 The content of illitic material in selected clay samples from Tri jezerca quarry and in underlying limestone (insoluble residue) after 0 to 100 wetting/drying cycles.



Fig. 22 Contact between greenish-grey clays and karstified "Istarski žuti" limestone (Tri jezerca quarry).

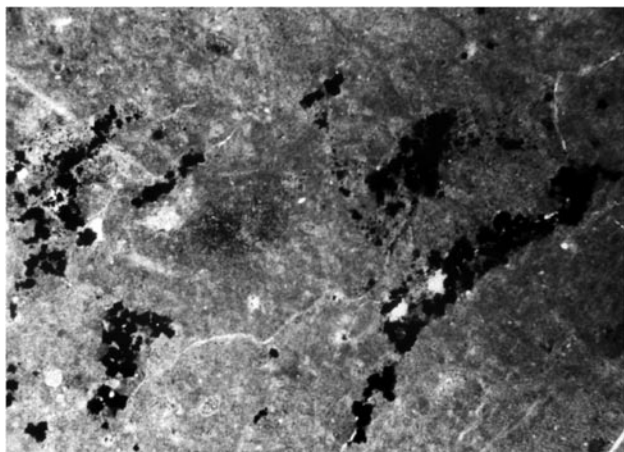


Fig. 23 Root remains, burrows and channels, mainly filled with pyrite framboids (upper part of profile shown on Fig. 25, 10–18 cm, Tri jezerca quarry); length of photograph = 3.3 mm.

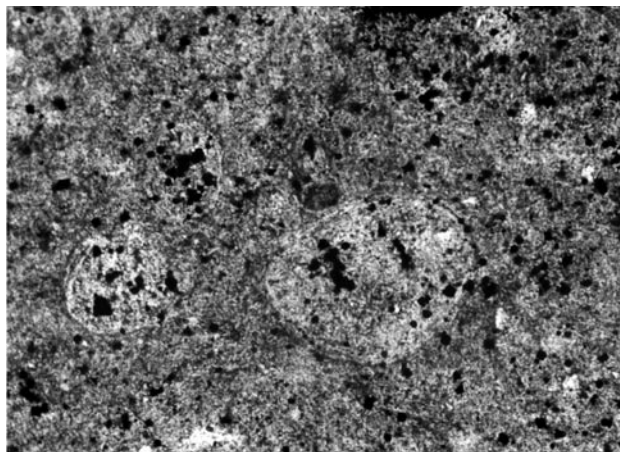


Fig. 24 Nodular pedofeatures (upper part of profile shown on Fig. 25, 10–18 cm, Tri jezerca quarry); length of photograph = 3.3 mm.



Fig. 25 Bright clay strikes may correspond to cross-striated b-fabric and masepic plasmic fabric (upper part of profile shown on Fig. 25, 0–8 cm, Tri jezerca quarry); crossed nicols, length of photograph = 3.3 mm.

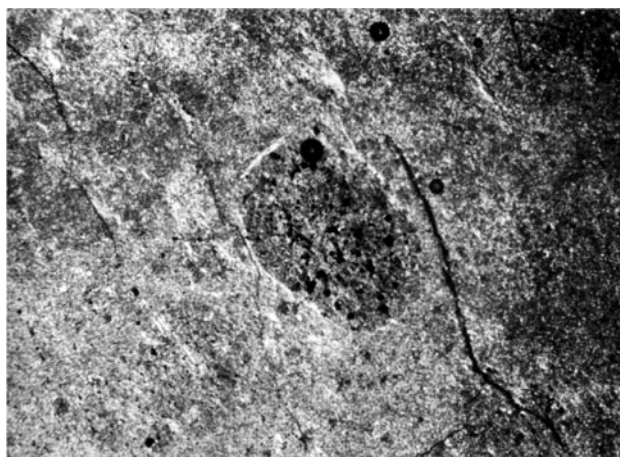


Fig. 26 Some of the features in the clayey matrix show the outline of former crystals, now replaced by clay (upper part of profile shown on Fig. 25, 10–18 cm, Tri jezerca quarry); crossed nicols, length of photograph = 3.3 mm.

4. QUATERNARY SEDIMENTS AND SOILS ON THE JURASSIC–CRETACEOUS–PALAEOGENE CARBONATE PLAIN OF SOUTHERN AND WESTERN ISTRIA

4.1. Introduction

Since the end of the Eocene (or probably earlier for the central parts of Istria – MATIČEC et al., 1996) the surface of the Istrian Peninsula has been affected by karst processes and weathering, which has led to the development of both surficial and underground features. Different types of sediments, polygenetic palaeosols and soils have been formed. Among them the most important are loess and *terra rossa*. The oldest Quaternary sediments were discovered in the Šandalja cave near Pula, and are represented by red breccia with faunal remains of Early Pleistocene age (MALEZ, 1981). According to CREMASCHI (1990a) deposition of loess was a very important recurrent process in Northern and Central Italy from at least the early Middle Pleistocene. He recognized the following loess depositional periods: (1) Middle Pleistocene; (2) Upper Pleistocene, with two main phases of loess sedimentation: the first during Early

Pleniglacial and second during the Second Pleniglacial, and (3) Younger Dryas (Late-glacial loess). Loess deposition also affected Istria. Loess is situated in the southern (Premantura and Mrlera) and northwestern parts of Istria (Savudrija) and is considered to be Upper Pleistocene in age (POLŠAK, 1970). Although there are no data about older loess deposits in Istria, they were recognized on the neighbouring Island of Susak. They are situated below the Upper Pleistocene loess and have a reddish alfisol developed on their top, which is thought to have formed in the Riss–Würm interglacial (CREMASCHI, 1990b).

Terra rossa is a common general term used among Croatian geologists and pedologists for reddish soil occurring on limestone and dolomite substrates. The nature and relationship of *terra rossa* to underlying carbonates is a long-standing problem, which has resulted in different opinions with respect to the parent material and origin of *terra rossa*. The bright red colour is a diagnostic feature of *terra rossa* and is a result of the preferential formation of haematite over goethite, i.e. *rubification*. Generally, *terra rossa* can be, according to different authors, considered as soil, relict soil (non-buried-palaeosol), palaeosol or a

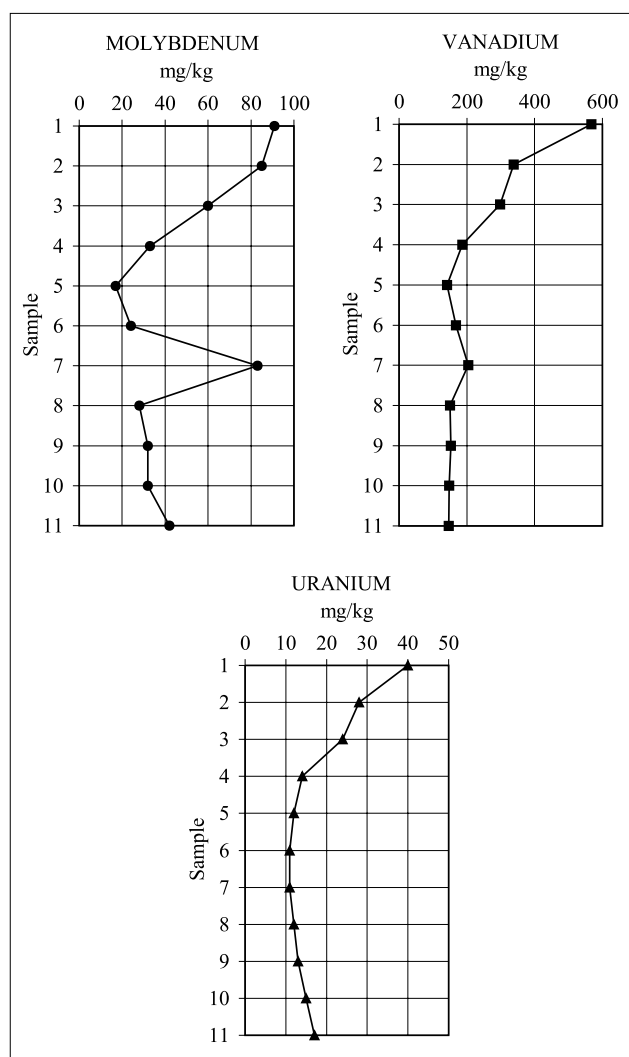


Fig. 27 Distribution of Mo, U and V along along the profile in the Trijezerca quarry.

pedo-sedimentary complex (soil-sediment). Most authors today believe that *terra rossa* is a polygenetic relict soil formed during the Tertiary and/or hot and humid periods of the Quaternary. However, some recent investigations (e.g. BRONGER & SEDOV, 2002) show that at least some *terra rossa* previously referred to as polygenetic relict soils should be regarded as Vetusols (soils which are marked by a continuity of pedogenetic processes in time), in accordance with the concept of CREMASCHI (1987). According to DURN et al. (1999), in some isolated karst terrains *terra rossa* may have formed exclusively from the insoluble residue of limestone and dolomite, but much more often it comprises a span of parent materials which derived from carbonate terrains via different transport mechanisms.

Terra rossa is found on the Jurassic-Cretaceous-Palaeogene carbonate plain of southern and western Istria. It fills cracks and sinkholes, and forms a discontinuous surface layer up to 2.5 metres thick. Since *terra rossa* has been exposed to various climatic fluctuations it can be affected by aeolian deposition, erosion, colluviation, eluviation, yellowing and secondary hydromorphy. Erosion and depositional processes which were superimposed on karst terrains and induced by climatic changes, tectonic move-

ments and/or deforestation might be responsible for both the patchy distribution of *terra rossa*, and thick colluvial accumulations (up to 14 m) of *terra rossa*-like materials, in *uvula* and *dolina* types of karst depressions (pedo-sedimentary complexes, soil-sediments).

The Upper Pleistocene loess in the northwestern part of Istria (Savudrija cape) covers red interglacial palaeosols and *terra rossa*. This indicates that the Upper Pleistocene loess post-dated *terra rossa* formation in Istria. However, the presence of aeolian dust was also recognized in the upper part of *terra rossa* in areas where loess is not present, or not clearly recognized (DURN, 1996). Namely, when the rate of aeolian dust accumulation increases to 40 $\mu\text{m}/\text{y}$, dust accumulates as surface loess (YAALON, 1997). When the rate of accumulation is less than 20 $\mu\text{m}/\text{y}$ the accreted dust manages to become completely assimilated by the prevailing pedoenvironment, and is leached or bioturbated into the soil profile (YAALON, 1997). This is why the addition of aeolian dust to a soil is usually difficult to identify. If we bear this in mind, it can be postulated that similar external materials might have contributed to *terra rossa* since the Middle Pleistocene. Consequently, DURN et al. (1999) presented evidence for the polygenetic nature of *terra rossa* in Istria, based on detailed mineralogical and geochemical investigation. Namely, neither the content and particle size distribution nor the bulk and clay mineralogy of the insoluble residue of limestone and dolomite support development of *terra rossa* entirely by dissolution of carbonate rocks. They concluded that both aeolian sediments older than those of Upper Pleistocene age and flysch might have contributed to the genesis of *terra rossa*. DURN et al. (1999) also found that arithmetic means of two populations (Fe_d of 45 *terra rossa* samples from various locations around the world and Fe_d of 40 samples from Istria) represent two independent estimates of the same population (Fe_d in *terra rossa*), and concluded that this supports BOERO & SCHWERTMANN's (1989) conclusion that the rather limited extent of variation of selected Fe-oxide characteristics may indicate a specific pedoenvironment in which *terra rossa* is formed. They suggested that this pedoenvironment is characterized by an association of Mediterranean climate, high internal drainage due to the karstic nature of a hard limestone, and neutral pH conditions.

In the frame of this excursion we will see polygenetic relict *terra rossa* soil in Novigrad (Stop 3).

4.2. Stop 3: Polygenetic relict *terra rossa* soil in the Novigrad town area (western Istria)

The Novigrad profile is situated on the coast of Novigrad bay, NW of Novigrad town (Fig. 4). It represents a polygenetic *terra rossa* soil about 150 cm thick, situated on fine-grained pelletal wackestone of Lower Cretaceous age (Upper Albian, Fig. 31). In the lowest part of the profile it is clear that the limestones were exposed to the process of rubification (Fig. 32). Dissolution voids and cracks in limestone at the contact with *terra rossa* are infilled exclusively with clayey matrix (Fig. 33). A detailed description of the Novigrad profile is presented in Fig. 34. The chemical composition and selected weathering indices of samples from Novigrad are given in Tables 7 and 8 and Fig. 35.

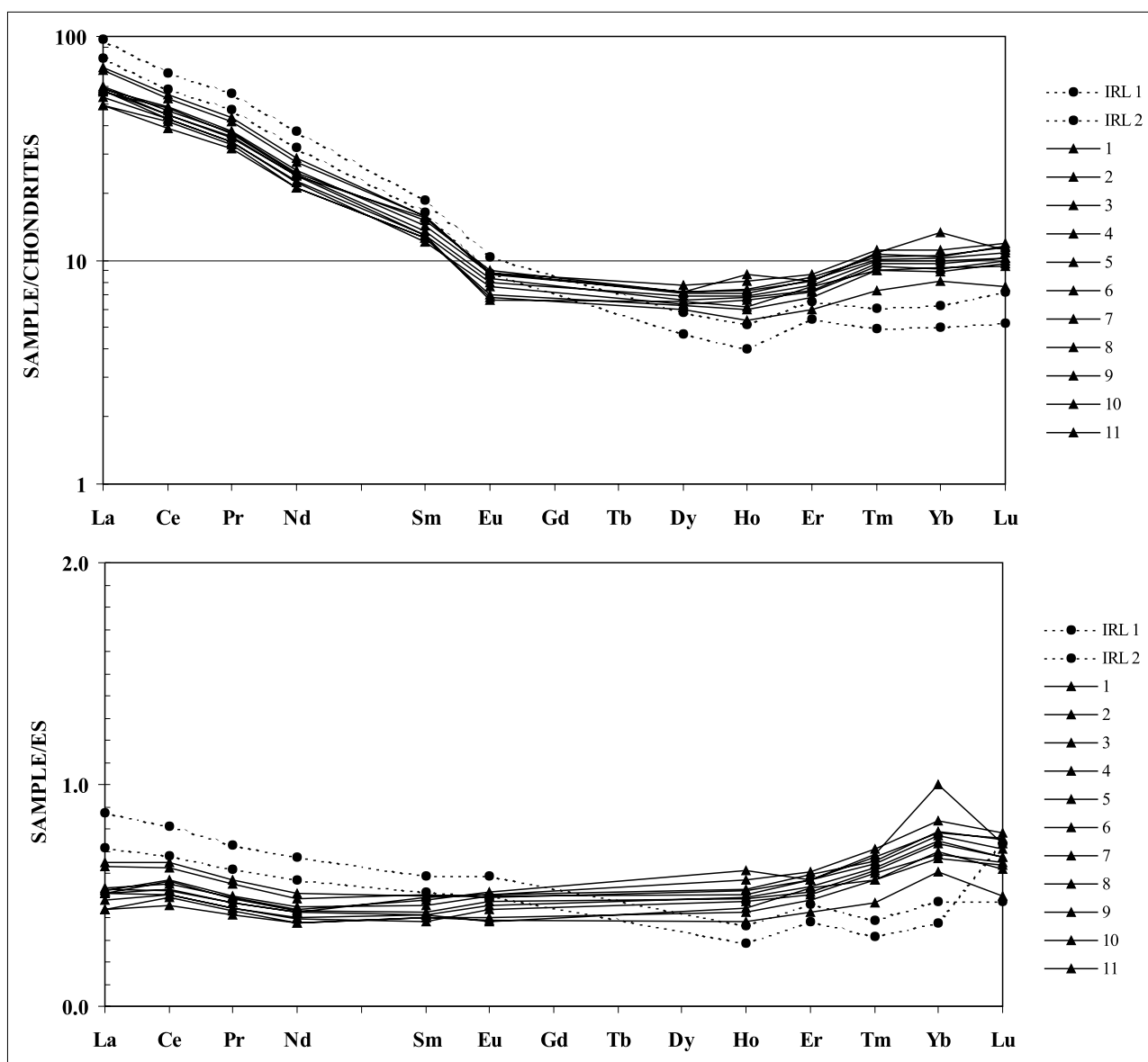


Fig. 28 Chondrite-normalized and European shale-normalized REE patterns of greenish-grey clays from the Tri jezerca quarry and the insoluble residue of limestone from the Tri jezerca and Kanfanar quarries (numbers of samples match those on Figs. 27 and 28). Legend: IRL1) insoluble residue of limestone (Istarski žuti) situated immediately bellow clay in the Tri jezerca quarry (Stop 2); IRL2) insoluble residue of limestone (Istarski žuti) situated immediately bellow clay in the Kanfanar quarry.

The contents of SiO_2 , TiO_2 , MnO and Na_2O are significantly higher, and Al_2O_3 and Fe_2O_3 lower in the upper part of the profile (Fig. 34 and Table 7; samples 131 and 132, horizons IIB1 and IIB2). A clear trend of decreasing content of SiO_2 and Na_2O and increasing content of Al_2O_3 and Fe_2O_3 both in the upper and lower part of profile (samples 133, 134, 135 and 136; horizons IIIB1t, IIIB2t, IIIB3t and IIIB4t(g)) is observed. Distribution of MgO and P_2O_5 do not show a clear trend with depth.

Weathering indices also show clear trends in the distribution of the major elements (Table 8). Although K_2O does not show a clear trend along the profile, decreasing content of Na_2O with depth is also manifested as a decrease in the $\text{Na}_2\text{O}/\text{K}_2\text{O}$ index with depth. The same trend is observed for other weathering indices. The trends of increasing contents of Al_2O_3 and Fe_2O_3 , and decreasing contents of SiO_2 and Na_2O with depth are compatible with the increasing amount of the clay fraction with depth (Table 8).

Both the upper and lower parts of the profile are mineralogically similar. They consist of quartz, plagioclase, K-feldspar, micaceous clay minerals (illitic material and mica), kaolinites (Kl_D and Kl), vermiculite, mixed-layer clay minerals (other than illitic material), haematite, goethite and an XRD-amorphous inorganic compound (Tables 9 and 10). However, the content of quartz and plagioclase is higher in the upper part, while the content of phyllosilicates and Fe-oxides is higher in the lower part of the profile. Dominant mineral phases in the clay fraction of the Novigrad profile are kaolinites (Kl_D and Kl) and illitic material, while vermiculite, mixed-layer clay minerals and quartz are present in subordinate amounts (Figs. 36 and 37). The content of kaolinite which does not form intercalation compounds with DMSO (Kl) is higher than that of kaolinite which intercalates with DMSO (Kl_D) (Fig. 37). The $\text{K}_2\text{Ox}100/\text{Al}_2\text{O}_3$ index, which can be in this case considered as a good approximation of the illite/kaolinite

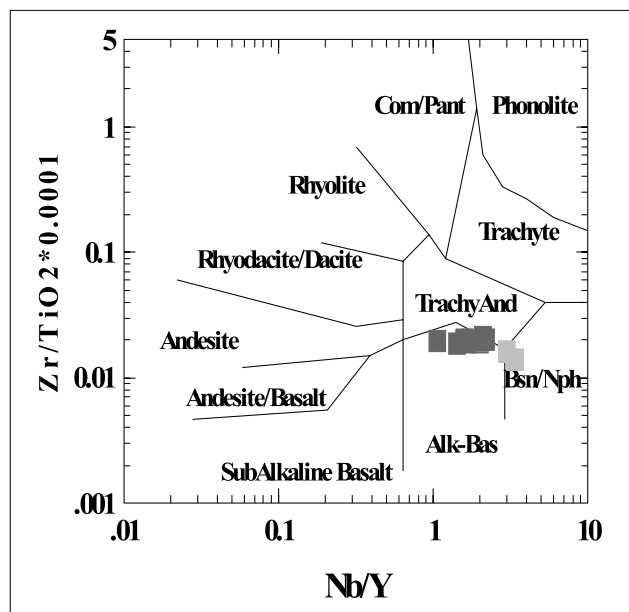


Fig. 29 Diagram after WINCHESTER & FLOYD (1977) for greenish-grey clays from Tri jezerca quarry (dark grey) and insoluble residue of limestone from the Tri jezerca quarry and Kanfanar quarry (light grey).

ratio (MORESSI & MONGELLI, 1988), decreases downwards (Table 8). This indicates that the amount of kaolinite increases downwards. DURN et al. (1999) concluded that kaolinite which does not form intercalation compounds with DMSO(KI) is the dominant mineral phase in the fine clay of *terra rossa* in Istria and is considered predominantly authigenic rather than being inherited from parent materials.

Samples from the Novigrad profile bear typical *terra rossa* Fe-oxide characteristics, e.g. Fe_d and Fe_d/Fe_t (DURN et al., 1999). Fe_d /clay ratios are relatively uniform along the profile and clearly indicate a predominance of co-illuviation of clay and Fe oxides, i.e. connection of Fe-oxides with the clay fraction (DURN et al., 2001). So, translocation of clay particles is responsible for the distribution of the red colour through the whole profile.

In order to characterize chemically insoluble residues of carbonate rocks and compare them with *terra rossa* and loess, DURN et al. (1999) among others also used Zr and

Nb, elements with a high ionic potential which are considered relatively immobile in soil environments and suitable for geochemical “fingerprinting” (MUHS et al., 1987, 1990). Zr/Nb ratios in the insoluble residue of Jurassic and Cretaceous limestones and dolomites are generally lower than these ratios in the Novigrad profile, although there is obvious overlapping of the lower part of the Novigrad profile with the insoluble residue field (Fig. 30).

The heavy mineral fraction of the Novigrad profile is enriched in epidote-zoisite group minerals, amphiboles and garnets (Fig. 38, samples 131, 134 and 136), which may indicate that at least part of the parent material from which *terra rossa* was formed belongs to the Po plain-Adriatic loess region provenance. However, the contents of epidote-zoisite group minerals, amphibole and garnet decreases, while contents of zircon, tourmaline and rutile increases with depth along the profile. This may indicate that the parent material is of mixed provenance. The content of the clay fraction in the highly weathered loess from Northern and Central Italy ranges from 58–75 wt.% and that of the sand fraction from 1–3 wt.% (CREMASCHI, 1990b). These results are very similar to the results obtained for *terra rossa* (Fig. 39). DURN et al. (2003) tentatively attributed red interglacial soil situated below the Savudrija loess complex, (which has significantly higher silt/clay ratios than *terra rossa* in the Novigrad profile, Table 8) to the Eemian interglacial period. There is sufficient evidence to propose that formation of *terra rossa* started earlier than this.

Materials other than the insoluble residue of limestones and dolomites which have contributed to *terra rossa* in Istria are aeolian sediments, the deposition of which was a very important recurrent process in Istria probably since the early Middle Pleistocene, and flysch sediments which extended further south from its present position (DURN et al., 1999). Based on detailed heavy mineral study, DURN et al. (2006) concluded that the main external contributor to *terra rossa* in Istria is Middle Pleistocene loess, followed by flysch and tephra (minor contributions). Upper Pleistocene loess might have become intermixed in the upper parts of already formed *terra rossa*.

Terra rossa is formed as a result of: (1) *decalcification*, (2) *rubification* and (3) *monosiallitization* (neof ormation of kaolinite). However, since they have been exposed to vari-

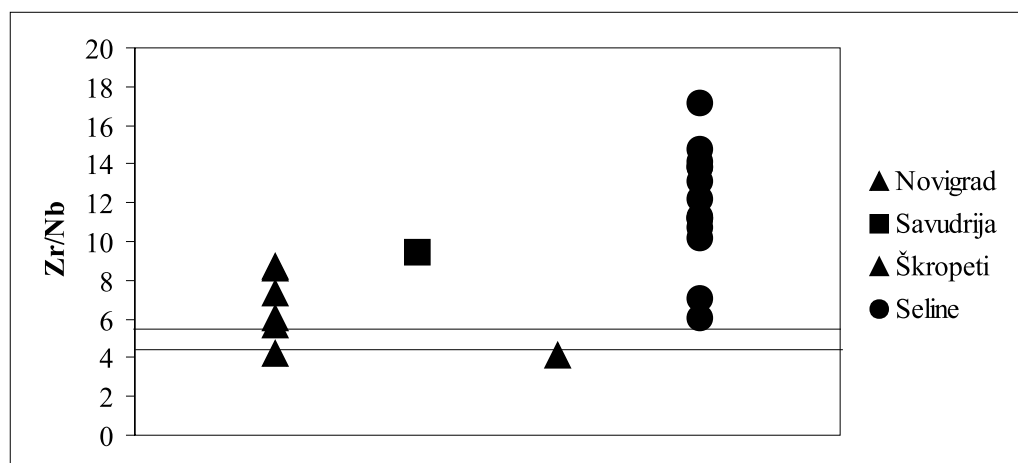


Fig. 30 Zr/Nb ratios for greenish-grey clays from the Tri jezerca quarry (Seline) and *terra rossa* (Novigrad, Savudrija and Škropeti). Two horizontal lines represent the minimum and maximum values for these ratios in insoluble residues of limestone. Data for *terra rossa* and insoluble residues of limestone from DURN et al. (1999).



Fig. 31 Polygenetic *terra rossa* soil in Novigrad. Cleaned profile prepared for detailed sampling.

ous climatic fluctuations *terra rossa* soils can be affected by aeolian deposition, erosion, colluviation, eluviation, yellowing and secondary hydromorphy (gleyzation). For example, pedorelics found in *terra rossa* may be the erosional remains of very old (from Miocene on?) soils formed exclusively from the insoluble residue of limestones and dolomites. Now they represent only one component of a fine colluvium, which may also contain erosional remains of other pre-existing soils, aeolian sediments (of different ages), flysch and bauxites.

Based on the field description of the profile and the laboratory analyses, we may conclude that the Novigrad profile represents a typical polygenetic *terra rossa* soil.



Fig. 32 *Terra rossa* and footwall limestone contact. Novigrad profile. Depth=150 cm. Length of photograph=1.5 mm.

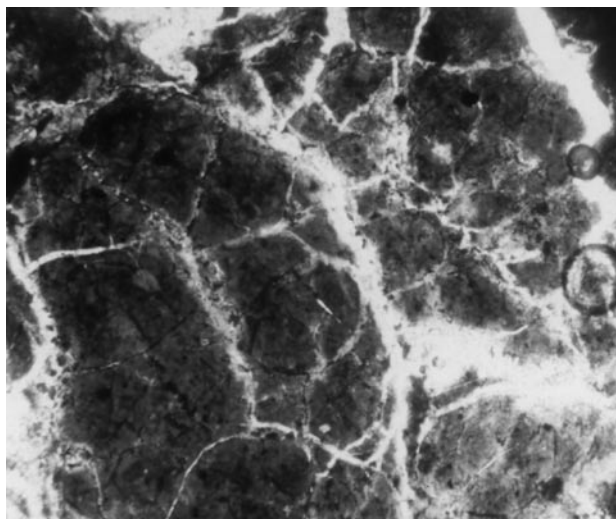


Fig. 33 Fissure microstructure. Basic mass consists of micromass only. Novigrad profile. Depth=145 cm. Length of photograph=7.5 mm.

5. REFERENCES

- BÁRDOSSY, Gy. (1982): Karst Bauxites, Bauxite Deposits on Carbonate Rocks.– Developments in Economic Geology, 14, Elsevier, Amsterdam, 441 p.
- BÁRDOSSY, Gy. & DERCOURT, J. (1990): Les gisements de bauxite tethysiens (Méditerranée, Proche et Moyen Orient); cadre paleogeographique et controles genetiques.– Bull. Soc. Geol. France (8), 4/6, 869–888.

sample	SiO ₂	TiO ₂	Al ₂ O ₃	Fe ₂ O ₃	MnO	MgO	CaO	Na ₂ O	K ₂ O	P ₂ O ₅	LOI	SUM
131	59.46	1.29	17.57	5.78	0.19	0.81	0.74	0.40	1.61	0.15	12.42	100.6
132	58.82	1.26	18.59	5.89	0.18	0.80	0.69	0.38	1.58	0.13	11.29	99.66
133	50.27	1.06	22.76	8.68	0.10	0.86	0.73	0.26	1.65	0.12	13.35	99.89
134	50.27	1.08	22.67	8.75	0.10	0.88	0.67	0.26	1.65	0.13	13.56	100.1
135	49.84	1.08	23.06	8.87	0.08	0.86	0.66	0.23	1.63	0.13	13.41	99.90
136	47.91	1.01	23.39	9.31	0.10	0.85	0.64	0.18	1.55	0.12	14.82	99.93

Table 7 Chemical composition (major elements) of samples from polygenetic *terra rossa* soil (Novigrad profile). For sample description see Fig. 34. Data from DURM (1996).

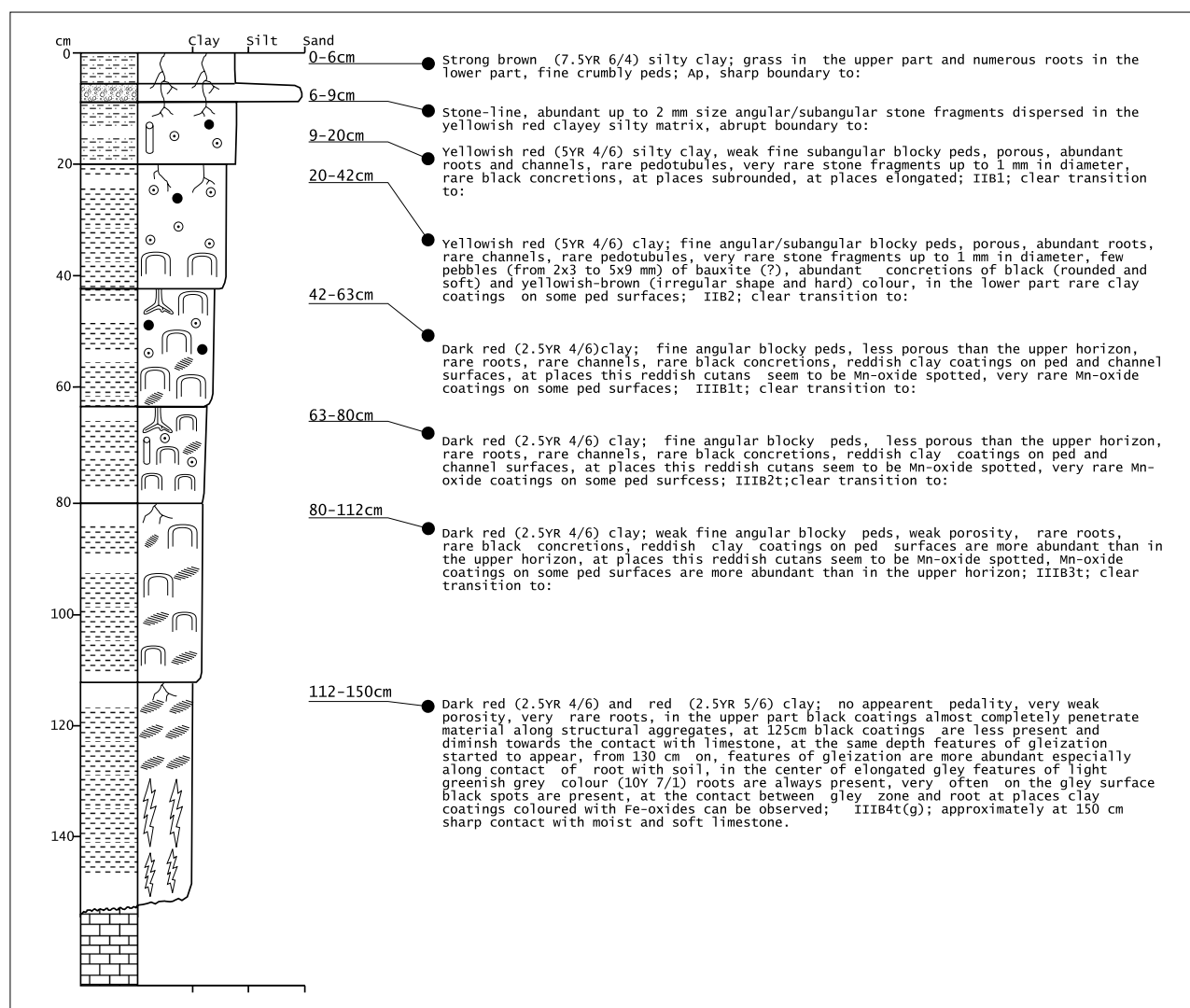


Fig. 34 Field description of polygenetic *terra rossa* soil (Novigrad profile). Modified from DURN (1996).

- BERNOULLI, D. (2001): Mesozoic–Tertiary carbonate platforms, slopes and basins of the external Apennines and Sicily.– In: VAI, G.B. & MARTINI, I.P. (eds.): *Anatomy of an Orogen: the Apennines and Adjacent Mediterranean Basins*. Kluwer Academic Publ., 307–326.
- BOERO, V. & SCHWERTMANN, U. (1989): Iron oxide mineralogy of terra rossa and its genetic Implications.– *Geoderma*, 44, 319–327.
- BORDEA, S. & MANTEA, G. (1991): Stratigraphical composition of the bauxite deposits in the Padurea Craiului Moun-

tains (northern Apuseni Mountains).– In: *Tethyan Bauxites IGCP-287, part II.*, Acta Geol. Hung., 34/4, 351–376.

- BRONGER, A. & SEDOV, S.N. (2002): Vetusols and paleosols: natural versus man-induced environmental change in the Atlantic coastal region of Morocco.– 17th World Conference on Soil Science, Paper no.1530, 1–12.

- CARANNANTE, G., D'ARGENIO, B., MINDSZENTY, A., RUBERTI, D. & SIMONE, L. (1994): Cretaceous–Miocene shallow water carbonate sequences. Regional unconformities and facies patterns.– In: CARANNANTE, G. & TONIELLI, R.

sample	Na ₂ O/K ₂ O	(CaO+MgO+K ₂ O+Na ₂ O)/Al ₂ O ₃	K ₂ Ox100/Al ₂ O ₃	SiO ₂ /Fe ₂ O ₃	silt/clay
131	0.38	0.33	9.16	27.34	0.77
132	0.37	0.30	8.5	26.54	0.64
133	0.24	0.25	7.25	15.39	0.41
134	0.24	0.25	7.28	15.27	0.36
135	0.21	0.24	7.07	14.93	0.35
136	0.18	0.23	6.63	13.68	0.28

Table 8 Weathering indices for samples from polygenetic *terra rossa* soil (Novigrad profile). For sample description see Fig. 34. Data from DURN (1996).

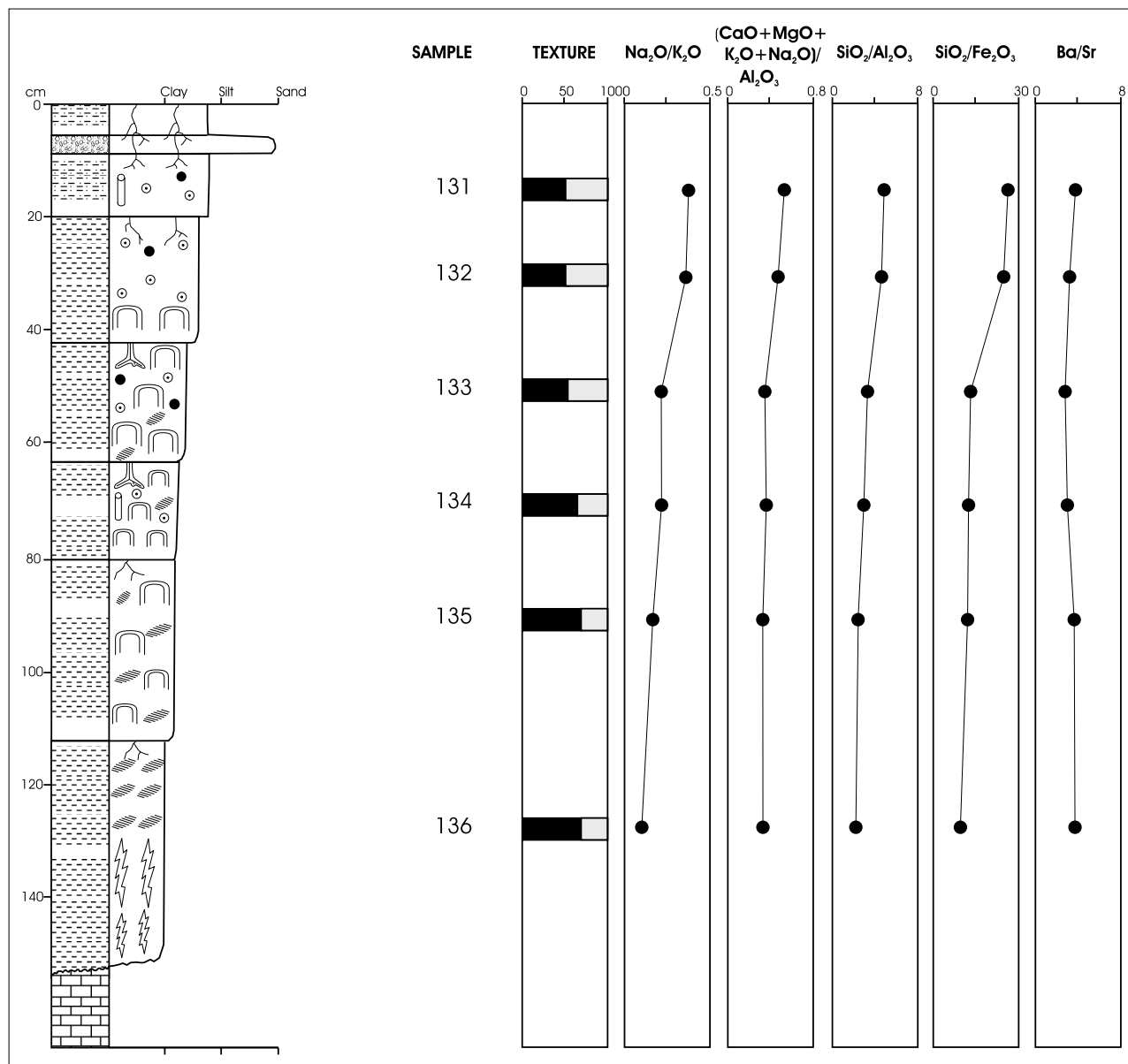


Fig. 35 Weathering indices for samples from polygenetic *terra rossa* soil (Novigrad profile). In column for texture black = clay content; grey = silt content. For sample description see Fig. 34. Modified from DURM (1996).

sample	Quartz	Plagioclase	K-feldspar	Haematite+Goethite	Phyllos.+am.
131	25	3	1	5	66
136	15	1	1	7	76

Table 9 Mineral composition of the <2 mm fraction of polygenetic *terra rossa* soil (Novigrad profile) in wt.%. Legend: Phyllos.+am.) phyllosilicates and amorphous inorganic compound. For sample description see Fig. 34. Data from DURM et al. (1999).

Sample	Illitic material	KI _b	KI	Vermiculite	Mc	Quartz
131	+	+	+	+	+	+
136	+	+	+	+	+	+

Table 10 Mineral composition of the <2 μm fraction of polygenetic *terra rossa* soil (Novigrad profile) after the removal of carbonates, humic materials and iron-oxides. Legend: KI_b) kaolinite which forms intercalation compounds with DMSO; KI) kaolinite which does not intercalate with DMSO; Mc) mixed-layer clay mineral. Data from DURM et al. (1999).

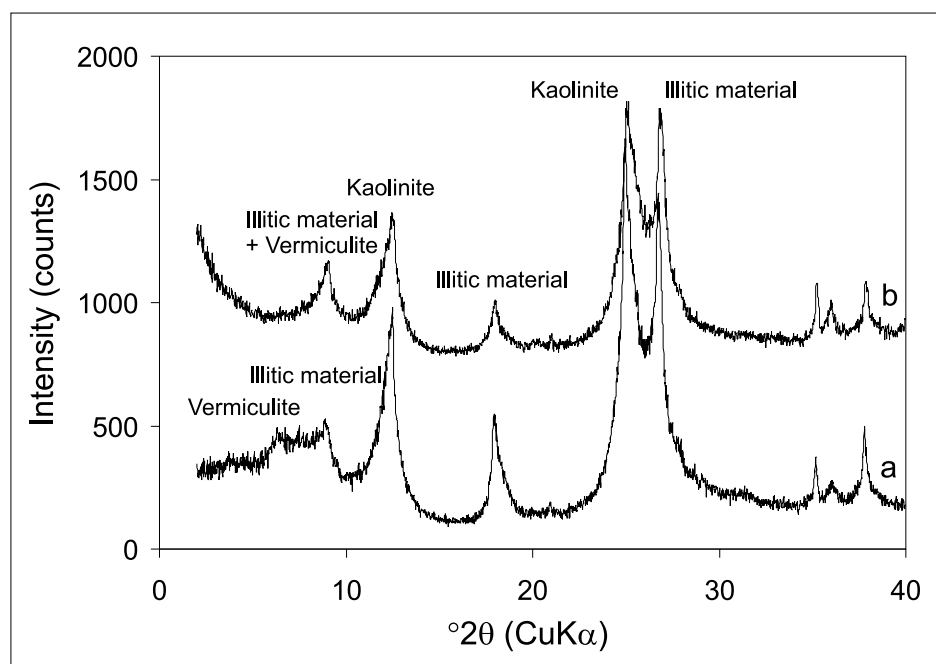


Fig. 36 Characteristic parts of XRD patterns of *terra rossa* sample 136 (<2 μm fraction): (a) Mg-saturated; (b) K-saturated.

(eds.): 15th IAS Regional Meeting, Ischia, Italy, Pre-Meeting Fieldtrip Guidebook, Exc. A2, 25–59.

CHANNEL, J.E.T. (1996): Paleomagnetism and paleogeography of Adria.– Geol. Soc. London, Spec. publ., 105, 119–132.

COMBES, P.J. (1990): Typologie, cadre géodynamique et genèse des bauxites Françaises.– *Geodynamica Acta* (Paris), 4/2, 91–109.

COMBES J.-P. & BÁRDOSSY, Gy. (1994): Typologie et contrôle géodynamique des bauxites tethysiennes.– *Compt. Rend. Acad. Sci. Paris, ser. II*, 318, 359–366.

CREMASCHI, M. (1987): Paleosols and Vetusols in the central Po plain, a study in Quaternary geology and soil development.– *Edizioni Unicopli, Milano*, 306 p.

CREMASCHI, M. (1990a): Stratigraphy and palaeoenvironmental significance of the loess deposits on Susak island (Dalmatian Archipelago).– *Quaternary International*, 5, 97–106.

CREMASCHI, M. (1990b): The loess in northern and central Italy: a loess basin between the Alps and the Mediterranean regions.– In: CREMASCHI, M. (ed.): *The Loess in Northern and Central Italy*. Centro di Studio per la Stratigrafia e Petrografia delle Alpi Centrali, Editrice Gutenberg, Milano, 15–19.

D'ARGENIO, B. & MINDSZNETY, A. (1991): Karst bauxites at regional unconformities and geotectonic correlation in the Cretaceous of the Mediterranean.– *Boll. Soc. Geol. It.*, 110, 1–8.

D'ARGENIO, B. & MINDSZNETY, A. (1992): Tectonic and climatic control on paleokarst and bauxites.– *Giornale di Geologia*, 54/1, 207–218.

D'ARGENIO, B. & MINDSZNETY, A. (1995): Bauxites and related paleokarst. Tectonic and climatic event markers at regional unconformities.– *Ecl. Geol. Helv.*, 88/3, 453–499.

DECONINCK, J.F. & STRASSER, A. (1987): Sedimentology, clay mineralogy and depositional environment of Purbeckian green marls (Swiss and Fench Jura).– *Ecol. Geol. Helv.*, 79, 753–772.

DECONINCK, J.F., STRASSER, A. & DEBRABANT, P. (1988): Formation of illitic minerals at surface temperatures in Pur-

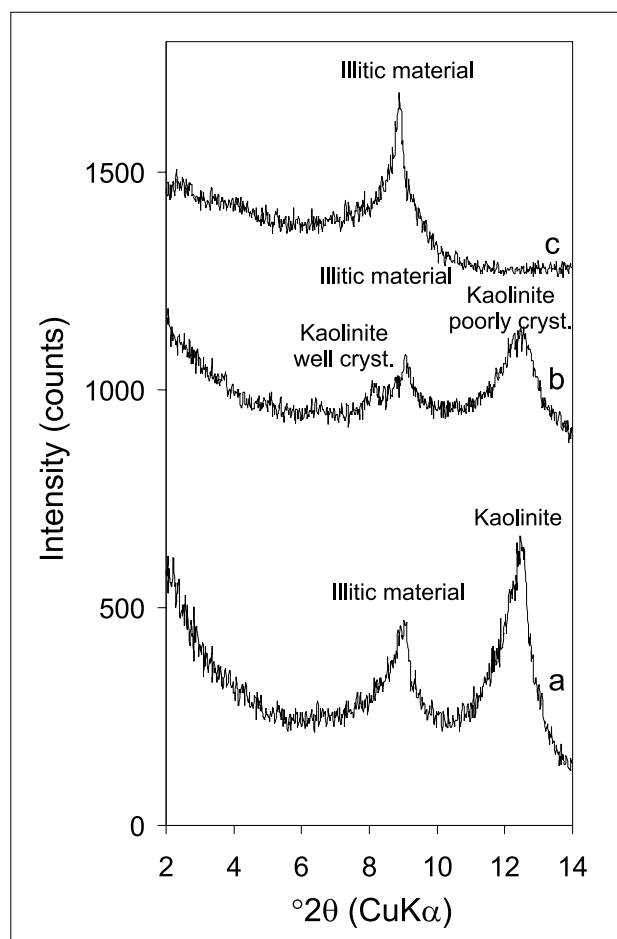


Fig. 37 Characteristic parts of XRD patterns of clay sample 136 (<2 μm fraction): (a) K-saturated; (b) K-saturated and DMSO-solvated; (c) Heated for one hour at 550°C.

beckian sediments (Lower Berriasian, Swiss and Fench Jura).– *Clay Miner.*, 23, 91–103.

DERCOURT, J., ZONENSHAIN, L.P., RICOU, E., KAZMIN, V.G., LE PICHON, X., KNIPPER, A.L., GRANDJACQUET,

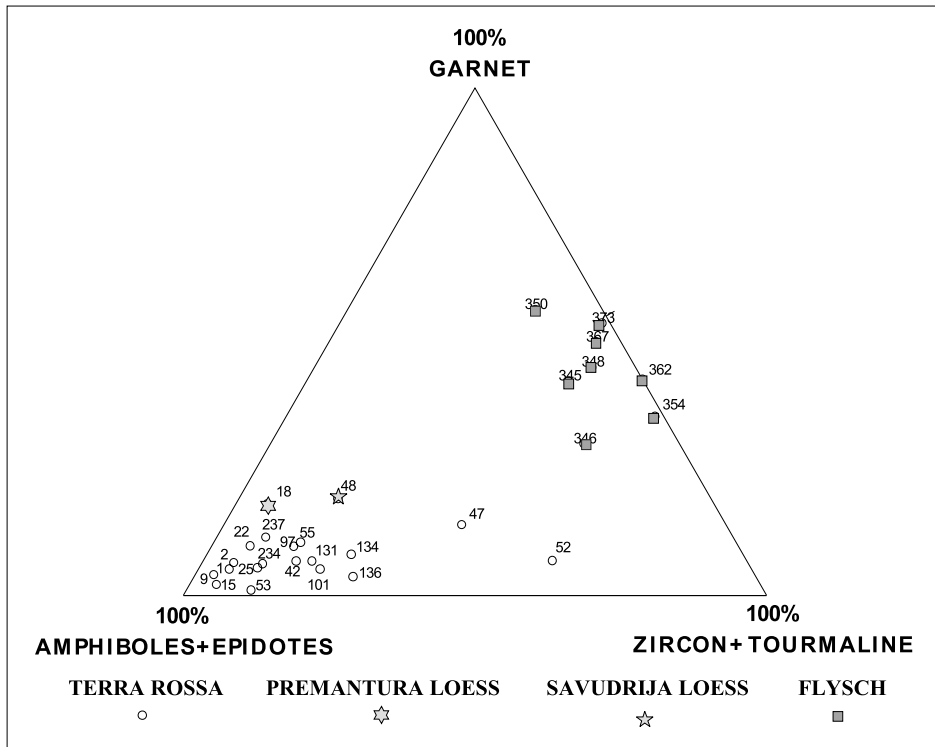


Fig. 38 Relationship between the composition of the selected heavy minerals in *terra rossa*, loess and flysch. Data for *terra rossa* and loess from DURN (1996), data for flysch from MAGDALENIĆ (1972).

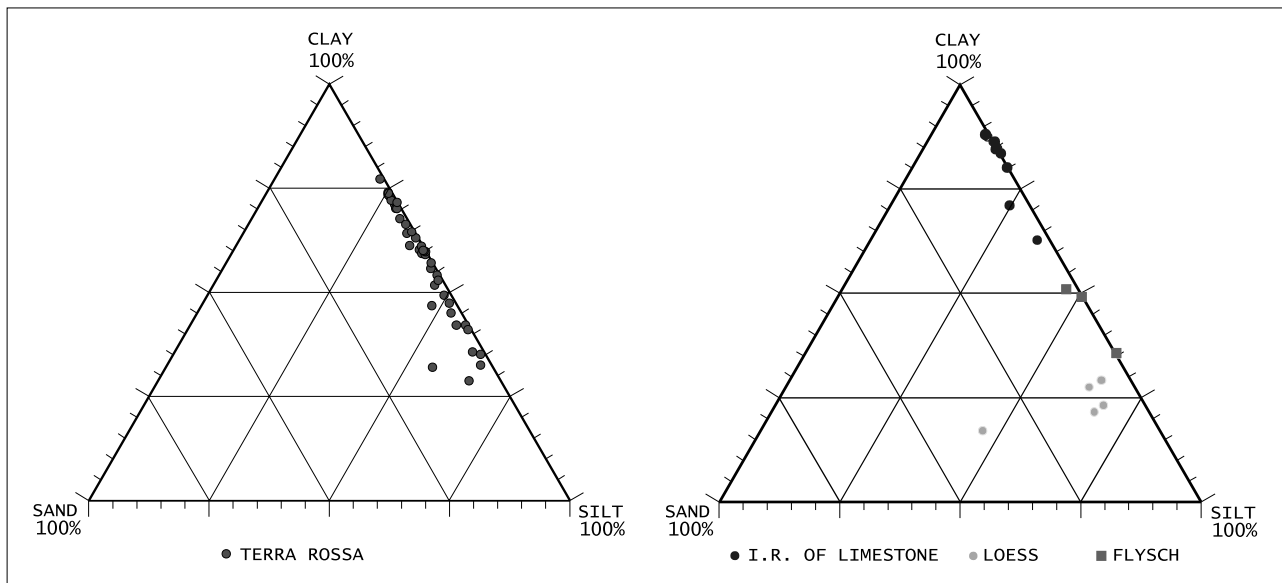


Fig. 39 Particle size analysis of *terra rossa* and insoluble residues of limestone, dolomite, loess and flysch (data from DURN et al., 1999).

C., SBORTSHIKOV, I.M., GEYSSANT, J., LEPVRIER, C., PECHERSKY, D.H., BOULIN, J., SIBUET, J.-C., SAVOSTIN, L.A., SOROKHTIN, O., WESTPHAL, M., BAZHENOV, M.L., LAUER, J.P. & BIJU-DUVAL, B. (1986): Geological evolution of the Tethys belt from the Atlantic to the Pamir since the Lias.– *Tectonophysics*, 123/1–4, 241–315.

DI STEFANO, P., MALLARINO, G., MINDSZENTY, A. & NICHITTA, D. (2002): Monte Gallo: A Jurassic angular unconformity marked by bauxites in the Panormide carbonate platform.– In: SANTANTONIO, M. (ed.): 6th Intern Symp. on the Jurassic System, Palermo, Italy. General field trip guidebook, 31–35.

DUDICH, E. & MINDSZENTY, A. (1984): Ásvány-közettani-geokémiai adatok a Villányi hegység és az Erdélyi Középhegység bauxitjának összehasonlításához (Comparison of the

lithology and geochemistry of the Villány and Apuseni bauxites).– *Földtani Közlöny (Bull. Geol. Soc. Hung.)*, 114/1, 1–18, Budapest.

DURN, G. (1996): Origin, composition and genesis of terra rossa in Istria.– Unpubl. PhD Thesis (in Croatian), University of Zagreb, 204 p.

DURN, G., OTTNER, F. & SLOVENEK, D. (1999): Mineralogical and geochemical indicators of the polygenetic nature of terra rossa in Istria, Croatia.– *Geoderma*, 91, 125–150.

DURN, G., SLOVENEK, D. & ČOVIĆ, M. (2001): Distribution of iron and manganese in terra rossa from Istria and its genetic implications.– *Geologia Croatica*, 54/1, 27–36.

DURN, G., OTTNER, F., TIŠLJAR, J., MINDSZENTY, A., & BARUDŽIJA, U. (2003): Regional subaerial unconformities

- in shallow-marine carbonate sequences of Istria: sedimentology, mineralogy, geochemistry and micromorphology of associated bauxites, palaeosols and pedo-sedimentary complexes.– In: VLAHOVIĆ, I. & TIŠLJAR, J. (eds.): Evolution of Depositional Environments from the Palaeozoic to the Quaternary in the Karst Dinarides and the Pannonian Basin. Field trip guidebook, 22nd IAS Meeting of Sedimentology, 209–255, Zagreb.
- DURN, G., ALJINOVIĆ, D., CRNJAKOVIĆ, M. & LUGOVIĆ, B. (2006): Heavy and light mineral fractions indicate polygenesis of extensive terra rossa soils in Istria, Croatia.– In: MANGE, M. & WRIGHT, D. (eds.): Heavy minerals in use. Developments in Sedimentology, Elsevier (in print).
- EBERL, D.D., SRODON, J. & NORTHROP, H.R. (1986): Potassium fixation in smectite by wetting and drying.– In: DAVIES J.A. & HAYERS, K.F. (eds.): Geochemical Processes at Mineral Surfaces.– Am. Chem. Soc. Symp. Ser., 323/14, 296–326.
- ELLENBERGER, F. (1955): Bauxites métamorphiques dans le Jurassique de la Vanoise, Savoie.– C.R. somm. Soc. Géol. Fr., Paris, 29–32.
- FERLA, P. & BOMMARITO, S. (1988): Bauxiti lateritiche mediojurassiche nei calcari della piattaforma carbonatica panormide di Monte Gallo (Palermo).– Boll. Soc. Geol. It., 107, 579–591.
- GRADSTEIN, F.M., AGTERBERG, F.P., OGG, J.G., HARDENBOL, J., VAN VEEN, P., THIERRY, T. & HUANG, Z. (1994): A Mesozoic time scale.– Journal of Geophysical Research, 99, 24051–24074.
- GUŠIĆ, I. & JELASKA, V. (1993): Upper Cenomanian–Lower Turonian sea-level rise and consequences on the Adriatic–Dinaric carbonate platform.– Geol. Rundsch., 82/4, 676–686.
- HOWER, J., ESLINGER, E., HOWER, M. & PERRY, E. (1976): Mechanism of burial metamorphism of argillaceous sediments. I. Mineralogical and chemical evidence.– Geol. Soc. Am. Bull., 87, 725–537.
- JENKYNS, H.C. (1991): Impact of Cretaceous sea level rise and anoxic events on the Mesozoic carbonate platform of Yugoslavia.– Amer. Ass. Petrol. Geol. Bull., 75, 1007–1017.
- MAGDALENIĆ, Z. (1972): Sedimentologija flišnih naslaga srednje Istre.– Acta Geol., 7/2, 71–100.
- MALEZ, M. (1981): Karst underground in Istria as a place for settling of fossil people (in Croatian).– In: EKL, V. (ed.): Liburnijske teme, 4 119–135, Opatija.
- MANATSCHAL, G. & BERNOULLI, D. (1998): Rifting and early evolution of ancient ocean basins: the record of the Mesozoic Tethys and of the Galicia–Newfoundland margins.– Marine Geophysical Researches, 20, 371–381.
- MARINČIĆ, S. & MATIČEC, D. (1991): Tektonika i kinematika deformacija na primjeru Istre (Tectonics and kinematic of deformations – an Istrian model).– Geol. vjesnik, 44, 247–268.
- MATIČEC, D., VLAHOVIĆ, I., VELIĆ, I. & TIŠLJAR, J. (1996): Eocene limestones overlying Lower Cretaceous deposits of western Istria (Croatia): Did some parts of present Istria form land during the Cretaceous?– Geologia Croatica, 49/1, 117–127.
- MINDSZENTY, A. & D'ARGENIO, B. (1994): Carbonate platform emergence and bauxite formation.– AAPG Annual Convention, Abstracts, Denver, 217.
- MOLINA, J.M., RUIZ-ORTIZ, P., VERA, J.A. (1991): Jurassic bauxites in the Subbetic, Betic Cordillera, Southern Spain.– In: Tethyan Bauxites IGCP-287 Part–I. Acta Geol. Hung., 34/3, 163–178.
- MORESI, M. & MONGELLI, G. (1988): The relation between the terra rossa and the carbonate-free residue of the underlying limestones and dolostones in Apulia, Italy.– Clay Minerals, 23, 439–446.
- MUHS, D.R., BUSH, C.A. & STEWART, K.C. (1990): Geochemical evidence of Saharan dustparent material for soils developed on Quaternary limestone of Caribbean and Western Atlantic islands.– Quaternary Research, 33, 157–177.
- MUHS, D.R., CRITTENDEN, R.C., ROSHOLT, J.N., BUSH, C.A. & STEWART, K.C. (1987): Genesis of marine terrace soils, Barbados, West Indies: Evidence from mineralogy and geochemistry.– Earth Surface Processes and Landforms, 12, 605–618.
- MUNSELL COLOR CHARTS (1994): Munsell Soil Color Charts.– Macbeth Division of Kollmorgem Instruments Corporation, New Windsor.
- NICHITTA, D. (1988): Stratigrafia e sedimentologia dei carbonati di piattaforma del Giurassico Superiore–Cretacico nel settore nord–orientale dei Monti di Palermo.– Unpubl. PhD Thesis, University of Palermo, 212 p.
- POLŠAK, A. (1970): Osnovna geološka karta SFRJ 1:100.000, Tumač za list Pula L33–112 (Basic Geological Map of SFRJ, 1:100000, Geology of the Pula sheet).– Institut za geološka istraživanja, Zagreb, Savezni geološki zavod, Beograd, 44 p.
- POLŠAK, A. & ŠIKIĆ, D. (1973): Osnovna geološka karta SFRJ 1:100.000, Tumač za list Rovinj (Basic Geological Map of SFRJ, 1:100000, Geology of the Rovinj sheet).– Institut za geološka istraživanja, Zagreb, Savezni geološki zavod, Beograd, 51 p.
- RADOJČIĆ, R. (1982): Carbonate platforms of the Dinarids: the example of Montenegro–West Serbia sector.– Bull. T. LXXX, Acad Serbe des Sci. et des Arts, Classe Sci. nat. et math., 22, 35–46, Beograd.
- RASMUSSEN, K. & NEUMANN, A.C.N. (1988): Holocene overprint of Pleistocene paleokarst: Bight of Abaco, Bahamas.– In: JAMES, N.P. & CHOQUETTE, P.W. (eds.): Paleokarst. Springer Verlag, 132–148.
- ROBINSON, D. & WRIGHT, V.P. (1987): Ordered illite–smectite and kaolinite–smectite: Pedogenic minerals in a Lower Carboniferous paleosol sequence, South Wales.– Clay Miner., 22, 109–118.
- SIMONE, L., CARANNANTE, G., D'ARGENIO, B., RUBERTI, D. & MINDSZENTY, A. (1991): Bauxites and related paleokarst in Southern Italy, Sicily and Sardinia.– In: Tethyan Bauxites IGCP-287 Part II. Acta Geol.Hung., 34/4, 273–306.
- ŠINKOVEC, B. (1974): Jurski glinoviti boksiti zapadne Istre.– Geol. vjesnik, 27, 217–226.
- ŠINKOVEC, B. & SAKAČ, K. (1991): Bauxite deposits of Yugoslavia – the state of the art.– In: Tethyan Bauxites IGCP 287 Part II., Acta Geol. Acad. Sci. Hung., 34/4, 307–316. 315316.
- STAMPFLI, G.M. & MOSAR, J. (1999): The making and becoming of Apulia.– In: GOSSO, G., JADOUL, E., SELLA, M. & SPALLA, M.I. (eds.): 3rd Workshop on Alpine Geological Studies. Memorie di scienze Geologiche, 51/1, 141–154, Padova.
- TIŠLJAR, J. (1978): Onkolitni i stromatolitni vapnenci u donjokrednim sedimentima Istre (Oncolites and stromatolites in Lower Cretaceous carbonate sediments of Istria (Croatia, Yugoslavia)).– Geološki vjesnik, 30/2, 363–382.
- TIŠLJAR, J. (1983): Coated grains facies in the Lower Cretaceous of the Outer Dinarides (Yugoslavia).– In: Peryt, T. (ed.):

- Coated Grains. Springer-Verlag, Berlin–Heidelberg–New York–Tokyo, 566–576.
- TIŠLJAR, J. (1986): Postanak crnih valutica i oblutaka (“black pebbles”) u periplimnim vapnencima titona zapadne Istre i barema otoka Mljeta (Origin of the black-pebbles and fragments in the peritidal limestones of the western Istria (Tithonian) and Island of Mljet (Barremian)).– *Geol. vjesnik*, 39, 75–94.
- TIŠLJAR, J. & VELIĆ, I. (1987): The Kimmeridgian tidal-bar calcarenite facies of Western Istria (Western Croatia, Yugoslavia).– *Facies*, 17, 277–284.
- TIŠLJAR, J. & VELIĆ, I. (1991): Carbonate facies and depositional environments of the Jurassic and Lower Cretaceous of the coastal Dinarides (Croatia).– *Geol. vjesnik*, 44, 215–234.
- TIŠLJAR, J., VELIĆ, I. & VLAHOVIĆ, I. (1994): Facies diversity of the Malmian platform carbonates in Western Croatia as a consequence of synsedimentary tectonics.– *Géologie Méditerranéenne*, 3–4, 173–176.
- TIŠLJAR, J., VLAHOVIĆ, I., MATIČEC, D. & VELIĆ, I. (1995): Platformni facijesi od gornjeg titona do gornjega alba u zapadnoj Istri i prijelaz u tempestitne, klinofornne i rudistne biolititne facijese donjega cenomana u južnoj Istri, ekskurzija B (Platform facies from the Upper Tithonian to Upper Albian in western Istria and transition into tempestite, clinoform and rudist biolithite facies of the Lower Cenomanian in southern Istria).– In: VLAHOVIĆ, I. & VELIĆ, I. (eds.): 1st Croatian Geological Congress, Excursion Guide-Book, 67–110, Zagreb.
- TIŠLJAR, J., VLAHOVIĆ, I., VELIĆ, I., MATIČEC, D. & ROBSON, J. (1998): Carbonate facies evolution from the Late Albian to Middle Cenomanian in southern Istria (Croatia): influence of synsedimentary tectonics and extensive organic carbonate production.– *Facies*, 38, 137–152.
- TIŠLJAR, J., VLAHOVIĆ, I., VELIĆ, I. & SOKAČ, B. (2002): Carbonate platform megafacies of the Jurassic and Cretaceous deposits of the Karst Dinarides.– *Geologia Croatica*, 55/2, 139–170.
- VANSTONE, S.D. (1988): Late Dinantian paleokarst of England and Wales: implications for exposure surface development.– *Sedimentology*, 45, 19–37.
- VELIĆ, I. & TIŠLJAR, J. (1987): Biostratigrafske i sedimentološke značajke donje krede otoka Veli Brijun i usporedba s odgovarajućim naslagama jugozapadne Istre (Biostratigraphic and sedimentologic characteristics of the Lower Cretaceous deposits of the Veli Brijun island and comparison with the corresponding deposits in SW Istria (western Croatia, Yugoslavia)).– *Geol. vjesnik*, 40, 149–168.
- VELIĆ, I. & TIŠLJAR, J. (1988): Litostratigrafske jedinice u doggeru i malmu zapadne Istre, zapadna Hrvatska, Jugoslavija (Lithostratigraphic units in the Dogger and Malm of western Istria).– *Geol. vjesnik*, 41, 25–49.
- VELIĆ, I., TIŠLJAR, J. & SOKAČ, B. (1989): The variability of thicknesses of the Barremian, Aptian and Albian carbonates as a consequence of changing depositional environments and emersion in Western Istria (Croatia, Yugoslavia).– *Mem. Soc. Geol. It.*, 40 (1987), 209–218.
- VELIĆ, I., TIŠLJAR, J., MATIČEC, D. & VLAHOVIĆ, I. (1995a): Opći prikaz geološke građe Istre (A review of the geology of Istria).– In: VLAHOVIĆ, I. & VELIĆ, I. (eds.): 1st Croatian Geological Congress, Excursion Guide-Book, 5–30, Zagreb.
- VELIĆ, I., MATIČEC, D., VLAHOVIĆ, I. & TIŠLJAR, J. (1995b): Stratigrafski slijed jurskih i donjokrednih karbonata (batgornji alb) u zapadnoj Istri (ekskurzija A) (Stratigraphic succession of Jurassic and Lower Cretaceous Carbonates (Bathonian–Upper Albian) in western Istria (Excursion A)).– In: VLAHOVIĆ, I. & VELIĆ, I. (eds.): 1st Croatian Geological Congress, Excursion GuideBook, 31–66, Zagreb.
- VERA, J.A., RUIZ-ORTIZ, P.A., GARCIA HERNANDEZ, M. & MOLINA, J.M. (1988): Paleokarst and related pelagic sediments in the Jurassic of the Subbetic Zone, Southern Spain.– In: JAMES, N.P. & CHOQUETTE, P.W. (eds.): Paleokarst. Springer Verlag, 364–384.
- VLAHOVIĆ, I. (1999): Karbonatni facijesi plitkovodnih taložnih sustava od kimeridža do gornjega alba u zapadnoj Istri (Carbonate facies of shallow water depositional systems from Kimmeridgian to the Upper Albian in Western Istria).– Unpubl. PhD Thesis (in Croatian with English summary), University of Zagreb, 327 p.
- VLAHOVIĆ, I., TIŠLJAR, J. & VELIĆ, I. (1994): Facies succession in the Cenomanian of Istria (Western Croatia): tectonic vs. eustatic control.– First International Meeting on Perimediteranean Carbonate Platforms, Abstracts, 169–171, Marseille.
- VLAHOVIĆ, I., TIŠLJAR, J., VELIĆ, I. & MATIČEC, D. (2000): Accumuli bauxitici e cicli peritidali shallowing upwards del giurassico superiore.– In: CARULLI, G.B. (ed.): Guida alle escursioni. 80a Riunione Estiva della S.G.I., Trieste, 245–252.
- VLAHOVIĆ, I., KORBAR, T., MORO, A., VELIĆ, I., SKELTON, W.P., FUČEK, L. & TIŠLJAR, J. (2002): Latest Cenomanian to Earliest Turonian platform drowning and Turonian recovery of shallow-water platform deposition in southern Istria.– In: VLAHOVIĆ, I. & KORBAR, T. (eds.) Abstracts and Excursion Guidebook – 6th International Congress on Rudists, Rovinj – Croatia. Institut za geološka istraživanja, Zagreb, 123–127.
- VLAHOVIĆ, I., TIŠLJAR, J., VELIĆ, I., MATIČEC, D., SKELTON, P.W., KORBAR, T. & FUČEK, L. (2003): Main events recorded in the sedimentary succession of the Adriatic Carbonate Platform from the Oxfordian to the Upper Santonian in Istria (Croatia).– In: VLAHOVIĆ, I. & TIŠLJAR, J. (eds.): Evolution of Depositional Environments from the Palaeozoic to the Quaternary in the Karst Dinarides and the Pannonian Basin. Field Trip Guidebook. 22nd IAS Meeting of Sedimentology, Opatija – September 17–19, 2003, 19–56, Zagreb.
- VLAHOVIĆ, I., TIŠLJAR, J., VELIĆ, I. & MATIČEC, D. (2005): Evolution of the Adriatic Carbonate Platform: palaeogeography, main events and depositional dynamics.– *Palaeogeography, Palaeoclimatology, Palaeoecology*, 220, 333–360.
- WINCHESTER, J.A. & FLOYD, P.A. (1977): Geochemical discrimination of different magma series and their differentiation products using immobile elements.– *Chemical Geology*, 20, 325–343.
- YAALON, D.H. (1997): Soils in the Mediterranean region: what makes them different?– *Catena*, 28, 157–169.

Field Trip 2
Ceramic and brick clays deposits and excessive flysch erosion

Stop 1

Deposit of brick clays Rečica

Boris KRUK¹, Ivan BROZOVIĆ², Željko KASTMÜLLER¹, Josip ZAJC³,
Darko TIBLJAŠ⁴ and Ljiljana KRUK¹

1. INTRODUCTION

The Rečica brick clays deposit have been chosen as a stop for the field trip in order to illustrate the deposit and type of clay that has been used as the raw material for brick production in Karlovac for a hundred years. Geological characteristics of the deposit, clay composition and the necessary technology for processing to obtain quality products with specific physical properties are presented.

For the past ten years the Wienerberger Ilovac d.d. company have produced porous bricks, called Porotherm block, using clays from the Rečica deposit modified by the addition of sawdust and quartz sand. Porosity in the bricks is created by the addition of burnable materials and is a recent technological advance. Due to the oil crisis at the beginning of the 1970's it became necessary to overcome the problem of how to construct buildings with a high thermal quality, with walls of low thermal conductivity. The buildings had to be durable and of stable construction while also creating a good internal microclimate. Full bricks ($\lambda=0.80$ W/mK) as well as block bricks ($\lambda=0.58$ W/mK) could not fulfil these requirements. In order to reduce the thermal conductivity of the walls close to the value of $k=d \times \lambda^{-1}=0.50-0.55$ m²K/W, it was necessary to improve the properties of the bricks. This was achieved by the inclusion of porosity by admixing combustible material (sawdust) to the clay. In this way, the qualities of the oldest and most widely used building material – brick – were improved.

2. GEOGRAPHIC LOCATION

Rečica, one of the biggest deposits of brick clays in Croatia, with proven reserves of 4.500,000 m³, is located in the Kupa river valley approximately 8 km northeast of the town of Karlovac, an important regional and transport centre. In the heartland of Croatia, Karlovac, with approximately 60,000 inhabitants, was founded as a six-pointed star fortress, constructed for protection from the Turks, near the old town of Dubovac, at the confluence of the Kupa, Korana, Mrežnica and Dobra rivers. It owes its name, which was originally Karlstadt, Carlstadt, or Carlstatt, to Archduke Charles II of Austria, upon whose orders construction began in 1579. The architect of the city was Matija

Gambon. The Renaissance core of the city, with its regular geometric arrangement of streets and central square, was the culmination of the architectural and fortification skills of that period, when city walls with bastions, palaces and squares, military and sacral buildings were built.

The deposit is located north of the Kupa River at the south-western rim of the Crna Mlaka Basin known as the Karlovačko Pokuplje (Fig. 1) in the lowlands area, 110 to 115 m a.s.l., characterized by ponds, swamps and fish-farms. The location of the deposit is 15°37'30" E and 45°32'10" N. It covers an area of 155 ha.

3. GEOLOGICAL AND GENETIC CHARACTERISTICS OF THE DEPOSIT

The deposit, as well as the whole of the Crna Mlaka Basin, is mostly composed of Quaternary clay beds, intercalated with layers and lenses of sands and fine-grained conglomerates, and Upper Neogene sands. Deeper parts of the basin are formed from Tertiary and Mesozoic sediments. The basin developed in the Pliocene–Pleistocene period. Older sediments in the footwall were dissected and covered by younger ones (BOJANIĆ & IVIČIĆ, 1974).

The Rečica clay deposit is represented by a series of sub-parallel and gently inclined, almost horizontal, layers of silty clay, which are laterally continuous (as confirmed by drilling). Layers of grey-blue sand and silt, containing some pebbles and clays, that represent an aquifer with sub-artesian water occur in the footwall. The major part of the clays is represented by the alternation of brown and grey, sometimes yellow clays that are underlain by greenish-grey and grey-blue clays. The clays are 8–12 m (average ~11 m) thick (Fig. 2).

The clay deposit is of an allochthonous fluvial–swamp–pond type. Clay was deposited during the Holocene under fluvial conditions, as well as in areas in which ponds, swamps and small lakes prevailed (DRAVEC-BRAUN et al., 1992).

4. GRANULOMETRIC, MINERALOGICAL AND CHEMICAL CHARACTERISTICS OF THE CLAY

Granulometric analyses revealed that clays of this genetic type at the Rečica locality contain 1.5–25.7 wt.% coarse silt,

¹ Croatian Geological Survey, Sachsova 2, HR-10000 Zagreb, Croatia (boris.kruk@hgi-cgs.hr)

² Wienerberger Ilovac d.d., Donje Pokupje 2, HR-47000 Karlovac, Croatia

³ Civil Engineering Institute of Croatia, Janka Rakuše 1, HR-10000 Zagreb, Croatia

⁴ Department of Geology, Faculty of Science, Horvatovac bb, HR-10000 Zagreb, Croatia

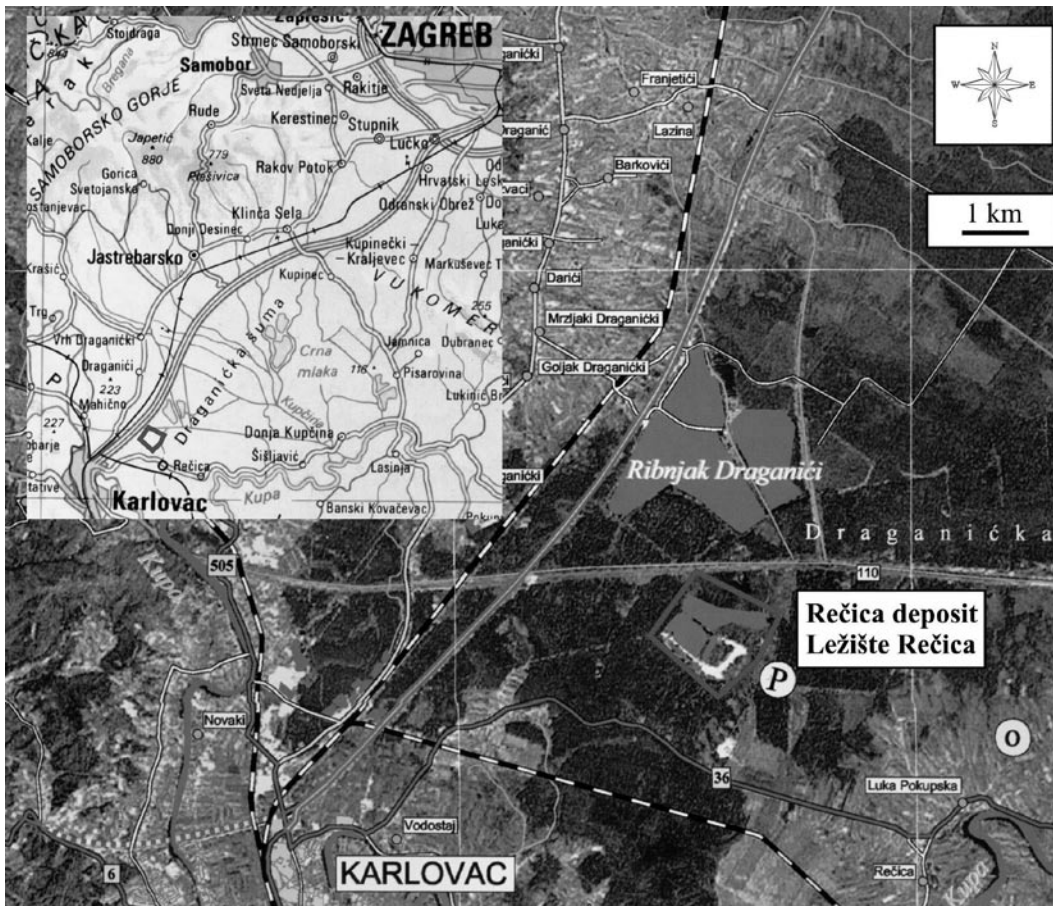


Fig. 1 Geographic location of the Rečica deposit.

10.4–25.7% mid-fine silt, and 32.5–88.1% clay size fraction, but usually they contain 40–60% clay. The average granulometric composition is given in Table 1.

Based on the results of X-ray, thermal and chemical analyses, clays from the Rečica deposit can be classified as a montmorillonite–illite variety, in accordance with their genetic type. The main mineral constituents are quartz, 10 Å phyllosilicate (illite and/or mica) and smectite group minerals, while goethite, kaolinite, chlorite, feldspars and dolomite are subordinate to accessory minerals. Quartz is mostly present in the silt fraction; clays with higher silt content also have higher quartz content.

Residue on the 4900 openings/cm² sieve is composed of quartz, feldspars, limonite grains, micas, rock particles and organic admixtures.

The average chemical content and ranges of oxides in these clays, based on 7 analyses, are given in Table 2.

Silica, together with alumina, is present in clay minerals and other silicates, but also as pure SiO₂. The presence of quartz in clays, if it is not too coarse, does not pose a problem. On the contrary, in the case of very plastic (fine) clays, it is used as a clay thinning medium, while in the pore-making process it is added to increase density.

Alumina, in contrast to silica, is not present in this clay as pure oxide; it is always bound in silicates. Higher contents of Al₂O₃ increase the refractory properties of the clay.

Iron is present in clays as cation in the clay mineral structures, however it can also be present in separate min-

erals (e.g. goethite). Since the colour of the brick is dependent on the iron content, >3% Fe₂O₃ is desirable. However if this exceeds 7%, due to the fact that iron acts as a fusing agent, it lowers the melting point and can have a negative influence on brick burning processes. In order to transform other iron minerals to red coloured Fe₂O₃ it is necessary to perform oxidative burning. Otherwise black stains of FeO will occur, especially if organic material is present. This phenomenon will have no effect on the quality of the brick, it is purely aesthetically undesirable.

Calcium and magnesium are present in the clay as carbonates (CaCO₃ and MgCO₃), or Ca²⁺ and Mg²⁺ cations within the crystal structures of clay minerals. They do not cause problems, unless they are present in carbonate grains coarser than 200 μm or if the carbonate content is higher than 20%. In the kiln, oxides are formed during carbonate decomposition. The presence of dispersed carbonates will result in the formation of very small pores.

5. LABORATORY INVESTIGATIONS OF OTHER QUALITY PARAMETERS

In addition to the above analyses several other technological parameters of the clay were measured (Table 3), on 13 samples.

These clays are characterized by their very fine grain size (residue on the 4,900 holes/cm² sieve is <4%, while on the 10,000 holes/cm² sieve it is ~ 9.9%), which demands special processing procedures. As a result of their grain size, these clays tolerate a high content of additives (up to

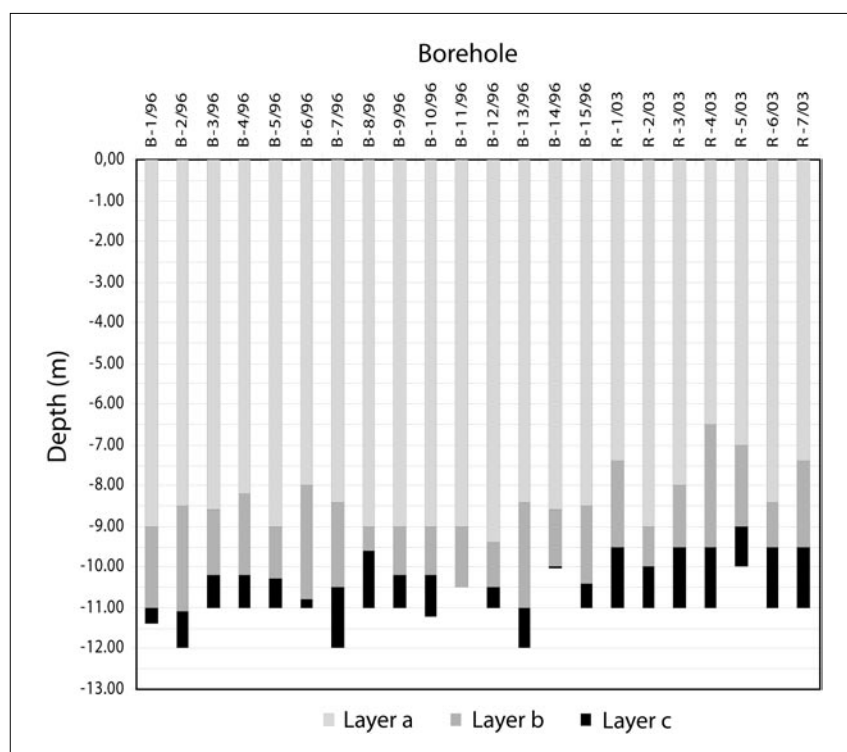


Fig. 2 Characteristic lithological cross sections in some boreholes in the Rečica deposit.

Table 1 Average granulometric composition of clays from the Rečica deposit.

Granulation (μm)	63–20	20–16	16–10	10–6	6–3	3–2	<2	Total
Average (wt. %)	14.55	5.56	10.03	8.43	4.14	1.83	55.48	100.00

40 vol.% of quartz sand and sawdust), while retaining a pressure strength above the required standard values (min. 10 MPa).

Investigation performed on single (124 analyses) and composite (13 analyses) samples showed that these clays have a very high (40–60%) clay size fraction content. Consequently they have high plasticity, and sensitivity during drying, requiring careful attention during brick production. This problem can be reduced by the addition of tempering material (sawdust and quartz), which will result in a more porous final product, that will still have satisfactory physico-mechanical properties. This was confirmed by high bending strength in both the dry and burnt states, as well as by the pressure strength of burnt cylinders. The same result was obtained from the final products that were made using the raw materials originating from the Rečica deposit. Clinkering temperatures are above 1000°C, and sintering temperatures are great enough, therefore no problem is expected during burning at high temperatures. When used in combination with tempering material, the clay is proven to be a suitable raw material for thin walled brick products (blocks, panels, partition ceiling elements, normal format bricks). In addition, energy consumption during the production process was reduced.

6. CLAY EXPLOITATION

Clays are excavated by hydraulic excavator, while a bulldozer is used for terrain levelling. Exploitation occurs on

Table 2 Chemical composition of clays from the Rečica deposit.

	Minimum	Maximum	Average
SiO ₂	54.70	64.70	60.76
Al ₂ O ₃	11.83	18.94	17.03
Fe ₂ O ₃	3.86	8.91	5.66
MgO	0.90	2.66	1.29
CaO	0.47	3.22	1.14
Na ₂ O	0.08	0.75	0.42
K ₂ O	1.67	2.11	1.89
TiO ₂	0.77	1.13	0.99
P ₂ O ₅	0.02	0.14	0.07
MnO	0.01	0.06	0.03
LOI	8.20	11.99	10.10
TOTAL	98.97	99.79	99.36

three benches, 2–4 m in height. Their width, prescribed by the mining project, is at least 20 m (determined by truck manoeuvrability). Excavated clays containing approximately 20% moisture are transported by trucks and stored on the stock in the plant. There it is levelled and flattened by bulldozers so that during the autumn and winter only the upper 10–15 cm are soaked. Clay that is stored in a proper manner retains its natural moisture level, which is optimal for shaping. Access roads to the deposit and warehouse have to be asphalted or covered by crushed bricks,

Table 3 Investigation results of technological parameters for the Rečica deposit clay.

	Minimum	Maximum	Average
Residue on the 4,900 openings/cm ² sieve	0.80	3.15	1.88
Bulk density (kg/dm ³)	1.80	1.88	1.83
Fracture strength in dry condition (N/mm ²)	6.60	14.07	10.23
Fracture strength after ignition at 950°C (N/mm ²)	12.73	13.35	13.07
Fracture strength after ignition at a 980°C (N/mm ²)	16.30	34.40	28.21
Plasticity after Pfeferkorn		very high	
Shrinkage after drying at 105°C (%)	8.75	10.50	9.52
Sensitivity of clay on drying – BIGOT		very sensitive	
Shrinkage after ignition at 930°C (%)	9.23	11.10	10.01
Shrinkage after ignition at 950°C (%)	9.55	12.50	10.68
Shrinkage after ignition at 980°C (%)	9.50	12.70	11.27
Clinkering temperature (°C)	1015.00	1093.00	1047.00
Sintering temperature (°C)	1065.00	1140.00	1097.69
Water uptake after ignition at 930°C (%)	11.58	18.19	13.46
Water uptake after ignition at 950°C (%)	11.20	11.90	11.44
Water uptake after ignition at 980°C (%)	8.02	16.11	10.58
Pressure strength-cylinders Φ=50 mm and h=35 mm (N/mm ²)	20.20	56.30	40.58

in order to prevent mixing of clays with limestone. Exploitation takes place on terrain that is partially covered by water; therefore water is collected in the excavations, and should be pumped into drainage channels. In order to prevent penetration of sub artesian waters present in the underlying aquifer, exploitation is performed so that the lowermost 0.5–1.0 m of clay is left in the deposit. Exploitation outwith the dry period of the year (April–October) would be possible, but more complicated, and is therefore avoided. During a year approximately 200,000 m³ (320,000 t) of clay is excavated.

In the clay deposit three to four clay beds are clearly visible. The thickness of the grey brown and yellow clays present in the upper part changes laterally, sometimes yellow clays are completely missing. They are underlain by grey–blue and greenish–grey clays that have slightly higher silt contents. During exploitation, different clays are excavated in amounts proportional to bed thickness. Material is stored in horizontal layers that are used vertically. In this way, a more or less uniform clay composition is achieved in accordance with brick production needs. The humus layer is very thin (approximately 30 cm); therefore it is removed annually from the area that will be exploited next year.

The area of the deposit is mostly covered by low plant cover and grass, therefore the mining activity does not result in environmental devastation. Small artificial lakes, with very clean water, stocked with fish, are ideal for recreational fishing, and remain after exploitation.

7. PRODUCTION TECHNOLOGY IN THE WIENERBERGER ILOVAC d.d. BRICK FACTORY

Raw materials for production of porous bricks are:

- clay,
- combustible matter – sawdust, and
- quartz sand.

Principal processes in brick making are:

- excavation and transport of raw materials,
- raw material preparation,
- shaping,
- drying,
- burning, and
- packing.

Details of some of the processes that are specific for porous brick production are given below.

Clays for porous brick production must have higher plasticity than those for normal bricks due to the fact that they should accept higher quantities of additives. Clays in the Rečica deposit occur in three to four beds, differing significantly in colour and other properties. Since clays from all beds can be classified as brick making clays, there is no waste, but it is necessary to mix them in quantities proportional to bed thicknesses during storage. This is accomplished quite easily by retaining equal widths of benches during excavation.

The favourable characteristic of this clay is the presence of all size fractions. A high content of the fine fraction (55.48% <2 μm) is of great advantage for present day technology, as it allows inclusion of high quantities of admixtures without reducing the pressure strength of the final product. Taking into account the rough method of raw material dosing (due to the valve on the trunk feeders), the fineness of the clay provides greater technological certainty.

The mineral composition is responsible for the higher sensitivity during drying; therefore more attention should be paid at this stage of the process. This characteristic is slightly reduced by the additives, as they counteract the sensitivity conditioned by the grain size. Variations in mineral composition are not crucial for brick making clays.

Burning material is crushed material that is burned in the kiln, leaving pores in the brick. In this way porous brick walls, that provide specific brick characteristics, are obtained. Usually this material is sawdust, which is also used in this process, but other materials such as coal dust or pulp from paper production, could also be used. Sawdust is not sorted in any way, and there is no exact data on its origin. According to the contract, suppliers do not have any obligation to provide such data. They have to provide dust that does not contain splinters or shavings, and is not rotten, as this makes mixing more difficult. Before mixing with clay, sawdust is sieved on rotational sieve. Sawdust is stored under cover to avoid excessive wetting and decay. The drying process is significantly improved by the addition of sawdust, and the most common problems, i.e. cracking and deformation, are reduced. Sawdust does not create any problems during raw material preparation and shaping; in contrast it accelerates and facilitates drying.

Quartz sand is used as an inert material that increases the density of the final product. The pore making process results in lower density, and consequently the sound insulation capability is also reduced. In order to achieve sound insulation that is within the prescribed limits it is necessary to add material of higher density. This addition has no significant influence on the production process, except during the cooling of burned products. Sand is stored under cover, otherwise it can become saturated, and this additional moisture could cause problems during processing.

Raw materials are prepared in ordinary brick making facilities, i.e. filter, trunk feeders, mixers, mills and ageing depot. The aim of the preparation is cleaning, fragmentation and homogenisation of the raw materials with respect to composition and moisture. The moisture content of the material ready for modelling is roughly 20%.

Clay, sand and sawdust are mixed together in an approximately 3:1:1 volume ratio. The ratio is determined empirically, taking into account both modelling parameters and the prescribed properties. Therefore the ratio is dependant on the product type as well as on the production line. The desired ratios are obtained by regulating bolts on the trunk feeders that are used for dosing. Raw materials are mixed and milled in special rotary mixers and two pairs of differential mills. When the mixture is too dry, as deduced from machinery strain, water can be added at this stage. Humidity is also controlled each hour by analytical balance. The mixture is left for three days at an ageing depot. If the humidity is too high $\text{Ca}(\text{OH})_2$ powder is added.

The mixture is transported to the **modelling** vacuum press. On the way to the press, it is homogenized once again in a circular homogenizer in which the clay is exposed to overheated steam in order to achieve a uniform temperature throughout product walls and to facilitate and speed up the drying process. If the mixture is prepared in the proper way, and the modelling parameters are well chosen, sawdust is not visible on the raw product; it is seemingly compact and homogenous.

Drying with recirculation of wet air is performed in tunnel dry kilns with a recurrent channel, which are filled through one and evacuated through another door. A mini-

mal number of door openings, i.e. highly uniform atmosphere in the kiln is achieved in this way. Initially, the air is taken from the first zone of the kiln, reheated and returned to the kiln. Due to this procedure the products in the first phase are warmed to approximately 40°C , without drying. Only in the second phase, at a constant temperature of $45\text{--}50^\circ\text{C}$ does the drying start. In the final stage of drying, which begins when the relative humidity reaches 50%, the humidity drops quickly, and temperature rises quickly to $85\text{--}95^\circ\text{C}$. A constant temperature indicates that drying is finished.

Burning takes place in a tunnel brick kiln equipped with a preheating chamber. Sawdust already starts to burn in the preheating area, therefore it is necessary to introduce cold air in order to inhibit excessive temperature rise. The burning is performed in an oxidative atmosphere in order to prevent reduction of Fe^{3+} to Fe^{2+} , which would produce black oxide. In addition, some sawdust would be carbonized, and consequently black spots would form – the quality of the bricks would still be the same, but they would not be aesthetically acceptable. The optimum capacity of the kiln is 50 wagons per day, and maximum temperature is roughly 900°C .

8. CHARACTERISTICS OF POROUS BRICKS

Optimum insulation properties

Despite scientific progress, a universal building material does not exist. Excellent properties of modern building materials become prominent only in combination with other materials and construction methods; therefore they are often too expensive or too complex for most uses. Modern brick blocks, having harmonized thermal, fire-prevention and sound insulation properties, are highly competitive with advanced building materials, and at the same time they enable fast and simple building. Table 4 gives a comparison of the thermo-technical properties of porous bricks and other materials.

Thermal insulation

High resistance to heat transfer classifies brick into the group of thermal insulators. This property is especially pronounced in porous bricks; therefore they can compete with other more complicated and expensive systems that are used in everyday practice. For example a single wall 38 cm thick made of porous brick (e.g. Wienerberger Porotherm) has much better thermal insulation properties than a common 29 cm thick brick wall protected by a 5 cm thick layer of thermal plaster. Consequently, in the field of modern housing construction, porous brick blocks are unrivalled.

Refractory properties

Brick is an entirely inorganic material, therefore it is non-combustible. In accordance with the German standards (DIN 4102, T4) on the basis of combustibility it is classified into class A – non-burnable material. Already a 115 mm thick brick wall has F90 class fire resistance; i.e. in the case of fire bricks will maintain their bearing power for at least

Table 4 Comparative thermo-technical properties of some building materials. Legend: * Wienerberger Porotherm type.

Material	Density φ [kg/m ³]	Coefficient of thermal conductivity λ [W/mK]	Resistance factor to the diffusion of water vapour M
Full brick	1200–1800	0.47–0.76	5–12
Hollow brick	1200–1400	0.52–0.61	4–6
Porous brick*	800	0.18	8
Perlitic mortar	500	0.13	4
Aerated concrete	400–800	0.14–0.29	2–7
Concrete	1800–2500	0.93–2.33	1–1.5

90 minutes, which is according to the standard the prescribed minimum for outer walls.

Furthermore, single brick walls have the important property that in the case of fire there is no development of smoke and toxic gases, therefore bricks represents a good choice for fire-prevention walls.

Sound proofing

These days sound proofing properties of building materials are very important. Various noise sources surround buildings in which we live and work, often they are present in buildings themselves. In such environments bricks are the optimum building material; thick outer walls guarantee good sound and thermal insulation at same time, in contrast to some other products, e.g. aerated concrete which is a good thermal insulator, but unfortunately has poor sound proofing characteristics.

Mechanical properties – mortar pockets system

The Porotherm S brick blocks system is characterized by its unique technological solution for construction in seismically active areas. A mortar pockets system contributes to a several fold increase of walls tensile strength, allowing building without tie column even in IX earthquake zone. In the case of buildings with multiple floors, tie columns are built; so that even in the earthquake zone IX, three-storey houses (ground floor + two floors + attic) can be built. In other areas four-storey (VIII zone) and five-storey houses

(VII zone) with attics are allowed. All Porotherm S blocks have a mortar pockets system that allows a complete choice of structural wall thickness, starting with Porotherm 20 S P+E block for 20 cm thick bearing walls. The biggest block available is Porotherm 38 S P+E for 38 cm thick walls.

Advantages of porous bricks in reference to the traditional bricks are:

- increase in thermal insulation capability – approximately 2.5 times better thermal insulation on the basis of thermal conductivity (λ),
- reduction of volume mass,
- higher water uptake,
- same or slightly higher brick pressure strength,
- higher wall tensile strength, in other words higher wall stability in the case of earthquake, for mortar pocket type (S class).

9. REFERENCES

- BOJANIĆ, L. & IVIČIĆ, D. (1974): General hydrogeologic characteristics of the Crna Mlaka Basin (northwestern Croatia) (in Croatian with English abstract).– *Geološki vjesnik*, 27, 265–271, Zagreb.
- DRAVEC-BRAUN, J., BRAUN, K., CRNIČKI, J & ZAJC, J. (1992): Brick making clays in Croatia (in Croatian).– Symposium: Industry of non-metallic raw materials in renewal and development of Republic of Croatia. 40–51, Zagreb.

Stop 2

Ivošević Gaj ceramic clay deposit in the vicinity of Vojnić

Radovan AVANIĆ¹, Koraljka BAKRAČ¹, Anita GRIZELJ¹, Lara WACHA¹, Mirjana ŠIMIĆ-STANKOVIĆ², Ljerka HEĆIMOVIĆ³, Darko TIBLJAŠ⁴ and Boris KRUK¹

The exploitation field Ivošević Gaj is located in the eastern part of Karlovac County, 25 km south of the town of Karlovac, and approximately 8 km northeast of the town of Vojnić (Fig. 3). The history of the investigations, geological characteristics of the region, as well as the mineral and chemical properties of the clay will be presented. The geological column Katinovac-1, recorded within the deposit, is used to present the sedimentary succession and to explain the depositional environment of the clays and overlying sediments during Pliocene–Pleistocene times.

1. HISTORY OF INVESTIGATIONS

Ceramic clays in the Ivošević Gaj deposit (Fig. 4) are used by the Inker d.d. company from Zaprešić, as raw materials for ceramic tiles, and to lesser extent, the production of sanitary ceramics. Initial investigation of the deposit, and the whole Vojnić area, began in 1968 and continued until 1974, as part of regional investigations of the Banija and Kordun minerogenic regions (ŠIMUNIĆ & MILOŠEVIĆ, 1969; ŠIMUNIĆ, 1974). The investigated area was divided into two parts. In the eastern part, during 1978–1989 a total of 1551 m of boreholes were drilled, and an average thickness of 3.2 m for the clay layer was calculated. Investigations in the Western part of the exploitation field, having an area of 12.9 ha, began in 1981, and were completed in 1989. In 1989 and 1990 a report on the reserves, based on 2272 m that were drilled, concluded that the clay occurs in 6 lenses, averaging 3.9 m in thickness. In 1996 both parts were merged into a single deposit. Planned annual production was 35,000 t of raw material for sanitary ceramics and tile production. At present the deposit is not exploited due to the fact that a new regional plan is under construction.

2. GEOLOGICAL CHARACTERISTICS OF THE WIDER AREA

In the area of the Ivošević Gaj deposit, rocks of the following ages have been found: Upper Palaeozoic, Lower Triassic, Middle to Upper Triassic, Upper Pliocene and Pleistocene.

Upper Palaeozoic (Pz₃) rocks occurring south of the deposit belong to the Palaeozoic rocks that crop out on the north-eastern slopes of Petrova gora. They are represented by conglomerates, greywackes, quartz-greywackes and shales (ŠIMUNIĆ, 1974). In the Vojišnica and Vujić Creek valleys, Lower Triassic sedimentary rocks (T₁) – silts, marls, shales and sandstones – of characteristic red, violet and brown colour, have been described. In the Vujić Creek area, Lower Triassic sediments are overlain by weathered basic extrusive rocks (spilites). Middle to Upper Triassic rocks (T_{2,3}) have been described east and southeast of the deposit in the Berek region. The main characteristic of these sediments is the presence of dolomites. South of the deposit in the Berek, Vojišnica and Vujić Creek area, beds of gravels, quartz sands and silts, determined as the lower part of Middle to Upper Pliocene layers (¹Pl_{2,3}) overlie them with erosional contact. The age of these sediments is not documented by fossils, therefore a Pliocene–Pleistocene age cannot be excluded. According to the geological map, the most wide-spread rocks are sands, silts and ceramic clays of Middle to Late Pliocene age (²Pl_{2,3}). It can be assumed that these sediments are also of Pliocene–Pleistocene age. The youngest deposits consist of Holocene deluvial and organogenic pondy clastics and humus.

3. MINERAL AND CHEMICAL PROPERTIES OF CLAY

Investigation drillings revealed that the upper part of the Middle to Upper Pliocene deposits (²Pl_{2,3}), which comprise ceramic clays are up to 50 m thick (STANKOVIĆ, 2000). Clays are underlain by yellow, grey and white sands that sporadically contain gravels. Multicoloured quartz sands containing gravels, with an average thickness of 8.24 m overlie them. Alternatively, they are covered by yellow or red-brown sandy clays (of variable thickness) and a thin, up to 0.5 m thick layer of humus.

The ceramic clays are plastic, yellow or light to dark grey in colour. They occur as larger or smaller discrete lenses in several levels. In the eastern part of the Ivošević Gaj deposit, three lenses, having an average thickness of 3.2 m occur. In the western part there are 6 lenses; their

¹Croatian Geological Survey, Sachsova 2, HR-10000 Zagreb, Croatia (ravanic@yahoo.com)

²Tehnokop d.d., Kuplensko bb., HR-47220 Vojnić, Croatia

³Inker d.d., Industrijska 1, HR-10290 Zaprešić, Croatia

⁴University of Zagreb, Faculty of Science, Horvatovac bb, HR-10000 Zagreb, Croatia

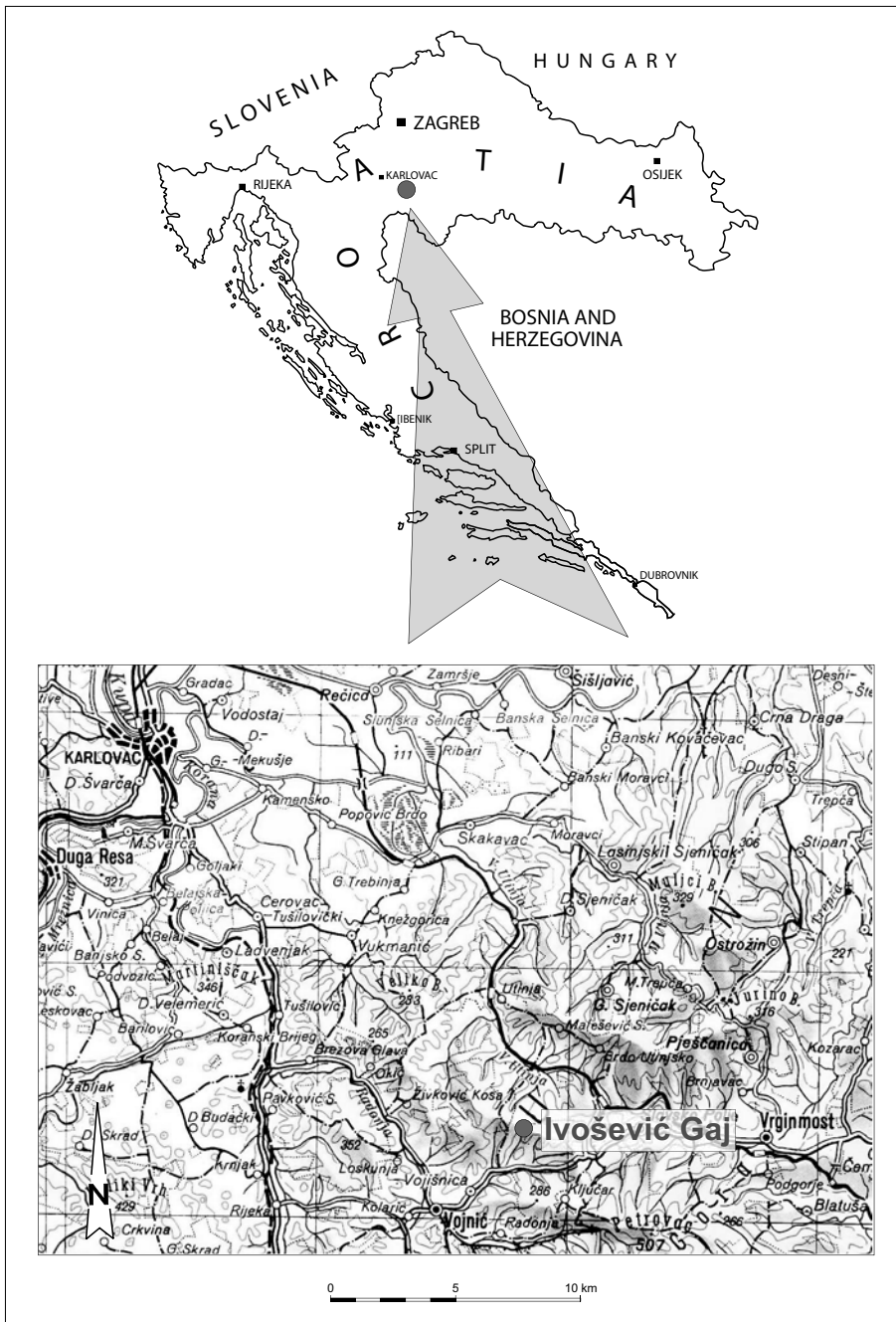


Fig. 3 Location map of the Ivošević Gaj clay deposit.

average thickness is 3.9 m. Their chemical composition expressed in wt.% is:

SiO ₂	68.92–79.08
Al ₂ O ₃	14.30–28.20
Fe ₂ O ₃	0.95–3.31
TiO ₂	0.11–1.61
CaO	0.20–1.75
MgO	0.10–2.20
K ₂ O	0.20–2.72
Na ₂ O	0.08–0.51
LOI	3.30–15.98

Volume weight is 1.937–1.98 t/m³. According to the results of mineralogical investigations of the clay minerals, kaolinite and illite, present in concentrations of 15–28% and 10–20%, respectively, are more abundant than montmorillonite.

4. COLUMN KATINOVAC–1

The geological column Katinovac–1 was recorded in the western part of the Ivošević Gaj ceramic clay deposit (Fig. 5), north-east of Vojnić near the Katinovac locality. Sediments within the column are 22 m thick and comprise several facies: Massive clays facies, Facies of sands with gravel lenses and Facies association A (Fig. 6). Lithostratigraphically these layers are comparable with the “Bistra formation”.

The Massive clays facies was observed in the lower part of the column (interval 1) as well as in the upper part as two intercalations (intervals 6 and 8). The total thickness of the layers belonging to this facies is 3.2 m, i.e. they form 14.6% of the total column thickness (Fig. 6). The Facies of sands with gravel lenses and Facies association A appear below and above the clays. The lower boundary is sharp, slightly



Fig. 4 Ceramic clay deposit Ivošević Gaj”.

wavy, while the upper one is sharp, erosional or smooth. The clay is massive, white to light grey (Fig. 7), sometimes dark grey due to a higher content of plant remains. Clays within the top 0.15 m of the interval 1 are limonitized (yellow–orange colour), and contain fine-grained sand laminae (Fig. 8). The laminae are 1–5 mm thick, horizontal to slightly wavy. Towards the top, the sand content increases, but the sand:clay ratio is never greater than 1:10. In the upper part of the column (interval 6), laminae of fine-grained sand (1–10 mm thick), having horizontal and wave lami-

nation are observed within the clays. Sometimes slumps are also present. The mineral and chemical composition of this clay corresponds to the previously mentioned clay composition from the deposit. Phytoclasts are the dominant organic remnant, but pollen grains of *Pinus* sp. and *Cichorium* sp. and phycoclasts of prasinophyte algae are also observed. By comparison to similar deposits in the surroundings of Zagreb, and, based on the poor palynological association, it can be concluded that this facies belongs to the Pliocene–Pleistocene.

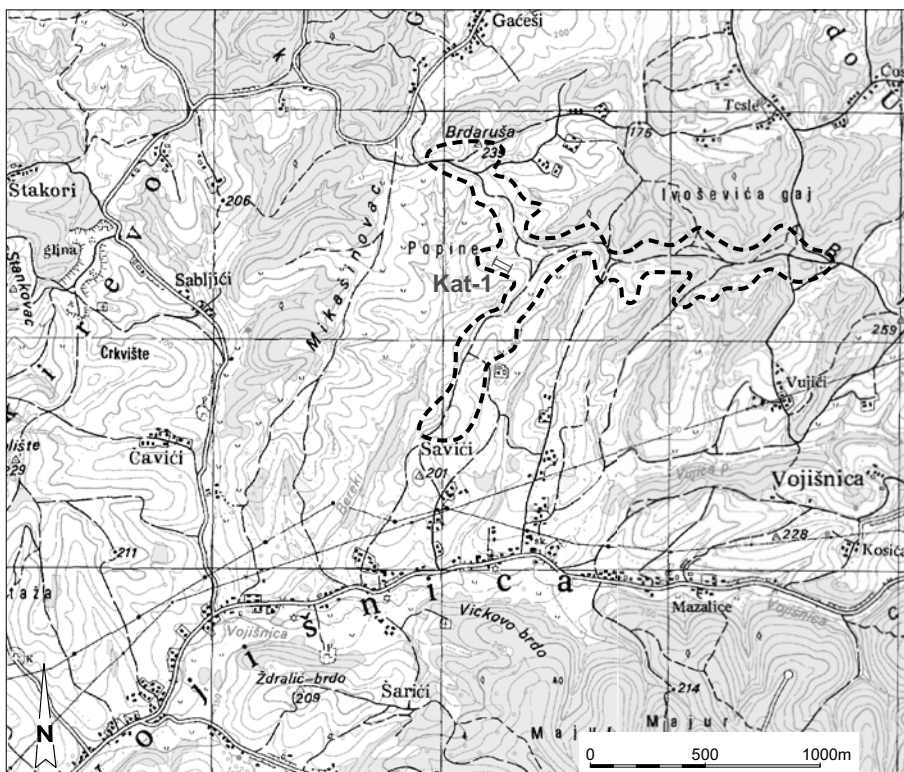


Fig. 5 Location map of the Katinovac-1 column.



Fig. 7 Massive clay facies.



Fig. 8 Massive clay facies and Facies of sands with gravel lenses.

Clays were deposited from suspension in stagnant water. However, fine-grained sands were partly deposited from suspension, and partly by traction by a very weak low-density current. The association with other facies, together with the observed palynomorphs and lignohumin remains, indicates that these sediments were most probably deposited in oxbow lakes and alluvial plains of fluvial environments.

The Facies of sands with gravel lenses occurs in the lower and upper parts of the column (intervals 2, 3, 4 and 7); its thickness is 11.2 m and it comprises 50.9% of the layers (Fig. 6). The Massive clays facies was observed below it (Fig. 8), while Facies association A (Fig. 11) and Massive clays facies are above it. The lower boundary is sharp,

smooth or erosional, while the upper one is sharp, erosional or uneven. Sands are fine- to coarse-grained, massive, white to grey, but also coloured due to the presence of iron hydroxides. In the lower part of the column, infrequent clay laminae (1–10 mm) are present, and horizontal and wave laminations are visible (Fig. 8). These sands are well sorted, and the grains are moderately to well-rounded. Within the light fraction, quartz is the dominant constituent (87%), rock fragments are less abundant (9–15%), K-feldspars are rare (0–4%). Chert fragments are the most common rock fragments, while quartzite fragments are rarer. Within the heavy mineral fraction, transparent minerals prevail (82–39%) over opaque ones (61–18%). The most common transparent minerals are tourmaline (55–10%), zircon (55–11%) and rutile (40–16%), while



Fig. 9 Clay laminae in the lower part of the Facies of sands with gravel lenses.



Fig. 10 Gravel lens in the sand.

chromite (8–0%) and staurolite (4–0%) are less abundant. Gravel occurs in lenses up to 0.2 m thick, and up to 10 m in lateral extent (Fig. 6). The lower bedding plane is sharp, erosional, while the upper one is sharp and uneven (Fig. 11). In the bottom of the lenses, lag deposits are observed, and sometimes normal gradation is poorly visible. Gravel is polymict, poorly sorted, clast- to matrix-supported. The matrix is medium-grained to granular sand. Pebbles are semi-rounded to rounded, bimodal, having diameters of 0.3–1 cm, and 5–10 cm rarely to 15 cm. They are mostly quartzite, with subordinate ortho-quartz conglomerate and sublithoarenite.

Fine- to coarse-grained sands, with a massive appearance and only sporadically visible lamination, that occur

within an alluvial environment MIALL (1996, 2000) classify within the sand facies as a result of gravitational flow. Such sands are characteristic of channels, in other words longitudinal channel sandbanks, and are the result of river bank collapse. Horizontally laminated clay was deposited from suspension, most probably in a flood plain environment. The erosional character of the lower boundary, together with large pebble dimensions indicates high water energy and deposition in the river channel. The matrix appearance and normal gradation indicate a reduction in current speed, while clast-support and lag deposits, together with gravel thickness indicate shallow sedimentary bodies (MIALL, 1996, 2000). In spite of the fact that the type of gravel facies cannot be determined unambiguously, the de-



Fig. 11 Erosional boundary between the Facies of sands with gravel lenses and Facies association A.



Fig. 12 Intraclasts and broken layers in Facies association A.

scribed sediments have the main characteristics of alluvial channel environments. However, there is visible evidence for rare and short term flood plain environments.

Facies association A is present in the upper part of the column within intervals 5 and 9 (Fig. 6). The total thickness is 7.6 m; it comprises 34.5% of all sediments. It is underlain by the Facies of sands with gravel lenses (Fig. 10) and Massive clays facies, which is also observed above (Fig. 13). The lower boundary is sharp and erosional, and the upper one is sharp and uneven. Facies association A is composed of a succession of small fining-upward cycles, which generally contain gravel, sand and clay (Fig. 6). Most of the cycles are incomplete, they contain gravel and sand, or rarely sand and clay. Their thickness varies from 5-50 cm. One

small coarsening-upward cycle was also observed. Fining-upward cycles contain fine- to coarse-grained gravels that form beds 3–40 cm thick. Their lower boundary is erosional, while the upper one is uneven. Within them normal gradation, clay intraclasts and fragmented clay layers are visible (Figs. 12 & 14), and some layers are amalgamated. These gravels are polymict, clast- to matrix-supported. The matrix is medium-grained to granular sand. Pebbles, having diameters 0.5–3 cm, and rarely up to 7 cm, are moderately- to well-rounded. They are mostly of quartzite and radiolarian cherts, and more rarely of sublitharenites and meta-sublitharenites. Sands occur on gravels (Fig. 11) and less frequently on clays, and have uneven or erosional bedding planes. Their grain size varies from granular to fine-



Fig. 13 Horizontal and wave lamination in massive clay between Facies association A and the Facies of sands with gravel lenses.



Fig. 14 A clay slump between Facies association A and the Facies of sands with gravel lenses.

grained. Normal gradation, cross- and parallel-bedding and clay intraclasts can be observed (Fig. 13). Sands are very poorly sorted, and grains are moderately rounded. Within the light fraction quartz is the most abundant (85%), while rock fragments (cherts and quartzites) are less common (15%). Among the heavy minerals, opâque minerals are more abundant (55%) than transparent ones (45%). Tourmaline is the most abundant transparent mineral (52%), rutile (24%) and zircon are less common (12%), while chromite (4%), undetermined grains (4%) and staurolite are rare (3%). Clay occurs at the top of the fining-upward cycles. It is underlain by sands, while gravel and sand occur above it. The lower bedding plane is uneven, and the upper one is uneven or erosional.

The nature of the lower erosional boundary, sand grain size and pebbles, clast support, as well as intraclasts and fragmented clay layers indicate that sediments belonging to Facies association A were deposited under high water energy conditions. The presence of a matrix in the gravels suggests pulsating flow, while normal gradation indicates reduction in flow rate. Gravels represent sediments of the channel base. Normally graded sands, horizontal and cross-bedding indicate strong currents with gradual decreasing flow rates. Sands were also deposited in the channel, but during periods of low water. Rare occurrences of clay indicate deposition from suspension on short-term alluvial plains. Fining-upward cycles suggest current speed decrease, occasional channel abandonment and formation

of short-term flood plains. Small coarsening-upward cycles possibly indicate channel reactivation. These characteristics of Facies association A suggest that sedimentation occurred primarily within the river channel which was characterized by rapid changes of filling and abandonment. During the filling phase the channel was active, and gravel and sand were deposited in it. During periods of abandonment, in the course of floods when small flood plains were formed, clays were deposited over these sediments.

The sedimentary succession within the Katinovac-1 column, beginning with a flood plain environment and finishing with the development of channel sediments, that show coarsening-upward tendency, generally suggests progradation of a river system.

5. REFERENCES

- MIALL, A.D. (1996): *The Geology of Fluvial Deposits. Sedimentary Facies, Basin Analysis and Petroleum Geology.*– Springer-Verlag, Heidelberg, 582 p.
- MIALL, A.D. (2000): *Principles of Sedimentary Basin Analysis.*– 3rd ed., Springer-Verlag, Berlin–Heidelberg, 616 p.
- STANKOVIĆ, M. (2000): *Elaborat o obnovi rezervi keramičke gline na eksploatacijskom polju "Ivošević Gaj" kod Vojnića.*– Arhiva Inker Zaprešić, Zaprešić.
- ŠIMUNIĆ, Al. & MILOŠEVIĆ, F. (1969): *Regionalna istraživanja minerogenog područja Banija–Kordun.*– Fond struč. dok., Hrv. geol. inst., Zagreb.
- ŠIMUNIĆ, Al. (1974): *Istraživanje keramičkih glina sjeverno od Vojnića (Regionalna istraživanja minerogenog područja Banija–Kordun za 1973. god.).*– Fond struč. dok., Hrv. geol. inst., Zagreb.

Stop 3

Excessive flysch erosion – Slani Potok

Vladimir JURAK, Dragutin SLOVENEĆ and Marta MILEUSNIĆ

A significant amount of Mid-Eocene flysch is present in the coastal parts of Croatia. Over the whole region, flysch is subjected to erosion to a greater or lesser extent. However, there is excessive flysch erosion in the Slani potok (“Salt Creek”) catchment (in the area of Vinodol) which, together with accompanying landslides, covers an area of approximately 3 km² (Fig. 15). Here, total site degradation occurs forming terrains of the “badlands” type. The Slani potok flysch, together with non-eroded flysch from the surrounding area, is represented mainly by calcareous clayey siltstone and calcareous silty claystone, and to a lesser extent with marls and silty sandstones (Fig. 16). There are no significant differences in the mineral content and grain size distribution of clayey siltstone and silty claystone in the whole area of Vinodol. These rocks contain muscovite and illitic material (<30 wt.%), quartz (<25 wt.%), calcite (<15 wt.%),

feldspars (<10 wt.%), chlorite, kaolinite and smectite, and in some samples a small quantity of pyrite (Fig. 17). There is a large amount of small particles: the particle size fraction smaller than 2 μm and the 2–4 μm fraction form up to 45 wt.% and 15 wt.%, respectively (Fig. 18).

In terms of engineering geology, the lithological components of flysch are transitional between hard soil and soft rock (HS–SR) (Fig. 19). Soil produced by weathering of this complex tends to slide and flow.

The phenomenon of an efflorescent salt crust on flysch in the Slani potok during dry periods of the year is unique to the area. The mineral content of this white salt crust as determined by XRD is represented by thenardite (sodium sulphate) and a negligible amount of gypsum (Fig. 20). The largest thenardite crystallites observed by scanning



Fig. 15 Location map (orthophoto) of the investigated area.

electron microscope (SEM) have a diameter of 2 μm (Fig. 21). Occurrence of this water soluble mineral indicates that some components of the flysch include sodium, which accelerates disintegration facilitating intensive erosion.

A series of physical and chemical tests were carried out in an attempt to verify this assumption. Flysch samples were submitted to physical stability tests (pinhole test and cyclic dry-wet repeat treatment – Civil Engineering Insti-

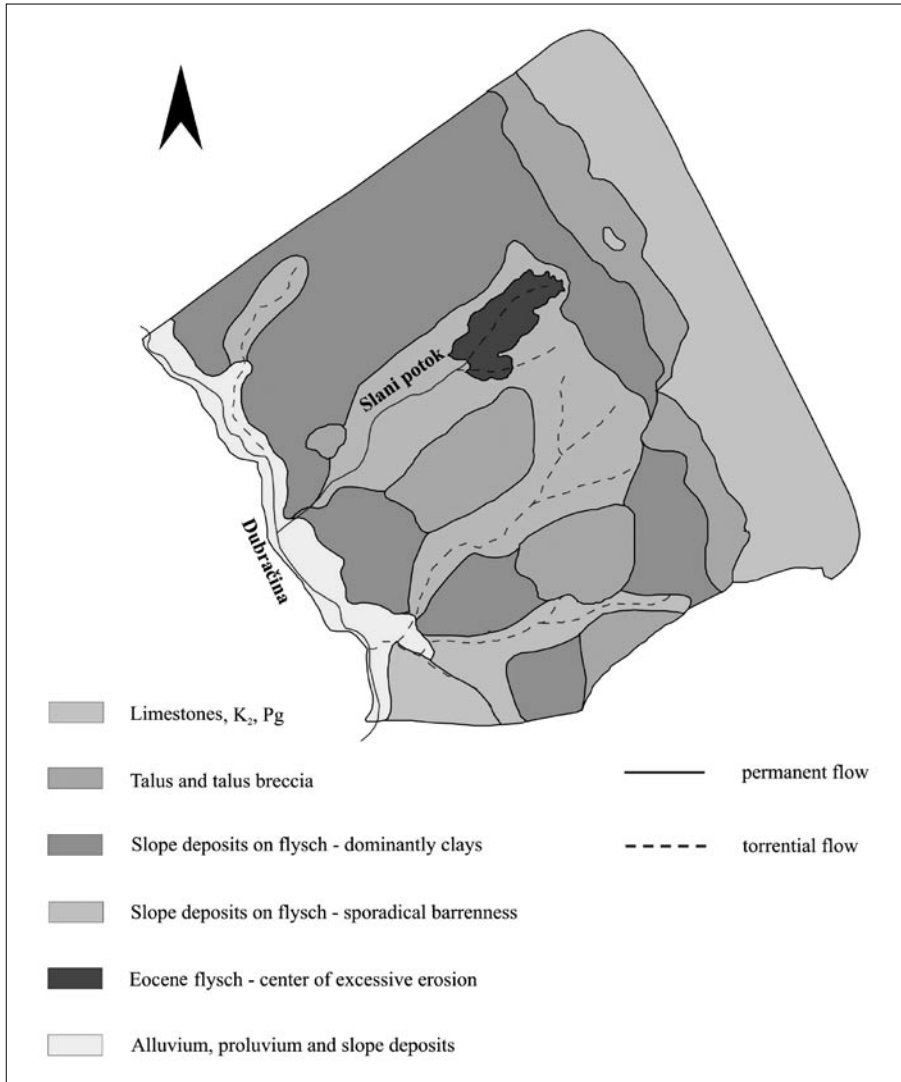


Fig. 16 Simplified geological map.

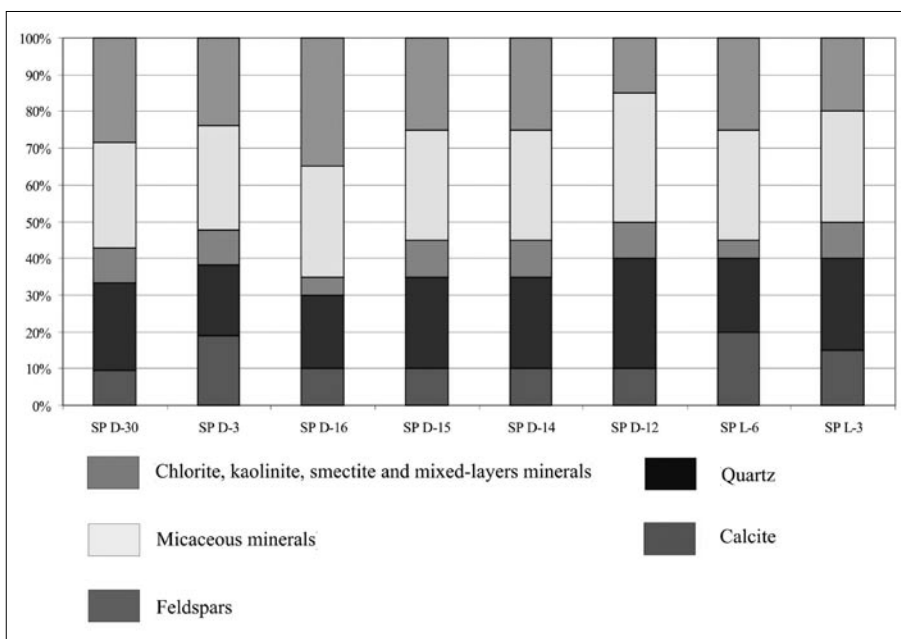


Fig. 17 Mineral content of the flysch samples (semiquantitative content).

tute of Croatia, Zagreb) indicating high soil erodibility. The degree of expansiveness of engineering soils is described by Fig. 22. Determination of soluble salts in flysch pore water was carried out following a modified procedure used by the International Soil Reference and Information Centre (VAN REEUWIJK, 2002). Using criteria established by SHERARD et al. (1976), the analysed flysch fall into the group of dispersive, i.e. erodible soils (Fig. 23). Analysis of stream water for soluble salts was also carried out. Measured concentrations of Na^+ and SO_4^{2-} are much higher than the average for fresh water. This illustrated discovery of thenardite is the first occurrence of this mineral in Croatia.

Excessive erosion of the Slani Potok flysch complex occurs due to its lithological nature where the composition is dominated by the presence of fine (including nanometer-

sized) particles, a group of materials known as HS-SR, the presence of swelling minerals, pore water rich in sodium, and occurrence of the sodium mineral – thenardite.

REFERENCES

SHERARD, J.L., DUNNINGAN, L.P. & DECKER, R.S. (1976): Identification and nature of dispersive soils.- Journal of the Geotechnical Engineering Division. ASCE, 102, GT 4, 287-301.

VAN REEUWIJK, L.P. (ed.) (2002): Procedures for soil analysis.- International Soil Reference and Information Centre, Technical paper, 6th ed., Wageningen.

WILLIAMS, A.A.B. & DONALDSON, G. (1980): Building on expansive soils in South Africa.- Proc. 4th Int. Conf. on Expansive Soils, Denver, 2, 834-838.

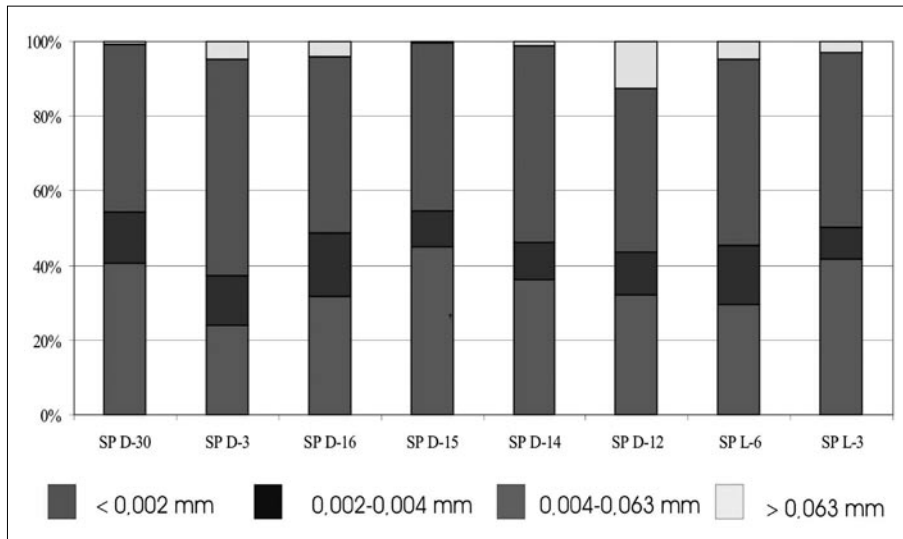


Fig. 18 Grain size distribution of the flysch samples (wt.%).

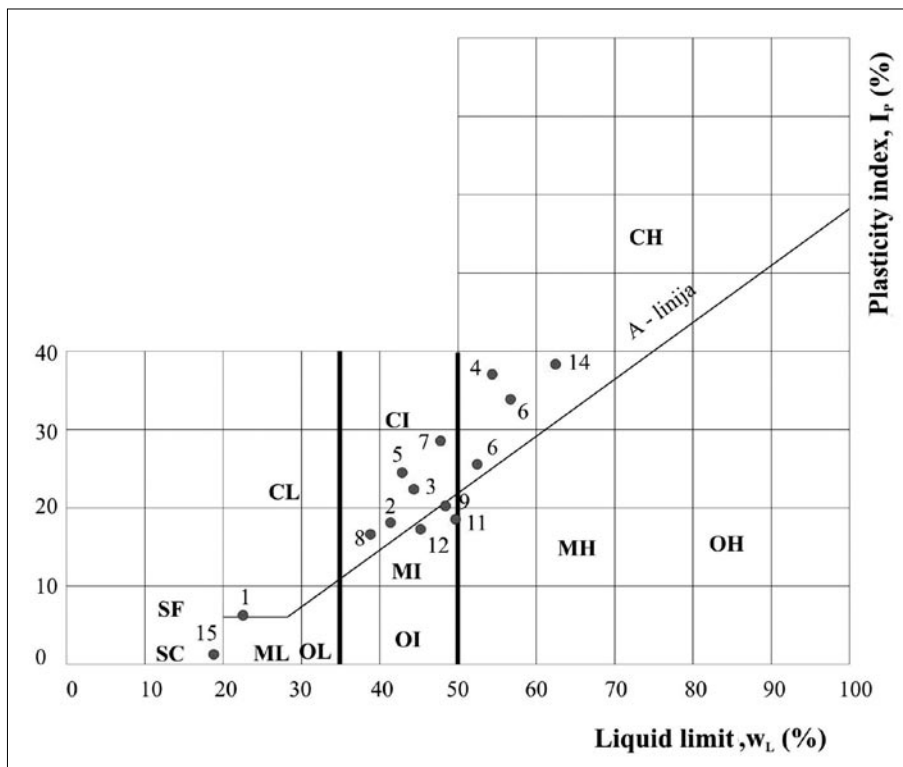


Fig. 19 Plasticity chart.

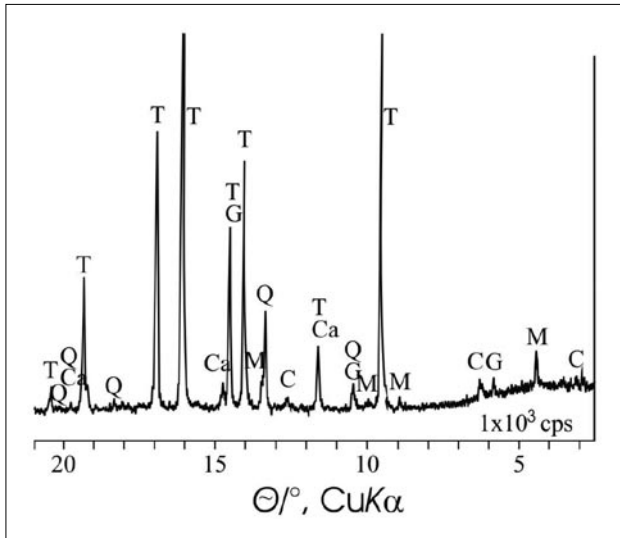


Fig. 20 A characteristic part of the XRD pattern of white powder on flysch. Legend: T – thenardite; C – chlorite; Ca – calcite; M – muscovite; Q – quartz; G – gypsum.

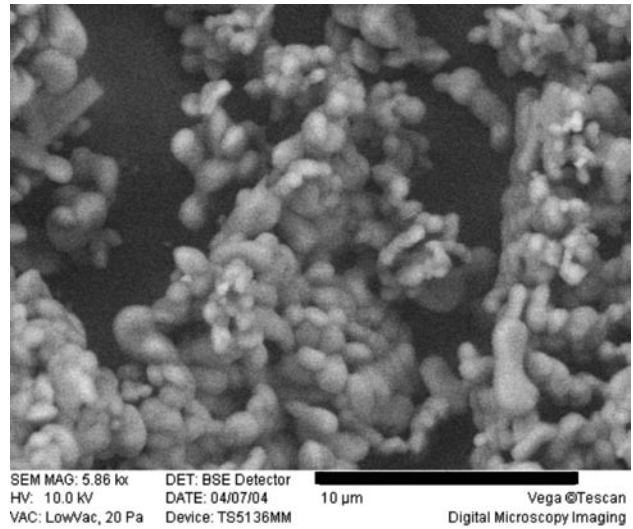


Fig. 21 SEM photograph of white powder on flysch (thanks to V. Beranec).

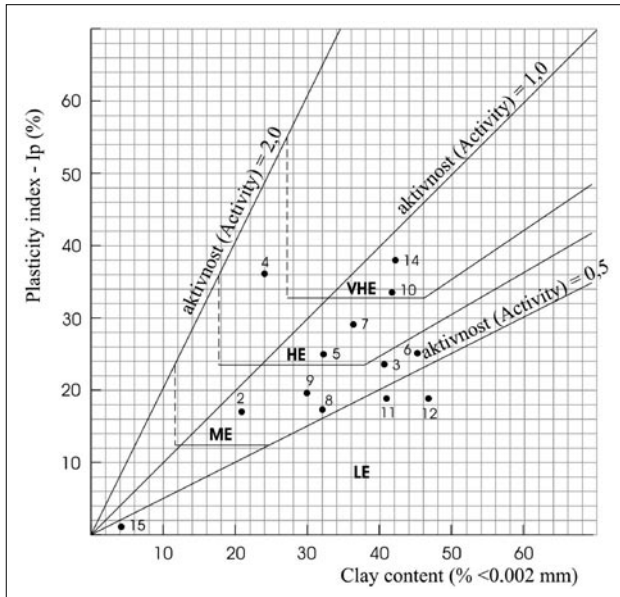


Fig. 22 Expansiveness chart (after WILLIAMS & DONALDSON, 1980). Legend: LE – low expansion; ME – medium expansion; HE – high expansion; VHE – very high expansion.

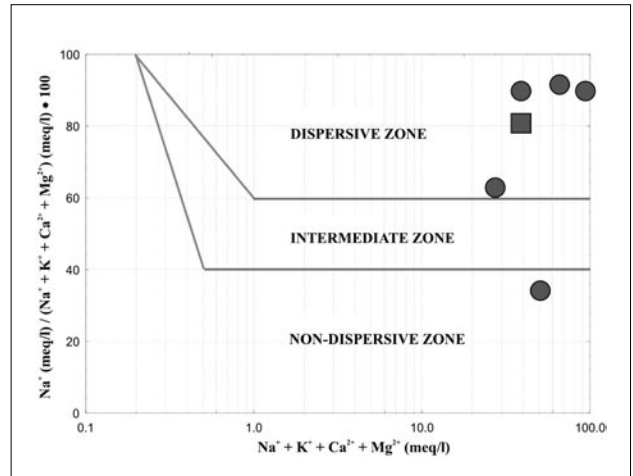


Fig. 23 Cations in the pore water of the flysch samples. Potential dispersivity chart after SHERARD et al. (1976). Stability after pinhole test: rectangle – nondispersive, circle – dispersive.

Field Trip 3
Clay minerals and selected ecological aspects of soils
on Veli Brijun Island, Croatia

Clay minerals and selected ecological aspects of soils on Veli Brijun Island, Croatia

Franz OTTNER¹, Monika SIEGHARDT², Tomislav ERSTIĆ³ and Marta MILEUSNIĆ⁴

1. INTRODUCTION

An academic cooperation agreement between the University of Natural Resources and Applied Life Sciences (BOKU) and the Faculty of Forestry of the University of Zagreb was established in September 2000. In the context of this agreement, the Institute of Forest Ecology of BOKU was asked to develop a sustainable concept for the continuation of the devastated arboretum at Brijuni.

The arboretum was established in 1987. The basic idea of the two initiators, Prof. Dr. Ž. Borzan and Prof. Dr. M. Vidaković, was to give a floristic general view on the Mediterranean flora as well as on trees and shrubs from completely different climatic zones of the world (BORZAN et al., 1993). Plants from various countries were chosen as examples to document the lively diplomatic activities of the former Yugoslavian President Tito. Costly facilities to maintain the arboretum, like paved pathways, water supply, a nursery and a house for employees and guests, were established. Due to warfare these investments were destroyed, the maintenance of the arboretum was neglected and furthermore completely abandoned. At present, the arboretum is in a poor condition. The fence is full of holes, so that deer can enter the arboretum regularly and feed on tree seedlings. Many of the non-autochthonous plants died as a consequence of the Mediterranean climate and lack of care.

The hypothesis of the ecological survey carried out by undergraduate student, Tomislav Erstić, was whether the general idea of the initiators of the arboretum could be sustainably continued, or whether an improved concept should be developed under the present ecological conditions with less maintenance efforts. Scientific soil research seemed to be a fundamental tool to prove these ecological hypotheses and was meant to support the elaborated concept. Data on mineralogical, physical, chemical and hydrological soil properties were collected and evaluated. Their ecological relevance was analyzed and served as fundament to the presented concept for the arboretum "Putevima Mira" (ERSTIĆ, 2005).

2. NATURE, HISTORY AND CULTURE ON VELI BRIJUN

The Brijuni archipelago (Fig. 1) was proclaimed a National Park in 1983. It covers an area of 7.42 km², comprising Veli Brijun (Big Brijun), Mali Brijun (Small Brijun) and Vanga (outside island), as well as several islets and the Kabula, Crnika and Stine reefs. The shores are mostly low and rocky with some pebble and sand beaches. The main characteristic of the archipelago is the extraordinary natural biological diversity enriched by man's traditional husbandry. Rich Mediterranean and Sub-Mediterranean vegetation is represented by holm oak, laurel, pine, olive, rosemary and underbrush. An extraordinary unity of natural elements and anthropogenesis has been achieved on Veli Brijun island, transforming farmlands and forests into landscape parks with vast meadows, tree-lined walks and gardens of sub-tropical vegetation. Some endangered plant species of Istria are quite widespread and develop freely. The ancient olive is about 1600 years old and it is one of the oldest trees in the Mediterranean (Fig. 2). Some of the smaller islands are excellent habitats of autochthonous birds as well as important seasonal habitats of northern bird species. The Saline bird reserve lies in the deep southern cove of Veli Brijun, with swampy plants and three small lakes. This bird reserve was developed on the remains of medieval salt pans which originate from ancient salt pans. Their traces are still visible today along the sea coast. The Brijuni National Park includes the surrounding sea with an exceptionally well preserved marine fauna with organisms typical of the northern Adriatic. Turtles and dolphins, the protected marine vertebrates, can occasionally be seen in the waters of Brijuni as well as other protected species, including different shells and some endemic species. The fish fauna makes the waters of Brijuni unique and different from other parts of the Adriatic. As a result of a millennium of anthropogenic influence on the archipelago of Brijuni, the animal kingdom on the islands, especially Veli Brijun, was enriched by many imported species (European hare, Akšić deer, Fallow deer, Mouflons) in addition to the autochthonous species, and these became acclimatised to

¹ University of Natural Resources and Applied Life Sciences, Vienna, Department of Civil Engineering and Natural Hazards, Institute of Applied Geology, Peter-Jordan-straße 70, A-1180 Wien, Austria (franz.ottner@boku.ac.at)

² University of Natural Resources and Applied Life Sciences, Vienna, Department for Forest and Soil Sciences, Institute of Forest Ecology, Peter-Jordan-straße 82, A-1190 Wien, Austria

³ wte Wassertechnik Austria GmbH, EVN Platz, A-2344 Maria Enzersdorf, Austria

⁴ University of Zagreb, Faculty of Mining, Geology and Petroleum Engineering, Pierottijeva 6, HR-10000 Zagreb, Croatia

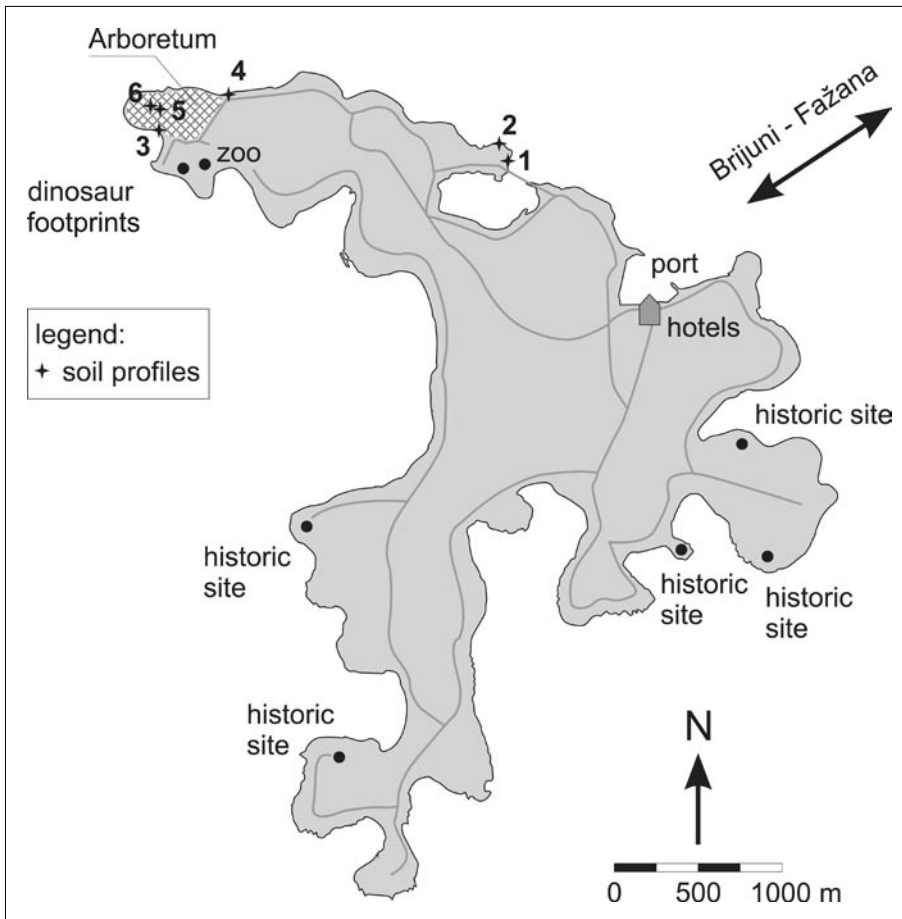


Fig. 1 Veli Brijun Island: location of soil profiles and tourist spots.



Fig. 2 Olive tree, about 1600 years old.

this habitat due to the almost ideal microclimatic conditions. The safari park lies on the northern edge of Veli Brijun, in an enclosed area. The park is the habitat of many exotic animals such as Indian elephants, llamas, zebras, nilgais and kob antelopes, Somalian sheep, Indian holy cows and autochthonous donkeys. The ethno park is an area within the Safari park representing a typical Istrian

homestead with its autochthonous animal species: Istrian ox (Boškarin), Istrian sheep (Istrian “Pramenka”), donkeys and goats. It is intended both as a habitat and presentation of domestic animals of Istria. Dinosaur footprints (Fig. 3) are the earliest, most fascinating, traces of animal life in the Brijuni archipelago.



Fig. 3 Dinosaur footprints.

The Brijuni islands have been inhabited since prehistoric times. Among the many archaeological sites, the most significant is the pre-historic settlement on Gradina from the earlier neolithic period. There are also rich remnants of architectural heritage from Roman (Fig. 4) and Byzantine times. The most important ones are the ruins of a typical Roman summer palace, the Roman temples of Venus and Neptune, very valuable ruins dating from the late ancient-Byzantine period with decorative mosaics, the Byzantine basilica of St. Mary, dating from the sixth century, and Gothic and Renaissance churches. Roman builders appreciated the qualities of the Brijuni stones and they used them as building material not only on Brijuni but also for many towns in the Adriatic region.

Veli Brijun (Fig. 1) is the largest and most important island, where the most important new objects are situated, such as representational and memorial objects reminiscent of Tito's activities, museum, a zoo and other tourist facilities.

3. GEOGRAPHIC LOCATION AND GEOLOGICAL SETTING

The Brijuni archipelago is located southwest of Pula, parallel to the peninsula of Istria, at 44°55'32" latitude and 13°44'40" longitude. It comprises 14 islands: Veli Brijun, Mali Brijun, Sv. Marko, Gaz, Okrugljak, Supin, Supinić, Galija, Grunj, Vanga, Madona, Vrasar, Jerolim and Kozada with some underwater rocks, and these can be arranged into three groups, according to their alignment: five islands surround the island Veli Brijun, five are adjacent to the island of Mali Brijun and two islands are located in the Fažana Channel which separates the archipelago from the Istrian Peninsula. The average distance to the mainland is 3 km. The coastline of the islands is 46.8 km long; the total area is 743.3 hectares.

Due to their favourable geographical location the Brijuni Islands are known for their mild northern Mediter-



Fig. 4 Verige bay with the Roman ruins.

anean type of climate, characterized by mild winters with precipitation maxima and warm dry summers. During the summer season the subtropical high-pressure belt influences the area, during winter, cyclones are transported by the westerly winds. The Adriatic Sea functions as an air-conditioner for Brijuni: during summer the sea cools, in winter it warms the region. Figure 5 shows mean monthly precipitation and mean monthly temperature for Veli Brijun island. Snowfall is rare, about 5 days per year. The prevailing wind direction is from the north-east. The so-called *bura* from the NNE or ENE, a cold wind mainly in the autumn and winter season coming from the Učka mountain

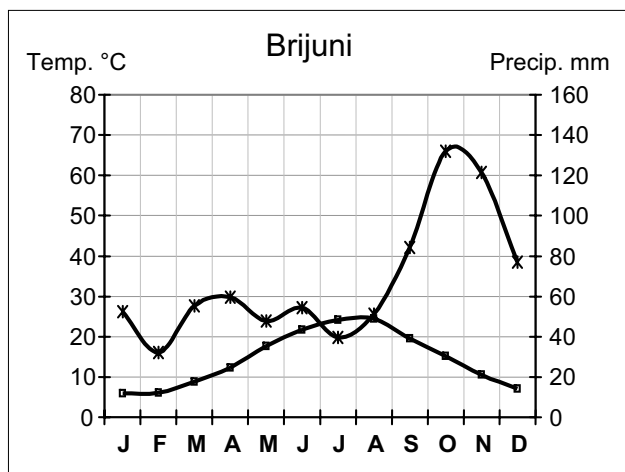


Fig. 5 Mean monthly temperature and precipitation for Veli Brijuni (1991-2000). Annual mean temperature: 14.5°C, Annual precipitation: 806 mm.

is typical. It lowers the air temperature, increases soil erosion in the coastal region by increasing wave intensity and influences the tree morphology.

Geologically and geo-morphologically Brijuni are the extension of the South Istrian plateau (Cretaceous limestone) covered with a thick layer of red soil, the so-called "Red Istria". Since the depth of the channel of Fažana is just 12 m, Brijuni were until some 10,000 years ago an integral part of Istria. The present relief of the Brijuni Islands is the result of gradual sinking of this karstic area since the last ice age. The geological setting of Istria is presented in more detail as part of the guide to the Field Trip 1 in this book. Figure 6 gives a general overview of the geology of the area. Paleosols of Jurassic, Cretaceous and Palaeocene ages are commonly observed across the entire region. As a result of processes during Neogene and the Quaternary, surficial sediments, e.g. loess, were formed, as well as palaeosols and soils of different stages of development. Of these soils, the "Terra Rossa", the Mediterranean red soil, is most widely spread (DURN et al., 1999).

4. RESEARCH AREA

The research area is situated in the arboretum "Putevima Mira", which is located in the NW of the island Veli Brijun on the Barban peninsula. Veli Brijun (Fig. 1) is the largest and most important island. It has a total area of 561 hectares and its coastline is 25.9 km long. The arboretum has a total area of 7.87 hectares. It was established in 1987 (Fig. 1) after the islands were declared a National Park and memorial site. Following the establishment of the necessary maintenance facilities, 72 selected areas were improved with up to 50 cm of topsoil (probably derived from the island), to increase soil depth and support and improve plant growth. The areas were between 20 and 400 m² and amount to a total of 1.45 ha. Each area represents a country which was visited by President Tito. Characteristic species of the respective countries were planted. Furthermore, selected areas should represent the diversity of a genus or a species. The morphological characteristics of woody plants,

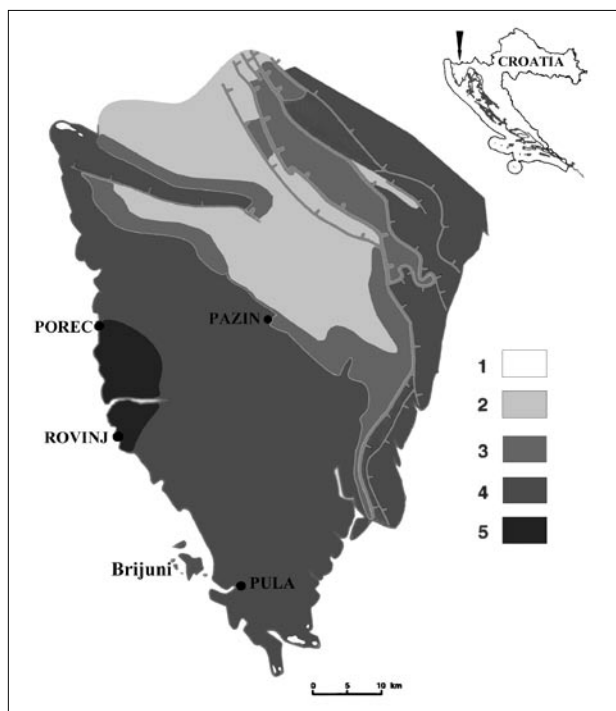


Fig. 6 Simplified geological map of Istria including Brijuni. Legend: 1 – Quaternary; 2 – Eocene; 3 – Paleocene; 4 – Cretaceous; 5 – Upper Jurassic.

their blossoms and fruits were supposed to become an attraction for visitors. Mediterranean plants as well as trees and shrubs from completely different climatic areas of the world were established. Outside of the defined areas in the arboretum the indigenous Mediterranean vegetation was kept.

At present the arboretum is in very poor condition. Apart from the network of paths, the entire infrastructure is destroyed or unusable. Both warfare and lack of maintenance by skilled personnel have led to the decay of the arboretum. The fence is holed and numerous deers enter the arboretum regularly and damage trees and seedlings. Non-autochthonous plants have died because of the Mediterranean climate and lack of care.

5. MATERIAL AND METHODS

5.1. Field methods

The map of Veli Brijun Island (Fig. 1) gives a general survey of the distribution of the investigated soil profiles on the island, as well the location of the arboretum. On the east coast, profiles 1 and 2 were dug at a distance of about 1.5 km apart from the arboretum. Profiles 3 and 4 are situated on the coastal part of the arboretum. Profile 3 is on the leeward side of the island, whereas profile 4 is situated on the windward side and is heavily influenced by the *bura*. In the arboretum, two soil profiles (5, 6) were dug with a soil depth of more than 50 cm. For comparison, one profile lies outside (Brijuni 5) and one in an area with additional soil deposit (Brijuni 6).

The profiles were prepared and the soil horizons were defined for soil classification according to the World ref-

Table 1 Chemical extraction and analytical methods.

Parameter	Extraction and analytic procedure	Reference
pH	suspension in deionised H ₂ O and 0.01 m CaCl ₂ electrometric determination	ÖNORM L1083
C _{org}	Leco S/C 444	ÖNORM L1080
H ₂ O-soluble compounds	cold water extraction; determination of electrical conductivity (WTW 90); Cl, SO ₄ with liquid chromatography (Dionex 5000)	ÖNORM L1092
adsorbed cations CEC	1 M ammonium acetate-extraction simultaneous ICP-OES (Optima 3000 XL, Perkin Elmer)	MEIWES et al. (1984)
pedogenous and active oxides	Extraction with dithionite-citrate and with oxal-acidic ammonium oxalate; determination of Fe-oxides with simultaneous ICP-OES (Optima 3000 XL, Perkin Elmer)	MEHRA & JACKSON (1960)

erence Base for Soil Resources (WRB; DECKERS et al., 1998). Soil colour was determined using MUNSELL COLOUR CHARTS (1994). Qualitative soil samples were taken from each genetic soil horizon for laboratory analyses.

To distinguish the potential rooting depth the actual soil depth throughout the arboretum was measured using a soil corer.

5.2. Laboratory methods

Vegetation roots were removed from the soil samples and the coarse and fine soil fractions were separated by dry sieving (2 mm). Mass and conversion factors for calculating oven-dry reference weights were determined.

5.2.1. Chemical methods

Chemical extraction and analytical methods are presented in Table 1.

5.2.2. Hydrological methods

To distinguish hydrological soil parameters water potential/water content curves were determined according to the Austrian standard procedure (ÖNORM L 1063), using undisturbed soil cores and a pressure-plate equipment (Soil Moisture Inc. Santa Barbara, USA).

Determination of density and bulk density was carried out according to the Austrian standard procedure (ÖNORM L1068 and B 3121), in addition to a helium pycnometer (Micromeritics, Instrument Corporation, Georgia, USA).

5.2.3. Mineralogical methods

XRD-Methods

The samples were studied by means of X-ray diffraction (XRD) using a Philips 1710 diffractometer with automatic divergent slit, 0.1° receiving slit, Cu LFF tube 45 kV, 40 mA, and a single-crystal graphite monochromator. The measuring time was 1 s in step-scan mode and step size of 0.02°. Bulk samples as well as the clay fractions (<2 µm) were analyzed.

The sample preparation generally followed the methods described by WHITTIG (1965) and TRIBUTH (1989). The dispersion of clay particles and destruction of organic mat-

ter were achieved by treatment with dilute (10%) hydrogen peroxide. The separation of the clay fraction was carried out using a Beckman labor centrifuge. The exchange complex of each sample (<2 µm) was saturated with Mg and K using chloride solutions and shaking. The preferential orientation of the clay minerals was obtained by suction through a porous ceramic plate similar to the methods of KINTER & DIAMOND (1956). To avoid disturbance of the orientation during drying, the samples were equilibrated for 7 days above a saturated NH₄NO₃ solution. Afterwards expansion tests were made, using ethylene glycol, glycerol and dimethylsulfoxide (DMSO) as well as contraction tests heating the samples up to 550°C. After each step the samples were X-rayed from 2–40°2θ.

The clay minerals were identified according to THOREZ (1975), BRINDLEY & BROWN (1980), MOORE & REYNOLDS (1997), and WILSON (1987). Semiquantitative estimations were carried out using the corrected intensities of characteristic X-ray peaks according to RIEDMÜLLER (1978).

The semiquantitative mineral composition of the bulk samples was estimated using the method described by SCHULTZ (1964).

Particle size distribution

The particle size analysis was carried out in combination with the clay mineral analysis. The coarse parts of the samples were fractionated using sieves with mesh-sizes ranging from 2000 to 40 µm. The fine particles were analyzed by means of sedimentation analysis with a sedigraph 5000ET (Micromeritics, Instrument Corporation, Georgia, USA).

6. RESULTS

6.1. Soil depth

Generally, the fine soil depth is very shallow over the entire arboretum, rock outcrops occur frequently. Sometimes the fine soil occurs only in fissures between boulders, where soil depths of more than 70 cm can be found. However, along the shore, the soil profile depth is higher due to the fact that the major part of the soil material was transported to the shore by solifluction.

In the western part of the arboretum, soil depths do not exceed 20 cm. Small slabs are scattered over the whole

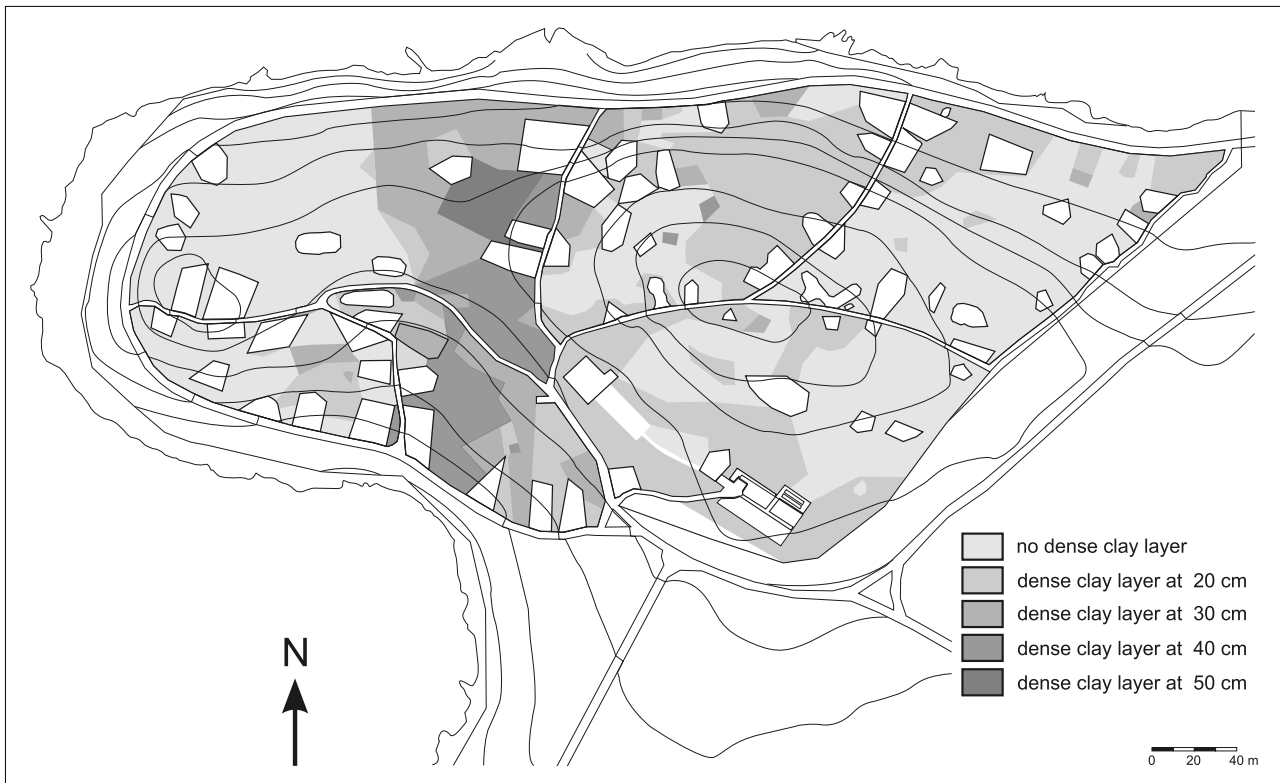


Fig. 7 The depth of the dense clay layer in the arboretum.

area which come from the transport of material to the arboretum. Many Medieval small quarries could also be the reason for the countless cairns which can be found in the entire arboretum. Unwanted limestone slabs were piled up into small cairns.

Soil depths in the arboretum increase in an eastward direction, however, a narrow belt which crosses the arboretum from the southern to the northern coast shows the highest soil depths. The soil depths found with the soil auger are 60 cm or more, but at depths of 70 cm the soil density increases due to the high clay content. Therefore, in these depths it was impossible to penetrate to the C-horizon. The site for the Brijuni 5 profile was chosen in this area. The soil depth then decreases again in an eastward direction.

Many extensive rock formations can be observed, in the arboretum and boulders protrude from the surface for up to 60 cm. A very dense clay layer (hardly penetrated by roots) was found almost throughout the arboretum at various soil depths. Figure 7 shows the position and depth of this dense clay layer.

6.2. Description and properties of the soil profiles

From all the profiles, only numbers 4, 5 and 6 (Fig. 1) can be visited during the field trip.

6.2.1. Brijuni 4 Profile

The profile Brijuni 4 is located on the east coast of Veli Brijun, which is the windward side, near the entrance to the arboretum at about 2 m above sea level. Figure 8 shows the profile in autumn 2004. Erosion marks due to wind,

water and mass movement can be seen nearby. The actual horizon descriptions are given in Table 2. The boundaries between horizons vary from gradual to diffuse and wavy.

Even if a definite E-horizon is not distinguishable, according to the World Reference Base for Soil Resources (WRB; DECKERS et al., 1998), it is classified as a chromic Luvisol on carbonate rocks with Mull and high bioturbation in the uppermost horizon (according to the Austrian Soil Classification System: Relictic Brown Soil; Mull-Reliktbraunerde).

Particle size distribution

To a depth of 110 cm a silt-clay-ratio of about 50 to 50 can be found. Below this, the soil becomes increasingly denser and the ratio shifts to 40 to 60. The sand content can be neglected. Figure 9 illustrates the particle size distribution with soil depth.

Bulk mineral analyses

Sheet silicates and quartz can be found with medium contents, whereas the amount of plagioclase decreases with the soil depth. Mica is present in traces and the amount of K-feldspar increases with soil depth. Haematite and goethite are present in the profile in small amounts.

Clay mineral analyses

Illitic material is the dominant clay mineral at 69–73 wt.%; no distinct changes in clay mineral distribution with the soil depth can be observed in this profile (Table 3). The vermiculite content is distributed irregularly within the soil profile. Kaolinite – mostly in its poorly-crystallized form



Fig. 8 The Brijuni 4 soil profile in autumn 2004.

as fire clay – constitutes between 18–24 wt.%. The mixed layer mineral in the soil profile shows a regular composition with vermiculite as one component and either illite or

secondary chlorite as the other. The quantification must be regarded as a rough estimate due to the low amounts of this mixed-layer mineral.

Chemical analyses

Selected soil chemical results are presented in Table 4. The data support both the particle size distribution and the soil classification. The cation exchange capacity (CEC) increases with soil depth, as does the proportion between pedogenic Fe-oxides and active Fe-oxides.

Due to the dense forest cover, which mostly consists of Mediterranean sclerophyllic trees and shrubs, the pH-values of the uppermost horizon are about 1 pH-unit lower than those in the Brijuni 1 and 2 profiles, where grass and herbaceous plants with few Mediterranean shrubs dominate the vegetation cover. The high organic carbon content in the uppermost A-horizon is noticeable and due to the forest cover and high bioturbation. The C/N ratio in the A-horizon is low (11) and an indication of the high biological activity.

The profile is influenced by seawater due to its proximity to the shore: the electric conductivity increases from a depth of 110 cm downwards and is mostly caused by the elevated water soluble Cl^- and SO_4^- contents. At this depth the CEC and Na contents are also significantly increased.

6.2.2. Brijuni 5 Profile

The Brijuni 5 profile was sampled in the arboretum but outside a planting area, so no additional soil material was

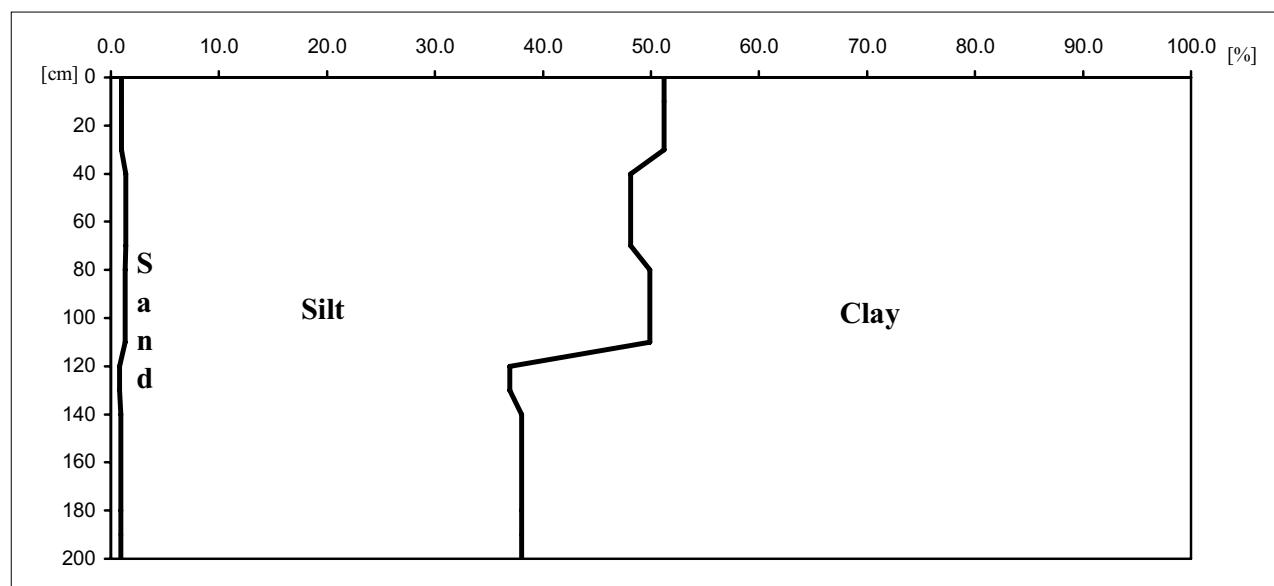


Fig. 9 Particle size distribution in the Brijuni 4 profile.

Table 2 Selected soil descriptive parameters for the Brijuni 4 profile.

A	0–30 cm; clay–silt; dark reddish brown (5YR 3/3); strong medium blocky subangular; many fine to medium roots
B1	30–75 cm; clay–silt; reddish brown (5YR 4/4); strong medium blocky; common medium to fine roots
B2	75–110 cm; clay–silt; reddish brown (5YR 4/4); strong medium angular blocky; few fine roots
Bt(g)	110–200 cm; clay–silt; reddish brown (5YR 4/4); up to 165 cm medium angular blocky, below fine angular blocky and weak prismatic with common limestone clasts (Ø 10–40 cm), few, faint, fine mottles; moderately salty

Table 3 Clay minerals (mass %) in the Brijuni 4 profile.

Lab. Nr.	Horizon	Vermiculite	Illitic material	Kaolinite	Mixed Layer
7094	0–30	3	70	22	5
7095	30–75	7	69	20	4
7096	75–110	4	73	18	5
7097	110–135	4	69	24	3
7098	135–200	5	72	19	4

Table 4 Selected chemical soil parameters for the Brijuni 4 profile.

soil depth (cm)	pH	H ₂ O CaCl ₂	C _{org} mg/g	CECeff mmolc/kg	Fe _{ped} / Fe _{act}	electric conductivity μS/cm	H ₂ O soluble Cl mg/kg	H ₂ O soluble SO ₄ mg/kg
0–30	7.0	6.2	32.00	70.4	5.5	60.9	121.3	78.8
30–75	7.4	6.4	8.44	58.2	6.6	91.6	236.2	221.5
75–110	7.1	6.1	7.75	53.4	5.5	114.7	325.1	384.0
110–135	6.4	5.9	7.32	80.4	7.6	407.0	1325.6	1711.8
135–200	7.0	6.4	7.78	85.0	7.0	293.0	1136.9	802.4

Table 5 Selected soil descriptive parameters for the Brijuni 5 profile.

A	0–12 cm; silty clay; dark reddish brown (5YR 3/3); strong coarse blocky subangular structure; many fine to medium roots
Bt1	12–35 cm; silty clay; reddish brown (5YR 4/4); strong medium angular blocky; common medium to fine roots
Bt2	35–50 cm; silty clay; reddish brown (5YR 4/4); very strong medium angular blocky to prismatic; very dense

present. The profile is situated on a flat terrain, about 10 m above sea level. Measurement of soil depth by auger showed that the fine soil depth exceeds 70 cm. The actual horizon description is given in Table 5. The boundaries between horizons are gradual to diffuse and wavy.

Again, according to the WRB, the soil is a chromic Luvisol with Mull and high bioturbation in the uppermost horizon (according to the Austrian Soil Classification System: Relictic Brown Soil, Mull-Reliktbraunerde).

Particle size distribution

The high clay content (up to 70 wt.%) throughout the entire soil profile are remarkable (Fig. 10). The fine clay fraction amounts to 46 wt.%. The sand fraction is negligible. The ratio of silt to clay is about 30 to 70.

Bulk mineral analyses

Layer silicates and quartz are present in this profile in high and medium amounts respectively. Plagioclase occurs in

small amounts, mica only in traces. Traces of K-feldspar can only be found in the uppermost as well as in the lowermost horizons.

Clay mineral analyses

The distribution of illite in the profile shows enrichment in the uppermost horizon (Table 6). The content of 81 wt.% is the highest amount of illitic material in all the samples of the investigated profiles. Vermiculite shows the opposite trend. Whereas the vermiculite content is only 2% in the upper horizons, it increases to 5% in the lower parts of the soil profile. As in the Brijuni 4 profile, kaolinite occurs in its poorly crystallized form. The kaolinite content is only slightly lower than that in the previous profile discussed above. Haematite and goethite are also present in small amounts.

Figure 11 shows the diffractogram of the clay fraction of the A-horizon (0–15 cm) of the Brijuni 5 profile, while Fig. 12 shows one for the Bt-horizon (30–40 cm).

Table 6 Clay minerals (mass %) in the Brijuni 5 profile.

Lab. Nr.	Horizon	Vermiculite	Illitic material	Kaolinite	Mixed Layer
7099	0–15	2	81	13	4
7100	15–30	3	77	17	2
7101	30–40	5	71	21	3
7102	40–50	4	68	22	6

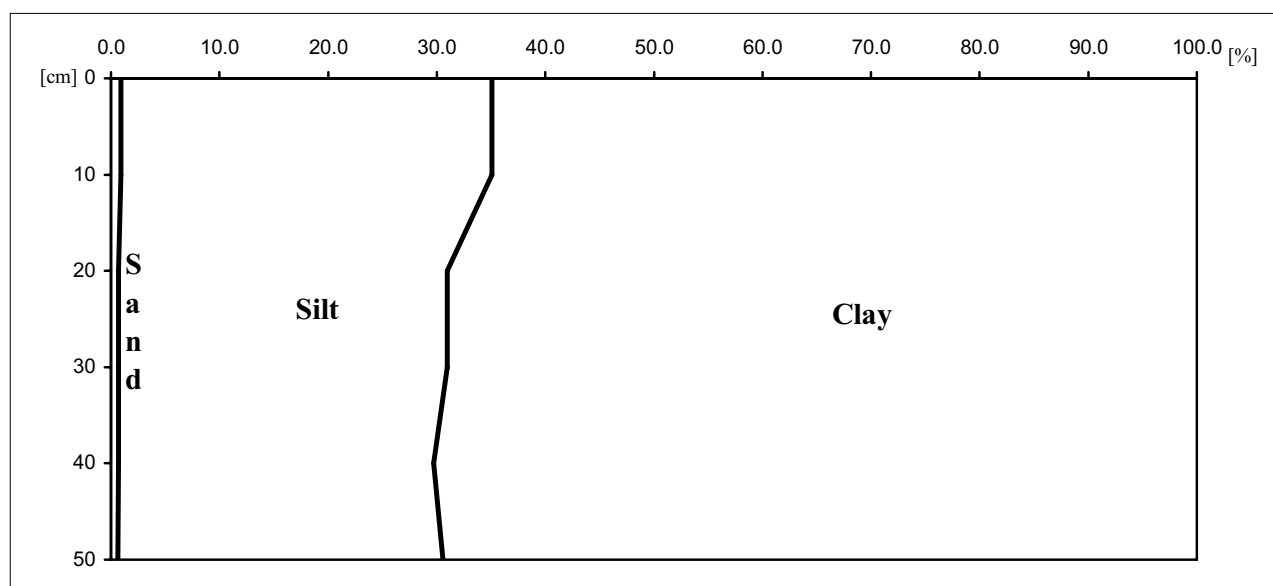


Fig. 10 Particle size distribution of the Brijuni 5 profile.

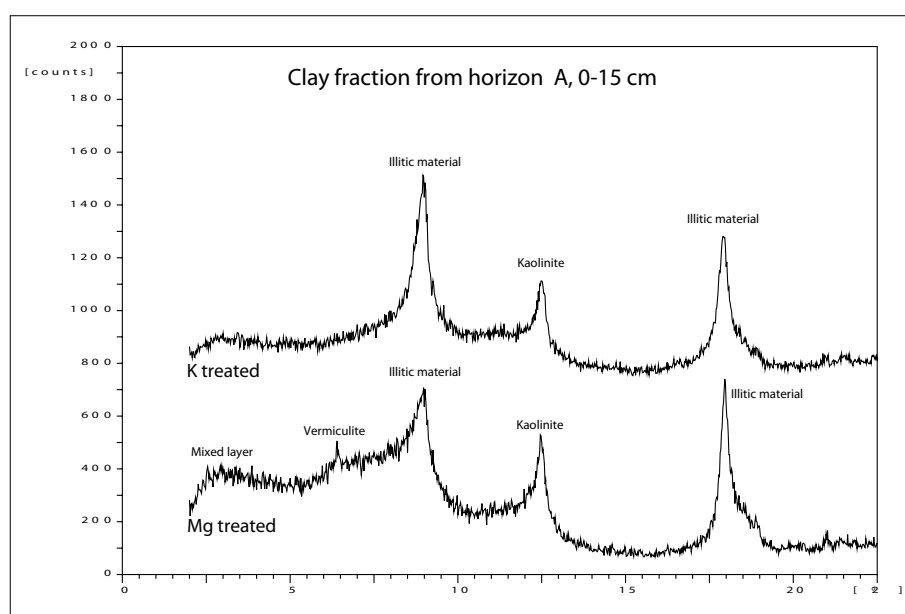


Fig. 11 Diffractogram of the clay fraction from the Brijuni 5 profile.

Chemical analyses

Selected soil chemical analytical results are presented in Table 7.

The data, together with the particle size distribution, support the soil classification. The cation exchange capacity (CEC) decreases with soil depth; the higher values in the A-horizon being the result of the high humus content as indicated by the high content of C_{org} . The ratio between pedogenic Fe-oxides and active Fe-oxides significantly increases with soil depth. The pH-values are clearly lower in all horizons than those of the profile Brijuni 4. This difference is related to the absence of sea water spray; the Cl^- and SO_4^{2-} content are 10-times lower than in Brijuni 4. The C/N-ratio with 19 in 30–40 cm depth is quite high, because of the high content of organic carbon, which may be attributed to root debris of the sclerophyllic vegetation and wind-protection of the site, whereas Brijuni 4 is fully

exposed to wind erosion of vegetation litter and has herbaceous undergrowth.

The pF-curves (not presented) for this profile show that the soil is even more dense than that of Brijuni 4. At a depth of 32 cm only 10% of the soil water is available at a water-potential of -1.0 bar. The data for bulk density, density and porosity given in Table 8 confirms these findings.

6.2.3. The Brijuni 6 Profile

The Brijuni 6 soil profile was excavated within an area of added topsoil (area 6, Japan) and is used here for comparison with Brijuni 5, where no material was added, and to analyse the material for soil depth melioration. The sampling point is at about 10 m a.s.l.; the profile is situated on level terrain. Only the first two horizons of the additional material were sampled, because at a depth of 30 cm a buried A-horizon was met (A2), which is the original genetic

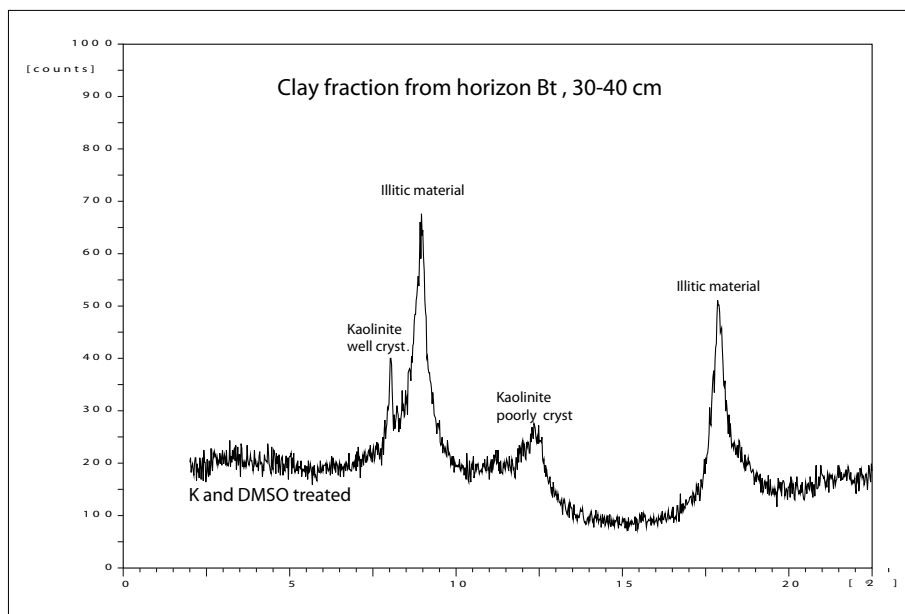


Fig. 12 Diffractogram of the clay fraction from the Brijuni 5 profile which shows the two types of kaolinite.

A-horizon. The rest of the profile below 30 cm is similar to the profile 5 which is only some metres beside. The horizon description for profile Brijuni 6 is given in Table 9. The boundary between horizon A1 and Bt1 is gradual to diffuse and wavy; between Bt1 and the buried A2 it is rather abrupt and smooth, while it is diffuse and irregular between A2 and A2/Bt2, the intermixed layer, as well as between A2/Bt2 and Bt2.

According to the WRB, the profile can be classified in two ways: firstly as an Anthroisol which might not really target the exact classification because it is used for soils with a long-lasting anthropogenic influence. Here, additional soil material was deposited in a single event twenty years previously and a new A-horizon developed, so this soils doesn't fit the requirements for such a classification. Secondly, the term anthric chromic Luvisol, reflects

the genesis of the profile in a better way. The topsoil shows forest Mull. According to the Austrian Soil Classification System it is an Anthropogenic Relictic Brown Soil ("Schüttungsboden").

Particle size distribution

This profile shows a low sand content, <2 wt.%. In the added material the silt:clay ratio is about 45:55 whereas in the "old" soil profile the respective ratio is 30:70.

Bulk mineral analyses

This profile shows a very similar mineralogical assemblage to the other soils. Sheet silicates and quartz are present in medium amounts. The plagioclase content decreases with soil depth, mica and K-feldspar only occur in traces.

Table 7 Chemical soil parameters for the Brijuni 5 profile.

soil depth (cm)	pH H ₂ O	pH CaCl ₂	C _{org} mg/g	CECeff mmolc/kg	Fe _{ped} / Fe _{act}	electric conductivity μS/cm	H ₂ O soluble Cl mg/kg	H ₂ O soluble SO ₄ mg/kg
0-15	6.7	6.3	47.05	100.06	2.9	70.0	30.0	30.2
15-30	6.5	5.8	16.91	77.38	5.8	31.0	34.7	27.9
30-40	6.5	5.6	9.30	70.55	8.0	26.2	35.8	49.5
40-50	6.5	5.6	7.57	69.68	8.6	29.0	29.4	96.7

Table 8 Bulk density, density and porosity of the Brijuni 5 soil profile.

genetic soil horizon	soil depth cm	bulk density g/cm ³	density g/cm ³	porosity pore vol. %
A	1-5	1.58	2.47	36.0
A	5-9	1.75	2.58	32.0
Bt	16-20	1.82	2.61	30.2
Bt	20-24	1.83	2.64	30.7
Bt	33-37	1.97	2.70	27.0
Bt	45-49	1.98	2.70	26.7

Table 9 Selected soil descriptive parameters for the Brijuni 6 profile.

A1	0–10 cm; new developed, recent A; silty clay; dark reddish brown (5YR 3/3); strong coarse subangular blocky; many fine to medium roots
Bt1	10–30 cm; new deposited B; silty clay; reddish brown (5YR 4/4); strong medium angular blocky; common medium to fine roots
A2	30–40 cm; original A-horizon, buried, silty clay; dark reddish brown (5YR 3/3); moderate medium to fine angular blocky; common medium to fine roots
A2/Bt2	40–55cm; silty clay; reddish brown (5YR 3/4); moderate medium to fine angular blocky, few fine roots
Bt2	55+ cm; silty clay, reddish brown (5YR 4/4); very strong medium angular blocky to prismatic; no roots, very dense

Table 10 Chemical soil parameters for the Brijuni 6 profile.

soil depth (cm)	pH		C _{org} mg/g	CECeff mmolc/kg	Fe _{ped} / Fe _{act}	electric conductivity μ S/cm	H ₂ O soluble Cl mg/kg	H ₂ O soluble SO ₄ mg/kg
	H ₂ O	CaCl ₂						
0–10	7.6	7.0	26.98	108.91	5.6	101.0	30.3	21.4
10–20	7.6	7.0	12.86	93.12	5.9	62.2	38.0	24.0

Clay mineral analyses

In this profile only 30 cm of the heaped-up material was analyzed. The slightly lower content of illite in the surficial horizon is noticeable. Vermiculite, haematite and goethite occur in small amounts.

Chemical analyses

The respective analytical results are presented in Table 10.

Both analyzed horizons are added material, and it can be concluded that this material came from the island and is the same as that used for the construction of the golf course as our analyses (not shown in this guide) indicate. The values for soil density (2.64 g/cm³) confirm this hypothesis, which is the same for the uppermost horizons of the profiles Brijuni 1, 2 and 6. The pF-curve demonstrates that at a soil water potential level of -1 bar 80% of the water is retained in the soil. This result is very similar to that of Brijuni 1, which is located at the boundary of the golf course.

7. DISCUSSION

7.1. Soil systematic position of “chromic Luvisol”

KUBIENA (1953) uses the terms “Terra Rossa” or “Mediterranean Red Earth” for reddish, clay rich soils derived from limestones in the Mediterranean region. As these soil types are within the soil class of “Terra Calcis”, their relationship to brown loam (“Terra Fusca”), red loam and red earth of the humid–temperate climate is evident. KUBIENA (1986) describes the matrix of the “Terra Rossa” as yellowish coloured with crystals of haematite, goethite and amorphous iron, with a very stable structure. According to DUCHAUFOR (1968), the main soil forming processes for the “Terra Rossa” are rubification, clay development, clay transformation, and processes that can be summarized as lessivage: clay mobilization by dispersion, clay transport

by descending percolating water (eluviation) and clay deposition (illuviation). DUCHAUFOR (1998) defines these soils as brown soils where a second process (lessivage) was superimposed on brunification. Two soil horizons are typical: the first, A or E, impoverished in clay and iron, with a lighter colour, and the second, the Bt, enriched in clay and iron, showing “argillans” around structural units. According to DUDAL (1978), the “Terra Rossa” is a chromic Luvisol, because of its clay-rich horizon. SKOWRONEK (1978) summarizes that all ideas for the systematic classification of the “Mediterranean Red Earth” contain an extremely clay-rich horizon.

The actual WRB version (ZECH & HINTERMAIER-ERHARD, 2002) also includes soils that have a clay-rich horizon below a horizon with low clay content, due to biological or geogenic (solifluction) processes as Luvisols. However, differences in clay content throughout the soil profile and the existence of a clay rich horizon are prerequisites for the classification of a soil as a Luvisol.

The three soil profiles shown here have all the properties necessary for classifying them as Luvisols, even if a lighter coloured distinct E-horizon cannot be distinguished: the clay contents and the iron contents increase with soil depth and the soil structure changes from subangular blocky to angular blocky to prismatic. In addition, the soil colour with a hue of 5YR allows the classification of the soils as chromic Luvisols (FAO–ISRIC–ISSS, 1998).

The “Terra Rossa” or chromic Luvisol is widely distributed in Istria. The typical reddish colour forms a soil cover over limestone of various depths, from some cm to several metres. This reddish colour is derived from Fe-oxides (haematite) that are formed because of dehydration from iron hydroxides (goethite) during hot and dry climatic periods. Several authors (e.g. DUCHAUFOR, 1998; DURN et al., 1999) show that these soils were developed during the Tertiary, thus being relictic and often polycyclic, sometimes with heavily eroded topsoil horizons.



Fig. 13 Location of the FAO reference profile.

7.2. Comparison of the analytical results

7.2.1. Clay minerals

Profile 5 is composed of distinct horizons, whereas profile 4 shows a more or less disturbed sequence. In profile 6 the deposited material which was added 20 years ago was analyzed.

In all the profiles illite is the dominant clay mineral accounting for 61–81 wt.%. In the undisturbed profile 5 noticeable enrichment of illite can be seen in the uppermost layers of the profile. This illitization derives from the greater availability of K from decaying plants, which is taken up by vermiculite, and then results in the formation of illite. In the Brijuni 4 profile which is influenced by solifluction, this process is less dominant, because the surficial layers of the profile were repeatedly covered with transported material.

Vermiculite with a basal spacing of 14 Å has been observed in all the profiles and shows the opposite trend to illite in its distribution. This means that the vermiculite is transformed into illite by the uptake of K.

Kaolinite characteristically occurs in “Terra Rossa” soils in high amounts. In all the investigated profiles the values did not exceed 28 wt.%, the lowest values were found in profile 4 at 18 wt.%. The majority of the kaolinite occurs in the form of fire clay – a poorly crystallized form of kaolinite. Only a small portion (about 10–20%) occurs as the well-crystallized form. These quantities of kaolinite are relatively low compared to other “Terra Rossa” profiles (DURN et al., 1999).

In almost all the examined soil samples a mixed-layer mineral was discovered. Due to the low amounts it was impossible to carry out an exact quantification. However, it could be determined that vermiculite, illite and partially chlorite are constituents of this mixed-layer mineral. The dense clay layer (Fig. 7) does not reflect changes in the clay mineral composition but is purely the result of increased clay content up to 70 wt.%. The bulk density of this compacted clay layer reaches values of almost 2 g/cm³, comparable to clay from industrially used brick clays.

In profile 3 (not shown in this guide) a remarkable clay component occurs: it is yellow and consists of illitic material which could be transformed smectites, derived from volcanic ash deposited 120 million years ago (OTTNER, 1999).

7.2.2. Chemical analysis

The lowest pH-values (6.5) can be found in the Brijuni 5 profile, which is located inside the arboretum and shows the impact of forest cover. The relatively high pH-values (7.6) in the uppermost horizon of profile Brijuni 6 confirm the assumption that the material was transported to the arboretum from outside the forest somewhere on the island and that it was mixed. The soil pH-data resemble those of the soils from the golf course. In all three profiles the A-horizons have a C/N-ratio between 11 and 13, which is typical for a mull. In all profiles the CEC-values clearly exceed 24 cmolc/kg clay and the pedogenic Fe-oxide contents increase with soil depth which is required by the WRB for classification as a Luvisol. Elevated water-soluble Cl⁻ and SO₄ contents and the high electrical conductivity of the Brijuni 4 profile are a consequence of its shore location and the subsequent influence of seawater. In addition, the PAK-content (not presented here) of the fine soil below 100 cm depth derived from the use of diesel on boats is worth mentioning.

Comparison of these profiles with the reference profile for the southern part of the Istrian peninsula north of Pula, (Fig. 13), from the soil map of Europe (FAO/UNESCO 1981), the analytical and descriptive data show similarities or even agreements with that agricultural soil. In these profiles the sand fraction is very low; the silt/clay-proportion is about 50/50, and the clay content increases to 75% with soil depth. When we consider the impact of agriculture (ploughing, removal of harvest, fertilization), the similarities refer to colour, pH, organic carbon, nitrogen and CEC. Only the carbonate content shows differences. Whereas the Brijuni-profiles have very low to no carbonate contents, the FAO-profile exceeds 35 mg/g.

8. FUTURE OF THE ARBORETUM

The results of this soil survey confirm the assumption that the visions and basic ideas of the initiators of the project “Arboretum Putevima Mira” can hardly be sustained without extraordinarily high expense and effort. It goes without saying that plants of completely different climatic zones cannot survive in the Mediterranean climate, even with daily care. The results of our extensive soil scientific investigations support this statement.

The soil depths are very shallow (20–30 cm) throughout the arboretum. Woody species can barely root in these shallow soils. However, the initiators of the project knew about this problem and therefore, soil material was heaped up to about 50 cm in restricted areas to enable the plants to develop a compact root system.

The soil results show that the additional soil material most likely comes from the island, thus being no improvement for the plants from a soil-science viewpoint. The analytical results of the profiles have shown that this material was the same as that used for the construction of the golf course. Instead of using well structured medium textured soil, material was used which has a clay content of more than 55%. The use of such a very dense soil is one of the reasons for the decay of the non-autochthonous plants in the arboretum. The pF-curves, together with the data on density and bulk density, are tools to estimate water availability. The reduced water storing capacity and water availability for tree roots are caused by the generally high clay content as well as by the shallow depth at which a dense, largely impenetrable clay horizon with a clay content of more than 70% occurs in the arboretum. In all the sur-

Table 11 Water potential of selected plant groups (after LARCHER, 2003).

Plant group	negative water-potential (bar)
tropical rain forest trees	15–40
beech	20
conifers	15–22
e.g. picea abies	20
sclerophyllic trees	35–45
mediterranean shrubs	40–80

veyed profiles the bulk density of the soil above the dense clay layer is about 1.8 g/cm^3 , the maximum density is 2.7 g/cm^3 , which is far too high for most deciduous or coniferous trees from temperate regions.

Table 11 shows evidence that trees from temperate climates, e.g. conifers, can deal with soil–water-potentials of about -15 to -22 bar, sclerophyllic trees about double, Mediterranean shrubs four times as much. Due to their extensive root system and the numerous stomata sclerophyllic plants (sclerophyllous evergreen) transpire and photosynthesize intensively when the water supply is good, e.g. after rain, whereas during dry periods they are able to reduce or even cease their evapotranspiration. Representatives of this group include bay (*Lauris nobilis*), ilex (*Quercus ilex*), arbutus (*Arbutus L.*), carob (*Ceratonia siliqua*), olive (*Olea europaea*) and myrtle (*Myrtus communis*).

Figure 14 shows the water storing capacity of soils which is dependent on fine soil depth, structure, texture and pore volume. In general, sufficient amount of water

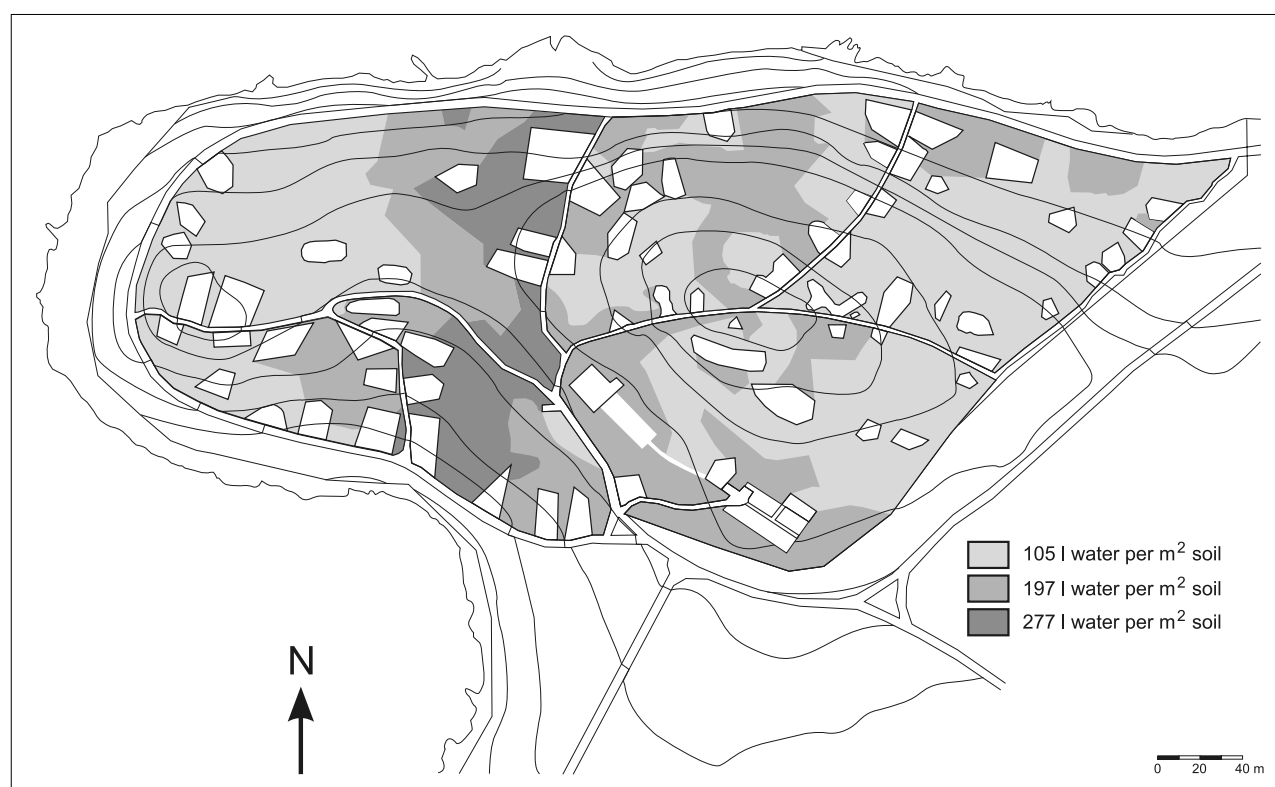


Fig. 14 Water storing capacity of soil in the arboretum.

can be stored in the soils for the adapted Mediterranean vegetation. However, the water potential values of the Brijuni soil samples show that the water is retained in the pores of the soil with such great tension that only a small amount of the water is available to the plants. This allows only woody species adapted to the climatic and pedological situation to survive without extensive care. The heaped-up soil material did not result in any improvement in terms of soil-hydrology. Therefore, it is necessary that only trees and shrubs that are adapted to the ecological conditions, the climate and the soil in this area are displayed in the arboretum. If we assume an annual precipitation of about 800 mm and an annual mean temperature of more than 14°C, the water requirements of non autochthonous plants cannot be met.

At present, the arboretum is in a very poor condition. With the exception of the network of paths, the whole infrastructure was destroyed or is unusable. However, it is clear that the idea to establish numerous areas that represent the species diversity all over Europe cannot be sustained. Four–five skilled persons would be needed for daily care and maintenance in the arboretum and it is doubtful that even then species indigenous to North Europe would grow. To stop further decay of the arboretum, the fence should be mended immediately so that deer can no longer enter and damage the existing trees and the regrowth of Mediterranean species.

An ecologically sustainable concept would be an arboretum with Mediterranean plants adapted to the actual climatic and pedological situation. The concept of the different areas for each European country should be abolished in favour of a concept with different areas which demonstrate the diversity of Mediterranean genera or species. Furthermore, it would be advisable to plant more shrubs and flowering plants to make the arboretum more attractive. At the moment there are almost only trees in the arboretum. The main building is in great need of renovation, as is the watering system for the plants. The arboretum must be an attraction for visitors giving a memorable experience for the whole family. Attractions such as a permanent soil profile or a “scented garden” could serve this purpose.

9. REFERENCES

- BORZAN, Ž., VIDAKOVIĆ, M. & MEŠTROVIĆ, S. (1993): Arboretum Brijuni – Znanstveno–nastavni i turistički objekt.– Glas. Šum. Pokuse, pos. Izd. 4, 73–86.
- BRINDLEY, G.W. & BROWN, G. (1980): Crystal structures of clay minerals and their X-Ray identification.– Mineralogical Society, London, 495 p.
- DECKERS, J.A., NACHTERGAELE, F.O. & SPAARGAREN, O.C. (eds.) (1998): World reference base for soil resources. Introduction.– Acco, Leuven, 165 p.
- DUCHAUFOR, Ph. (1968): *L'évolution des Sols. Essai sur la Dynamique des Profils.*– Masson et Cie, Paris, 94 p.
- DUCHAUFOR, Ph. (1998): *Handbook of Pedology: Soils, Vegetation, Environment.*– A.A. Balkema, Rotterdam, Brookfield, 264 p.
- DUDAL, R. (1967): *Definition of soil units.*– FAO, Rome.
- DURN, G., OTTNER, F. & SLOVENEK, D. (1999): Clay minerals as an indicator of polygenetic origin of terra rossa in Istria, Croatia.– *Geoderma*, 91/1–2, 125–150.
- ERSTIĆ, T. (2005): *Die Böden des Arboretums auf Brijuni/Kroatien: Eine Planungshilfe für die Neugestaltung.*– Unpubl. MSc Thesis, Universität für Bodenkultur, Wien, 151 p.
- FAO–ISRIC–ISSS (1998): *World Reference Base for Soil Resources. World Soil Resource Report 84.*– Food and Agricultural Organization, Rome, Italy.
- FAO–UNESCO (1981): *Soil Map of the World, Europe, Volume V.*– United Nations Educational, Scientific and Cultural Organization, Paris, France.
- KINTER, E.B. & DIAMOND, S. (1956): A new method for preparation and treatment of orientied–aggregate specimens of soil clays for X-Ray diffraction analysis.– *Soil Sci.*, 81, 111–120.
- KUBIENA, W. (1953): *Bestimmungsbuch und Systematik der Böden Europas.*– Ferdinand Enke Verlag, Stuttgart, Madrid,, 248 p.
- KUBIENA, W. (1986): *Grundzüge der Geopedologie und der Formenwandel der Böden.*– Österreichischer Agrarverlag, Wien, 128 p.
- LARCHER, W. (2003): *Physiological Plant Ecology, Ecophysiology and Stress Physiology of Functional Groups.*– Springer, Berlin, Heidelberg, New York, 513 p.
- MEHRA, O.P. & JACKSON, M.L. (1960): Iron oxide removal from soils and clays by a dithionite–citrate system buffered with sodium bicarbonate.– *Clays Clay Miner.*, 7, 317–327.
- MEIWES, K.H., KÖNIG, N., KHANNA, P.K., PRENZEL, I. & ULRICH, B. (1984): *Chemische Untersuchungsverfahren zur Charakterisierung und Bewertung der Versauerung von Waldböden.*– Ber. Forschungszentrum Waldökosystemforschung, 7, 142 p.
- MOORE, D.M. & REYNOLDS, R.C.Jr. (1997): *X–Ray Diffraction and the Identification and Analysis of Clay Minerals.*– Oxford Univ. Press, New York, 378 p.
- OTTNER, F. (1999): *Herkunft und Zusammensetzung von Peliten der Unterkreide Istriens, Kroatien: Sedimente oder Paläoböden.*– Habilitationsschrift Univ. Bodenkultur, 151 p.
- ÖNORM B3121 (2000): *Testing of natural stone; density, apparent density, bulk density.*– Austrian Standards Institute.
- ÖNORM L1063 (2005): *Physical analysis of soil; determination of the relation pressure potential versus water content of undisturbed soil samples.*– Austrian Standards Institute.
- ÖNORM L1068 (2005): *Physical investigation of soil; determination of soil density.*– Austrian Standards Institute.
- ÖNORM L1080 (1999): *Chemical analyses of soils; determination of organic carbon by dry combustion.*– Austrian Standards Institute.
- ÖNORM L1083 (2005): *Chemical analysis of soils; determination of acidity (pH value).*– Austrian Standards Institute.
- ÖNORM L1092 (2006): *Chemical analysis of soils; determination of water soluble substances.*– Austrian Standards Institute.
- RIEDMÜLLER, G. (1978): *Neoformations and transformations of clay minerals in tectonic shear zones.*– *TMPM Tschermaks Min. Petr. Mitt.*, 25, 219–242.
- SCHULTZ, L.G. (1964): *Quantitative interpretation of mineralogical composition from X-Ray and chemical data of the Pierre shales.*– *Geol. Surv. Prof. Paper*, Washington, 391C, 1–31.

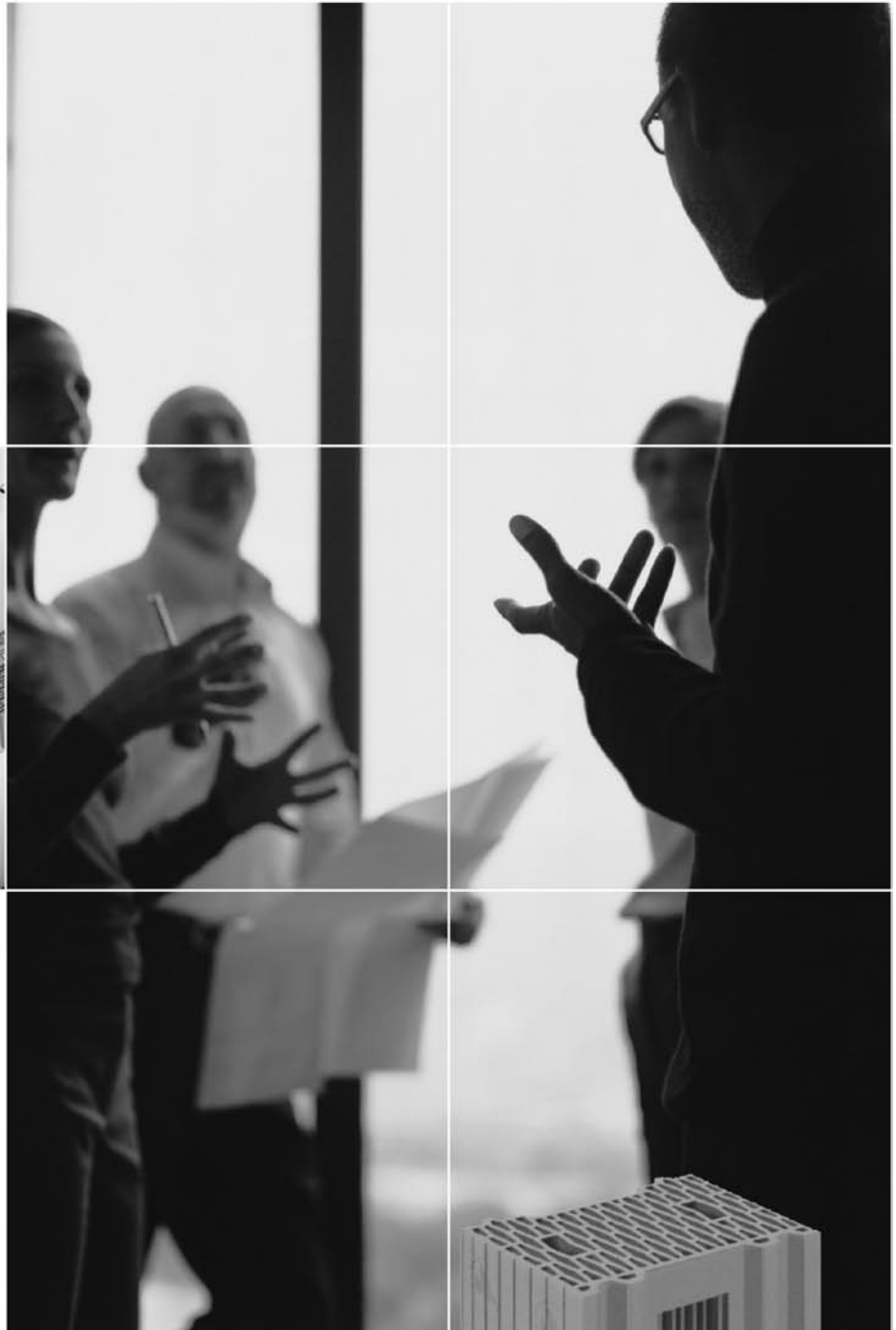
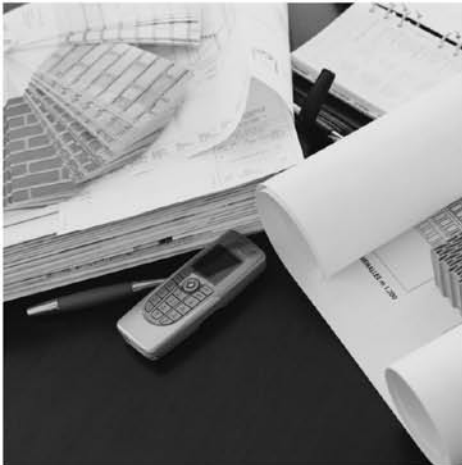
- SKOWRONEK, A. (1978): Untersuchungen zur Terra Rossa in E- und S-Spanien – ein regionalpedologischer Vergleich.– Würzburger geogr. Arbeiten, 37.
- THOREZ, J. (1975): Phyllosilicates and Clay Minerals – A Laboratory Handbook for Their X-ray Diffraction Analysis.– Editions G. Lelotte, Liege, 579 p.
- TRIBUTH, H. (1989): Notwendigkeit und Vorteil der Aufbereitung von Boden- und Lagerstättentonen.– In: TRIBUTH, H. & LAGALY, G. (eds.): Identifizierung und Charakterisierung von Tonmineralen. 29–33, Giessen.
- WHITTIG, L.D. (1965): X-ray diffraction techniques for mineral identification and mineralogical identification.– In: BLACK, C.A. (ed.): Methods of Soil Analysis, 671–698. 1. Amer. Soc. Agron., Madison, Wisconsin.
- WILSON, M.J. (1987): A Handbook of Determinative Methods in Clay Mineralogy.– Verlag Blackie, Glasgow and London, 308 p.
- ZECH, W. & HINTERMAIER-ERHARD, G. (2002): Böden der Welt. Ein Bildatlas.– Spektrum Akademischer Verlag Heidelberg, 120 p.

www.ina.hr

life in motion **INA**

 **ENVIRONMENT.**

Reliable
partners are
the best
foundation.



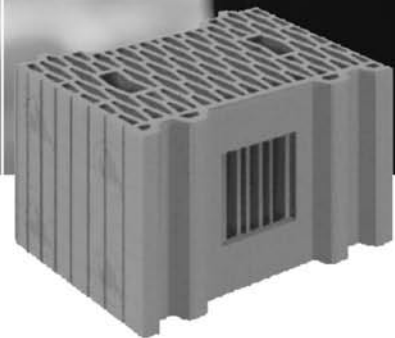
We are focused on those areas where we are among the best in the world – our core business bricks and roof tiles.

Brick is a sustainable product. Building with bricks represents a wise economic and ecological investment in the future.

Our primary goal is to create a long-term, balanced increase in value for our shareholders, customers, and employees.

Continual improvement is the requirement for above-average performance. Our motto: grow, but also optimize.

We are competitive because we are a multi-cultural company. We are successful because our employees act like entrepreneurs.



Bricks. Designed for Living.

www.wienerberger.hr



POROTHERM